IMPACT OF OIL ADDITIVE ON BIOFUEL ENGINE WEAR USING ELECTRON MICROSCOPY AND CONFOCAL MICROSCOPY

PANYAKORN RUNGSRITANAPAISAN

A THESIS REPORT SUBMITTED IN PARTIAL FULFILLMENT
OF THE REQUIREMENTS FOR THE DEGREE OF
MASTER OF ENGINEERING IN AUTOMOTIVE ENGINEERING
INTERNATIONAL COLLEGE
KING MONGKUT'S INSTITUTE OF TECHNOLOGY LADKRABANG
ACADEMIC YEAR 2018
KMITL-2018-IC-M-004-015

IMPACT OF OIL ADDITIVE ON BIOFUEL ENGINE WEAR USING ELECTRON MICROSCOPY AND CONFOCAL MICROSCOPY

PANYAKORN RUNGSRITANAPAISAN

A THESIS REPORT SUBMITTED IN PARTIAL FULFILLMENT
OF THE REQUIREMENTS FOR THE DEGREE OF
MASTER OF ENGINEERING IN AUTOMOTIVE ENGINEERING
INTERNATIONAL COLLEGE
KING MONGKUT'S INSTITUTE OF TECHNOLOGY LADKRABANG
ACADEMIC YEAR 2018
KMITL-2018-IC-M-004-015

THESIS TITLE	Impact of Oil Additive on Biofuel Engine Wear using Electron Microscopy and Confocal Microscopy
STUDENT NAME	Mr. Panyakorn Rungsritanapaisan
STUDENT ID	60610027
DEGREE	Master of Engineering
PROGRAME	Automotive Engineering
ADVISOR	Asst.Prof.Preechar Karin
CO-ADVISOR	Dr.Ruangdaj Tongsri
CO-ADVISOR	Prof.Dr.Katsunori Hanamura

ABSTRACT

Soot particles are produced inside the combustion chamber of the internal combustion engines and will later be exhausted into the thermosphere. Part of these particles will contaminate the engine oil. When this happens, diesel engine abrasion or, in a worst-case scenario, lubricant starvation will occur. This circumstance will eventually cause engine wear. This research uses X-ray fluorescence (XRF) technique to analyze the additive element in engine oil. For wear test, this research uses tribology Four-ball wear tester to substitute point contact wear mechanism. Then the images will be analyzed with Scanning Electron Microscope (SEM) and three-dimensional models of wear scars from Confocal Microscope will be used to study the effect of additive on soot dispersion in engine oil, which affects the metal wear mechanism. This research focuses only soot between 0.01-1 μm which can enter into contact area and cause wear. Base on Four-ball wear test, average wear scar in the group of low-grade engine oil were clearly larger because they had lower amount of anti-ware additive. Carbon black was the cause why wear scar diameters increased significantly on low-grade engine oil and wear mechanism was three body abrasive wear because the hardness of the carbon black is higher than the steel ball. Anti-wear additive has an important role on preventing metallic wear, both in the case of with and without carbon black contamination, by building oil film layers to protect metal surfaces.

ACKNOWLEDGEMENT

I would like to express my sincere gratitude to my thesis advisor Asst.Prof.Dr. Preechar Karin of the faculty of engineering at King Mongkut's institute of technology Ladkrabang for the continuous support of my master's degree study and research, for his patience, motivation, enthusiasm, and immense knowledge. His guidance helped me in all the time of research and writing of this thesis. I would also like to thank the experts who were involved in the validation survey for this research project: Dr.Dhritti Tanprayoon and Dr.Ruangdaj Tongsri from National Metal and Materials Technology Center (MTEC) and Prof. Dr. Katsunori Hanamur of the Departments of Mechanical Engineering, Tokyo institute of technology, Japan. Without their passionate participation and input, the validation survey could not have been successfully conducted.

I would also like to acknowledge financial support in this research from the project of Research and Researchers for Industries (RRI) under the operation of Thailand Science Research and Innovation (TSRI). I am thankful to Bangchak Corporation Pub. Co., Ltd. that provide materials for this research and expertise that greatly assisted the research.

Finally, I must express my very profound gratitude to my parents and Ms.Wayama Ruangrit for providing me with unfailing support and continuous encouragement throughout my years of study and through the process of researching and writing this thesis. This accomplishment would not have been possible without them.

Panyakorn Rungsritanapaisan

TABLE OF CONTENTS

Chapter	Page
ABSTRACT	I
ACKNOWLEDGEMENT	II
TABLE OF CONTENTS	III
LIST OF FIGURES	VII
LIST OF DEFINITIONS	X
CHAPTER 1 INTRODUCTION	11
1.1 Research Background	11
1.2 Objective	11
1.3 Scope of work	12
1.4 Structure of the research	12
1.5 Expected benefits	12
CHAPTER 2 LITERATURE REVIEW	13
2.1 Tribological contacts [1]	13
2.2 Lubrication Conditions [2]	14
2.2.1 Boundary layer	14
2.2.2 Full film lubrication	14
2.2.3 Mixed lubrication	15
2.2.4 Stribeck Diagram	16
2.3 Wear [2]	17
2.3.1 Abrasive wear [3]	17
2.3.2 Adhesive wear	18
2.3.3 Rolling Contact Fatigue	18
2.4 Diesel engines [5]	19

2.5 Oil analysis 20
2.5.1 Engine oil additive 20
2.5.2 Viscosity 23
2.5.3 Density [11] 24
2.5.4 Total base number [1] 24
2.5.5 Element and structural analysis [12] 24
2.6 Wear analysis 25
2.6.1 Scanning Electron Microscope [1] 25
2.6.2 Confocal Microscope [23] 26
2.7 Literature reviews 27
2.7.1 Particle Emission Characteristic 27
2.7.2 Impact of Soot on metal wear [18] 32
2.7.3 Soot hardness calculation [19] 34
2.7.4 Tribology Test [11] 37
CHAPTER 3 RESEARCH METHODOLOGY 39
3.1 Experimental equipment 39
3.1.1 Engine oil related with API standard 39
3.1.2 Carbon black 39
3.1.3 Laser Diffraction Particle Size Analyzers 41
3.1.4 Fourier-transform infrared spectrometer 41
3.1.5 Four ball wear tester 42
3.1.6 Optical Microscope 43
3.1.7 Confocal Microscope 43
3.1.8 Scanning Electron Microscope 44
3.2 Experimental procedure 44

3.2.1 The study of engine oil property 44
3.2.2 The impact of oil additive with soot on metal wear 44
CHAPTER 4 RESULTS AND DISCUSSIONS 46
4.1 Engine oil properties 46
4.1.1 Fourier-transform infrared spectroscopy 47
4.1.2 Laser particle size distribution 47
4.2 Impact of anti-ware additive 49
4.3 Impact of soot on metal wear 49
4.3.1 Wear scar diameter 49
4.3.2 Surface roughness 52
4.3.3 Wear mechanism 55
4.3.4 Ball surface element analysis 61
CHAPTER 5 CONCLUSIONS 65
REFERENCES 66
APPENDIX A 68
APPENDIX B 79
APPENDIX C 82
APPENDIX D 86
APPENDIX E 88
AUTHOR BIOGRAPHY 98

LIST OF TABLES

Table **Page**

Table 2.1 Wear scar diameter, roughness and friction torque [18]. 32

Table 2.2 The properties of various forms of carbon [19]. 35

Table 2.3 Carbon atom density and its hardness of soot primary particle from the references [19]. 36

Table 3.1 The condition of Four Ball wear tester (ASTM D4172) [24]. 42

Table 3.2 Engine oils contaminated with carbon black N330 45

Table 4.1 Engine oil properties 46

Table 4.2 Qualitatively analyze wear mechanisms when engine oil is contaminated with carbon black N330. 55

Table 4.3 Element analysis of ball surface (Low grade engine oil) 61

Table 4.4 Element analysis of ball surface (High grade engine oil) 62

LIST OF FIGURES

Figure **Page**

Figure 2.1 Tribological contacts are affected by different conditions [1]. 13

Figure 2.2 The tribological contact can be observed at macroscale (left) or at microscale (right) [1]. 14

Figure 2.3 Hydrostatic lubrication as a form of fluid friction [2]. 15

Figure 2.4 The Stribeck graph [2]. 16

Figure 2.5 Two-body abrasion is shown in (a); the abrasive particles are fixed to a substrate during rubbing. In (b), the particles are forced against the fixed surface by the third body [4]. 17

Figure 2.6 Adhesion loci are produced by sites of real contact between conforming surfaces (a) and (b) [4]. 18

Figure 2.7 Schematic illustration of the process of surface crack initiation and propagation [3]. 19

Figure 2.8 The lubricated parts in an engine (left) and the corresponding lubricating conditions indicated in the diagram (right) [5]. 20

Figure 2.9 Multilayer adsorption of friction modifier (FM) additives promotes separation of surfaces. The layers are easily sheared, giving low friction [1]. 22

Figure 2.10 Explanation of viscosity [10] 23

Figure 2.11 Principle of SEM [1]. 26

Figure 2.12 Principles of Confocal Microscopy [23]. 27

Figure 2.13 Artist's conception of diesel particulate matter [14] 28

Figure 2.14 TEM micrograph of diesel engine soot [15]. 28

Figure 2.15 Idealized diesel exhaust particle number and mass weighted size distribution [16]. 29

Figure 2.16 TEM images of (a) biodiesel engine's and (b) diesel engine's ultrafine particles in the operation condition 80% of engine load and 2400 rpm of engine speed [15]. 30

Figure 2.17 Size distributions of (a) biodiesel engine's and (b) diesel engine's nanoparticle emission using TEM image processing method. The engine operation condition is 20, 40, 60 and 80% of engine load and 1600 rpm of engine speed [15]. . 31

Figure 2.18 Carbon black and wear particles (a) size distribution and (b) cumulative volume in lubricating oil before and after Four-ball tribology test by Laser Particle Diffraction Spectroscopy [18].....33
Figure 2.19 Soot primary particle conceptual model for calculation carbon atom density [19]. 34
Figure 2.20 Plots of carbon density and its hardness [19]. 36
Figure 2.21 Types of contact and movement of friction and wear testers [11]. 38
Figure 3.1 Carbon Black N330 [21]. 39
Figure 3.2 TEM Micrograph of carbon black N330 at (a) 50,000 and (b) 100,000 magnification. 40
Figure 3.3 Laser particle size distribution analyzer (MALVERN, Mastersizer 3000) 41
Figure 3.4 Fourier Transform Infrared Spectrometer (Perkin Elmer, Spectrum One) 41
Figure 3.5 Schematic of Four-ball wear tester followed ASTM - D4172. 42
Figure 3.6 Optical Microscope 43
Figure 3.7 LEXT OLS4000 3D Laser Measuring Microscope.....43
Figure 3.8 SEM-EDX JEOL JSM-IT-500HR.....44
Figure 4.1 Fourier Transform Infrared Spectroscopy 47
Figure 4.2 Carbon black N330 (a) size distribution and (b) cumulative volume in engine oil by Laser Particle Diffraction Spectroscopy. 48
Figure 4.3 The average wear scar diameter measured by OM (μm).....49
Figure 4.4 The average wear scar diameter of carbon black contaminated engine oil measured by OM (μm).....50
Figure 4.5 Wear scar diameter measured by OM. 51
Figure 4.6 Ra value from confocal microscope at low magnification 20x (μm).....52
Figure 4.7 Ra value from OM at high magnification 100x (μm) 52
Figure 4.8 Example of wear profile between (a) low-grade and (b) high grade engine oil. 52
Figure 4.9 Roughness measurement by confocal microscope 54
Figure 4.10 Average wear mechanism (%).....55
Figure 4.11 SEM Micrographs of wear scar at 120 magnification.....57
Figure 4.12 SEM micrograph of wear scar at 500 magnification.....58
Figure 4.13 SEM micrograph of wear scar at 500 magnification with wear description 59

Figure 4.14 SEM micrographs of wear scar with colored wear analysis..... 60
Figure 4.15 Elemental analysis of ball surface. 62
Figure 4.16 SEM micrograph with EDX analysis. 64

LIST OF DEFINITIONS

API	American Petroleum Institute
CB	Carbon Black N330
EDX	Energy Dispersive X-Ray Analysis
OM	Optical Microscopy
SEM	Scanning Electron Microscopy
TEM	Transmission Electron Microscopy
TBN	Total Base Number
WSD	Wear Scar Diameter
FT-IR	Fourier-transform infrared spectroscopy

CHAPTER 1

INTRODUCTION

1.1 Research Background

In the present, internal combustion engines are mechanical, which use fuel to transform heat energy into mechanical energy. However, a part of the mechanical energy is wasted by friction caused by tractions between moving parts. This friction causes deteriorations of the parts and eventually defunct them. Therefore, engine oil is used to protect the engines from deterioration by decreasing frictions and separating surfaces to reduce contacts between them.

Biodiesel is an alternative fuel from plants. It is nontoxic, biodegradable, and has a comparable technical qualification to the diesel. Studies shown that horsepower and torque of engines that use biodiesel is not far from ones with diesel. In fact, if a biodiesel engine is modified properly, its performance can overcome a diesel one, thanks to its more complete combustion done by oxygen atoms in biodiesel molecules.

However, a better combustion does not mean a complete one. The biodiesel engine combustion is still incomplete, which does not only produce particle pollution that effects environment by releasing carbon as soot together with the exhaust gas, but also contaminates the engine oil with these particles.

This contaminated engine oil can harm the lubrication in many ways, for example, causing oil deterioration, reducing oil film thickness, producing sticky stain, making the oil more acidic and corrosive to metal, increasing abrasive wears, etc. Due to the mentioned possible damages, oil additives are utilized to improve both its physical and chemical properties. So, appropriate oil additives are important for prolonging the life and the efficiency of the engine.

1.2 Objective

To investigate the impact of soot and oil additive on metallic wear by Tribotester.

1.3 Scope of work

1) Do research and study on academic papers about mechanism of internal combustion engine, occurrence of soot, lubrication, physical and chemical properties of engine oil, mechanism of wear, contamination of fuel and soot in engine oil and oil additive.
2) Testing and analyzing the physical and chemical properties of lubricants with additives, as contaminated by soot, with scientific instruments.
3) Testing and analyzing the example of soot contaminated lubricant, that has additives, with Four ball wear tester and advanced tribology technic.
4) Explain the mechanism of metal wear cause by soot contamination in engine oil and the additive's properties that influence physical and chemical properties of lubricant, which also impact metal wears, by using Four ball tester, Small engine, Scanning Electron Microscope and Confocal Microscope

1.4 Structure of the research

The research methodologies are divided as follows.
Chapter 1 discuss the research background, objective and scope of work.
Chapter 2 discuss the relevant theory and literature including fundamental of tribology, engine oil analysis, soot contamination and metallic wear.
Chapter 3 discuss the research materials and methods.
Chapter 4 discuss the results of soot contamination on metallic wear using Four-ball wear tester, optical microscopy, confocal microscopy, scanning electron microscopy and laser diffraction spectroscopy.
Chapter 5 make conclusion and discussion

1.5 Expected benefits

This research can explain the impact of soot and engine oil additive on metal wear.

CHAPTER 2

LITERATURE REVIEW

2.1 Tribological contacts [1]

A tribological contact is when two solid bodies are in contact under relative motion. It can be either unlubricated or lubricated. Figure 2.1 shows the characteristic of tribological contact, which defined by its operating conditions, such as velocity, load and type of motions; material parameters, such as surface material, surface roughness and hardness; environmental conditions, such as temperature and humidity; and lubricant properties in the lubricated case, such as viscosity. Figure 2.2 shows different scales that tribological contact can be observed: macroscopic scale and microscopic scale. The macro scale will give global information of the contact, while the micro scale will give local information within the contact. For example, a contact that appears smooth at macro scale may appear very rough and uneven at micro scale. The overall contact area between the two surfaces consists of many small areas where surface peaks get into contact. Therefore, the apparent contact area at the macro scale is much larger than the real contact area between the two surfaces in micro scale.

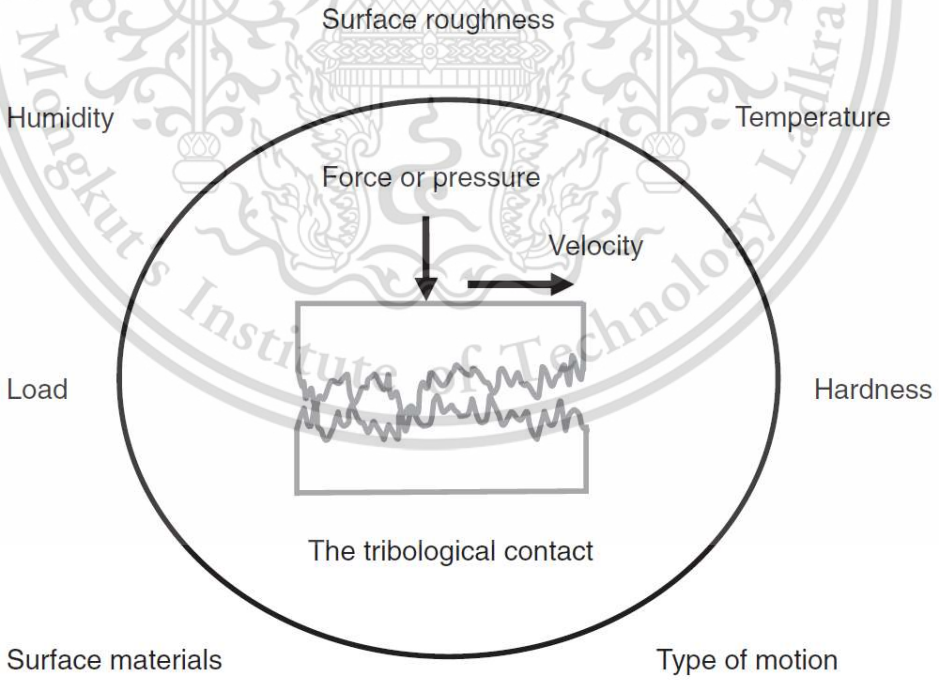

Figure 2.1 Tribological contacts are affected by different conditions [1].

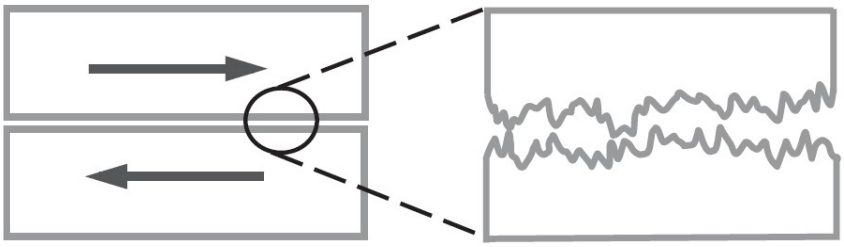

Figure 2.2 The tribological contact can be observed at macroscale (left) or at microscale (right) [1].

2.2 Lubrication Conditions [2]

2.2.1 Boundary layer

Boundary layer or additive layer is a molecular layer of a substance that cover two contact surfaces. The properties of these layers can significantly impact the characteristics of friction and wear. Creating additive layers in a variety of dynamic, geometric and thermal conditions is one of the most important objectives of lubricant development. These layers are significantly important when the thick and long-lasting lubricant films between two surfaces are not present. Additive layers are created from surface-active substances, their chemical reaction products, adsorption, chemisorption, and tribochemical reactions. Although boundary friction of these additive layers is often allocated to solid friction, the difference between them and the understanding of lubrication and wear processes, especially when the additive layers are formed by the lubricants, are significant to lubricant development.

2.2.2 Full film lubrication

In this form lubrication, both surfaces are fully separated by a fluid lubricant film. This film is either formed hydrostatically or more commonly, hydrodynamically. Figure 2.3 shows hydrodynamic or hydrostatic lubrication. It is when liquid or fluid friction is caused by the frictional resistance, because of the rheological properties of fluids.

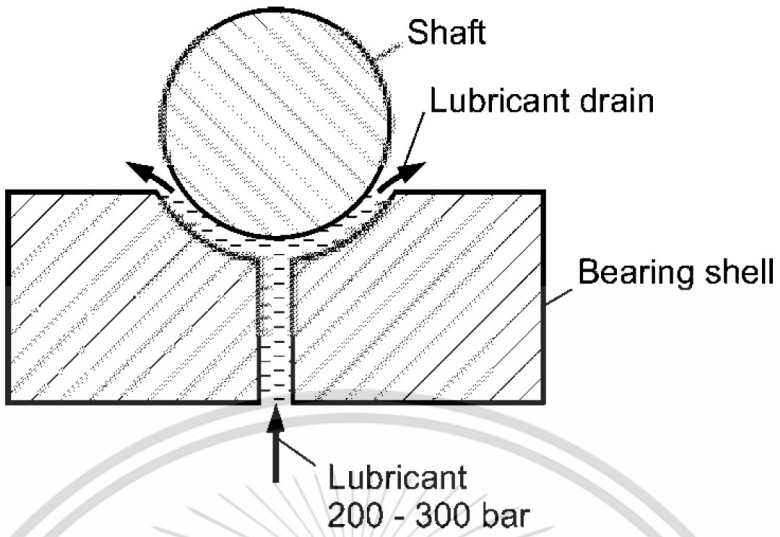

Figure 2.3 Hydrostatic lubrication as a form of fluid friction [2].

2.2.3 Mixed lubrication

Mixed lubrication occurs when boundary layer combines with full film lubrication. From a lubrication technology standpoint, this form of friction requires sufficient load-bearing boundary layers to form. Machine elements that are normally hydrodynamically lubricated experience mixed lubrication when starting and stopping. For rolling bearings, it has been shown that the reference viscosity either of, lubricating oils or of the base oils, is not enough to ensure the formation of protecting lubricant layers, or the required minimum lifetime. Under mixed lubrication conditions, it is important to choose the appropriate lubricant. For example, one that can form tribolayers by using anti-wear and extreme pressure additives.

2.2.4 Stribeck Diagram

Figures 2.4 shows the different between boundary and fluid friction by using Stribeck diagram. These are based on the starting-up of a plain bearing whose shaft and bearing shells are separated only by a molecular lubricant layer when stationary. As the speed of revolution of the shaft increases, a thicker hydrodynamic lubricant film is created. This film initially causes random mixed friction which significantly reduces the coefficient of friction. As the speed continues to increase, a full, uninterrupted film is formed over the entire bearing faces, which sharply reduces the coefficient of friction. As speed increases, internal friction in the lubricating film adds to external friction. The curve passes a minimum coefficient of friction value and then increases, solely as a result of internal friction. The lubricant film thickness shown in this Figure depends on the friction, lubrication conditions, and the surface roughness.

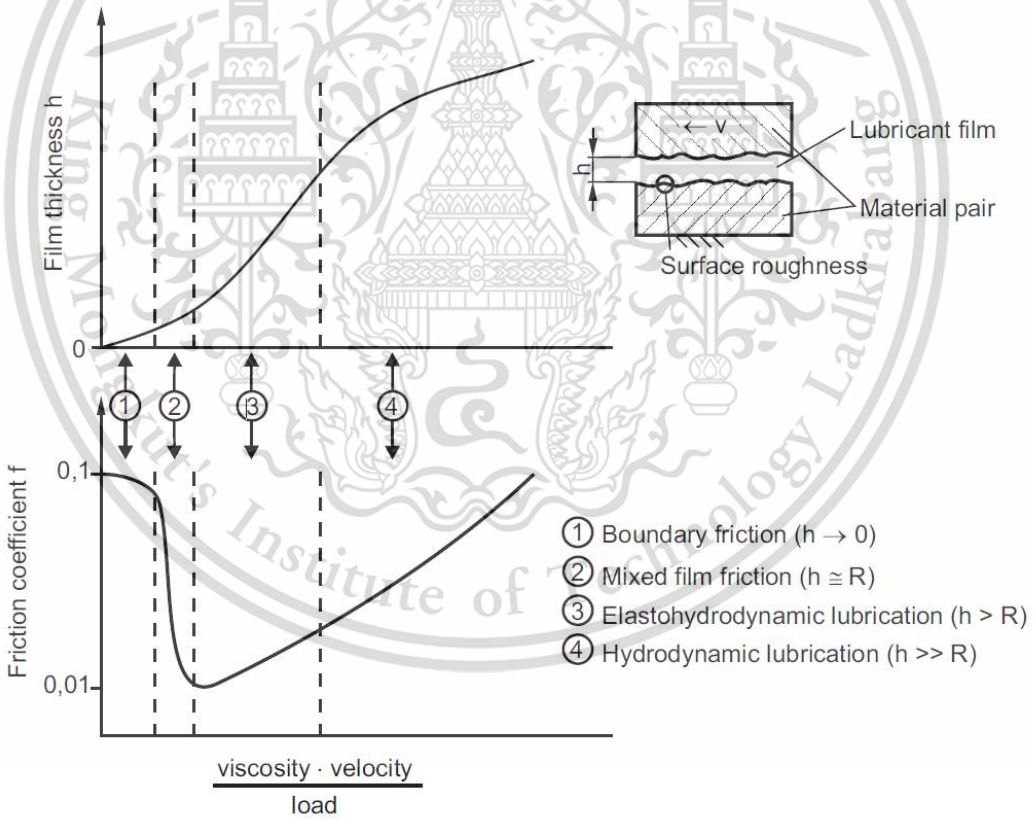

Figure 2.4 The Stribeck graph [2].

2.3 Wear [2]

Wear is loss of material from a solid surface. Wear can appear in many ways depending on the material of the interacting contact surfaces, the environment and the operating conditions. At least three principal wear processes can be distinguished: abrasive wear, adhesive wear and surface fatigue wear. These are briefly described as follows:

2.3.1 Abrasive wear [3]

Abrasive wear occurs whenever a solid object is loaded against material that have equal or greater hardness. A common example is the wear of shovels on earth-moving machinery. The level of abrasive wear is larger than may be realized. Any material may cause abrasive wear if hard particles are present even if it is very soft. For example, an organic material, such as sugar cane, can cause abrasive wear to cane cutters and shredders, because of the small fraction of silica present in the plant fibers. In fact, there are almost always several different mechanisms of wear that occur on materials, all of which have different characteristics.

The process when a rough hard surface mates a softer material, where the asperities of the hard material scratch the softer surface, is called two-body abrasive wear. While the situation when hard loose wear particles are present between the mating surfaces, and one or both surfaces can be worn by scratching, is called three-body abrasive wear as shown in Figure 2.5.

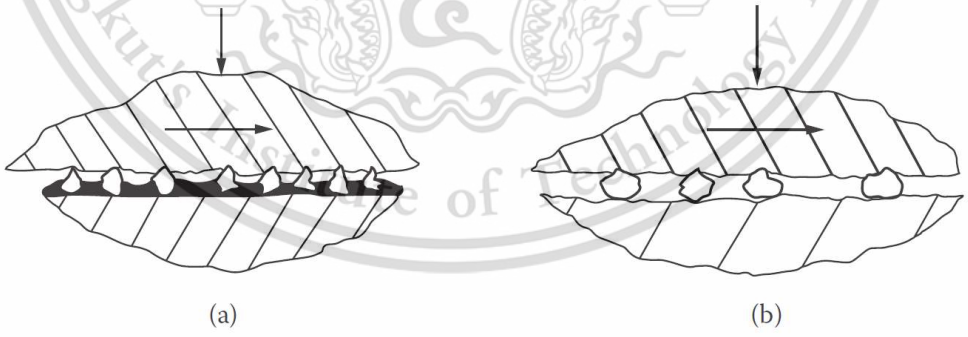

Figure 2.5 Two-body abrasion is shown in (a); the abrasive particles are fixed to a substrate during rubbing. In (b), the particles are forced against the fixed surface by the third body [4].

2.3.2 Adhesive wear

Adhesive wear occurs under sliding conditions where asperities are plastically deformed and welded together by high local pressure and temperature. When the sliding continues, the asperity bonds are broken, and results in removal of material or transfer of material from one surface to the other. Extensive adhesive wear is commonly described as scoring, galling or seizure as shown in Figure 2.6.

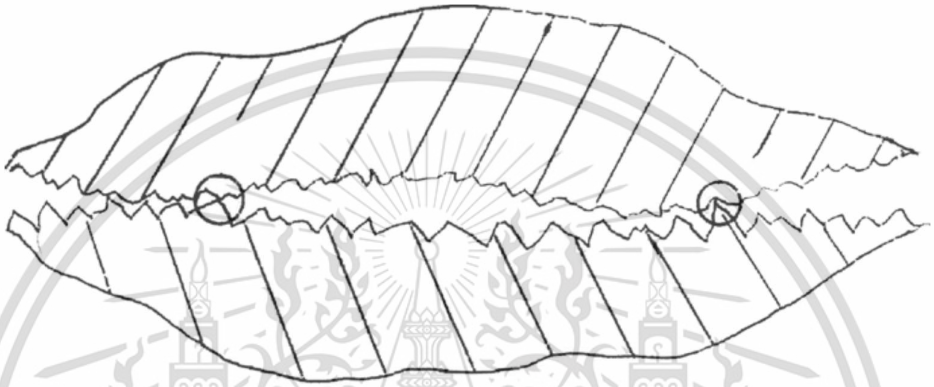

Figure 2.6 Adhesion loci are produced by sites of real contact between conforming surfaces (a) and (b) [4].

2.3.3 Rolling Contact Fatigue

Rolling contact fatigue is material removal or damage caused by repeated rolling of a solid shape on a contacting solid surface. The usual manifestations include pitting, micro pitting or cracking. There are many degrees of these manifestations, but these examples present the “flavor” of this form of wear [4].

Examination of worn surfaces in cross section reveals intense deformation of the material directly below the worn surface. For example, it is shown that under conditions of severe sliding with a coefficient of friction close to unity, material within 0.1 mm of the surface shifted in the direction of sliding due to deformation caused by frictional force. Also, close to the surface, the grain structure is drawn out and orientated parallel to the wearing surface. Obviously, under the lower coefficients of friction which prevail in lubricated systems, this surface deformation is less or may

even be absent. Strains caused by shearing in sliding are present below the surface reaching the extreme values at the surface [3].

Cracks and fissures have frequently been observed on micrographs of worn surfaces. Figure 2.7 shows the skeptical illustration of the mechanism of surface fatigue wear that is initiated by cracks. A primary crack starts at the surface at some weak point and propagates downward along weak planes such as slip planes or dislocation cell boundaries. A secondary crack can develop from the primary crack or, alternatively, the primary crack can connect with an existing subsurface crack. When the developing crack reaches the surface again a wear particle is released [3].

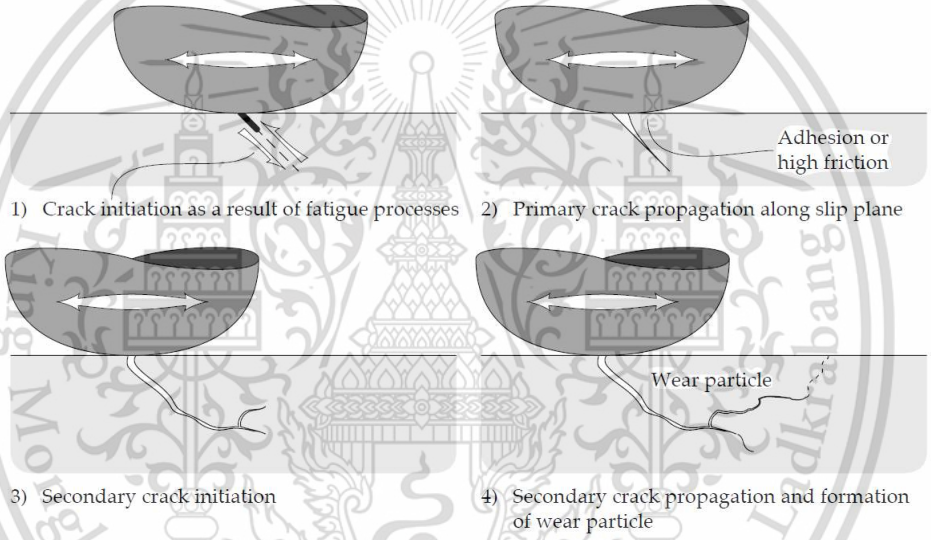

Figure 2.7 Schematic illustration of the process of surface crack initiation and propagation [3].

2.4 Diesel engines [5]

The engine operation will be described from the four-stroke engine perspective as showed in Figure 2.8. Air is sucked into the combustion chamber during the intake. Fuel is injected during the compression stroke. Different fuels are used for different engines. Fuels generally consist of carbon and hydrogen, C_xH_y. They may include gasoline that has 5–12 carbons, diesel or biodiesel that has 10–15 carbons, ethanol or gaseous fuels such as natural gas, biogas or landfill gas. Fuel and air react during the compression stroke. The combustion energy released pushes the

piston downwards, yielding power, heat and friction during the expansion stroke. The final stroke releases the exhaust components. The current emission legislation such as Euro V has limits on the allowable exhaust components. For example, CO, hydrocarbons, NOx and particulate matters like soot. Emissions may be reduced by after-treatment of the exhaust gas or optimizing the combustion.

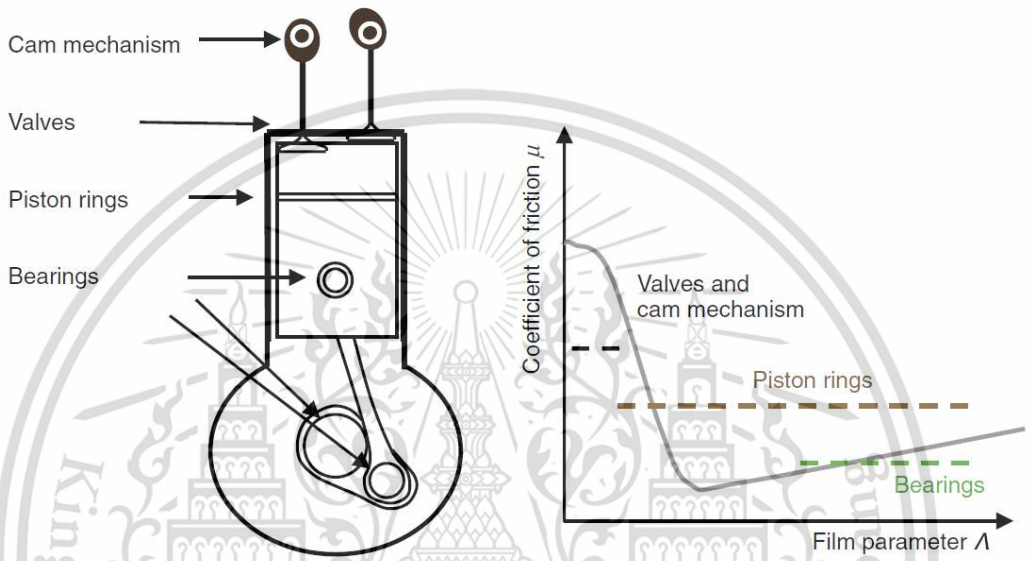

Figure 2.8 The lubricated parts in an engine (left) and the corresponding lubricating conditions indicated in the diagram (right) [5].

2.5 Oil analysis

2.5.1 Engine oil additive

2.5.1.1Soot dispersant additive [7]

Dispersants are metal-free additives that suspend oil-insoluble resinous oxidation products and particulate contaminants in the oil. By doing so, they minimize sludge formation, particulate-related abrasive wear, the increase of lubricant viscosity, and oxidation-related deposit formation.

Dispersants perform these functions by doing the following:

- They include polar contaminants in their micelles.
- They associate with colloidal particles to prevent aggregation to larger particles to prevent them from separating out of oil.
- They suspend aggregates in the lubricant.
- They modify soot to minimize its aggregation and then prevent soot-related oil thickening.
- They lower the surface or interfacial energy of the polar products to decrease their tendency to adhere to surfaces.

The unwanted polar materials, generally described as dirt, are a consequence of the oxidative degradation of the lubricant and thermal decomposition of the thermally labile lubricant additives, such as extreme-pressure or anti-wear agents; and the reaction of the resulting chemically reactive species, such as carboxylic acids, with the metal surfaces or wear debris in the engine. The lubricant consists of three components: the base fluid, the additives, and a viscosity modifier in the case of a multi-grade lubricant. As all three are organic, they are easy to be attacked by oxygen, resulting in the formation of the highly oxygenated polar materials.

In diesel-fueled engines, soot from the combustion chamber is the key component of the carbon and lacquer deposits, which occur on pistons and sludge. As stated earlier, soot combines with resin to form lacquer and carbon deposits. In general, lacquer is rich in resin, and carbon is rich in soot. Sludge results when soot combines with the oxygenated species, oil, and water. The local piston temperatures and the lubricant's ash producing tendency have a profound effect on the composition of the carbon deposits. High temperatures and the lubricants with high metals content mainly produce deposits with high residue and low organic content. Basic detergents are considered to contribute deposits, as they contain metals, which are the main source of ash that is a part of some deposits. Zinc dialkyl-dithiophosphate only slightly contributes deposits because their amount in lubricants is much smaller than that of the detergents.

2.5.1.2 Antiwear additive [1]

Figure 2.9 shows anti-wear additives that lengthen the tribological contact life by modifying the metal surfaces and reduce wear in the mixed lubrication regime. They are active in the mixed lubrication regime that has higher temperatures and loads than Friction Modifiers (FMs). They are commonly added at 1–3%. They are used in engine oils, hydraulic fluids, Automatic Transmission Fluids (ATFs), etc. [1]

Anti-wear additives mainly chemisorb to metal surfaces. The monolayer of chemisorbed anti-wear additive offers durable wear protection of the surface in the mixed lubrication regime. Anti-wear additives require moderate activation temperatures, loads and shear rates, but has to be higher than friction modifiers. [8].

The chemistry involves nitrogen, phosphorus and/or sulfur. Phosphorus is the most widely used because it offers anti-wear protection at relatively low loads. The most frequently used anti-wear additive is ZDDP (zinc dialkyl-dithiophosphate), which also has antioxidant and detergent properties.

Nontraditional anti-wear or extreme pressure additives will be more extensively used as environmental awareness increases. Nowadays there are alternatives reported in the literature, such as graphite, PTFE, inorganic carbon nanoparticles and CHON-based additives. [8, 9].

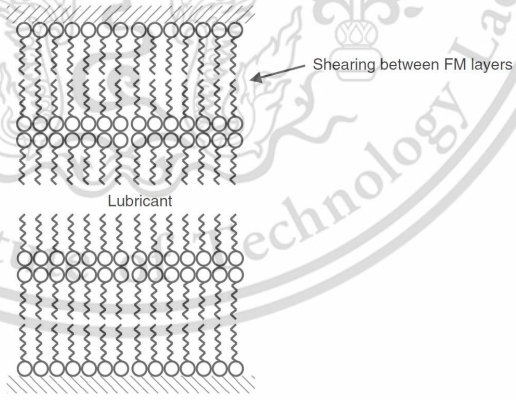

Figure 2.9 Multilayer adsorption of friction modifier (FM) additives promotes separation of surfaces. The layers are easily sheared, giving low friction [1].

2.5.2 Viscosity

Viscosity is the most important performance property, as it determines the lubricant film thickness and the performance of the lubricated contact. In general, a high viscosity gives a thicker lubricant film, while a low viscosity gives a thinner one. If the lubricating film is too thin, roughness surfaces will be brought in contact with each other and friction will increase. On the other hand, if the film is too thick, it requires more energy to move the surfaces. Therefore, a lubricant with extremely high viscosity may, in the worst case, not be able to pump into the contact, because it becomes harder to pump when viscosity increases. This will result in starvation of lubricant which cause wear or seizure. During the development of lubricants, the aspects of temperature, pressure and shear rate that impact viscosity are dealt with, so lubricants are available in different viscosity grades to satisfy the requirements in different applications. Lubricant with the lowest viscosity that still forces the two moving surfaces apart is generally the most demanded in the market [1].

Viscosity is the main parameters to create lubrication efficiency and the application of lubricants. Its terms appear in nearly all lubricant specifications and is also the only lubricant value which is used in the design process for hydrodynamic and elastohydrodynamic lubrication. Figure 2.10 shows viscosity explanation [10].

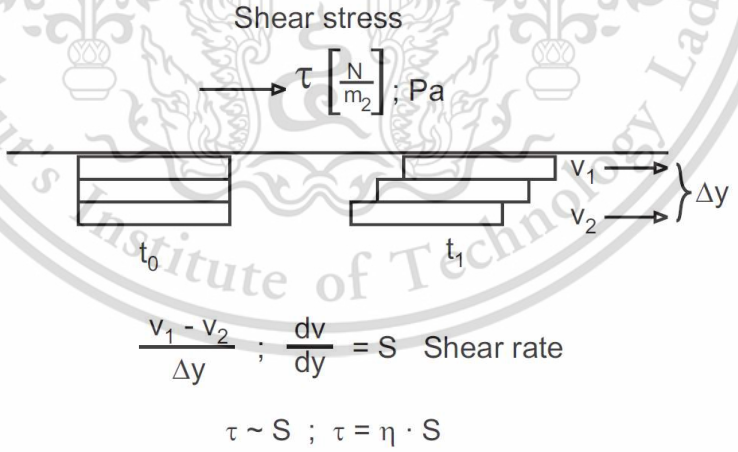

Figure 2.10 Explanation of viscosity [10].

2.5.3 Density [11]

The density is one of the most common physical properties of a lubricant. A liquid lubricant is usually considered to be incompressible while its thermal expansion is ignored, so that the density is considered as a constant. The density of 20°C is usually considered to be standard. The density of a lubricant is the function of pressure and temperature. The density of a lubricant should be variable under some conditions, such as in the elastohydrodynamic lubrication state.

2.5.4 Total base number [1]

The total base number (TBN) is another measure of the condition of lubricant as a high TBN indicates a good condition. Unused lubricants may contain basic additives such as detergents and dispersants with its TBN remains high. These basic additives are added to the lubricant to neutralize acidic components that may form. Therefore, the TBN will gradually be lowered when these additives are consumed, usually followed by oxidation and an increase of viscosity. So, the TBN is a good indicator of the remaining life of engine oils.

The TBN test is performed by diluting lubricant sample in a beaker. There are two methods for measuring the TBN: using a strong acid, such as hydrochloric acid or a weak acid such as perchloric acid to titrate the basic components of engine oil. The acid will react to the basic components in both cases, but there are some differences. The perchloric acid can determine both detergents and dispersants, so it is commonly used to measure the TBN of unused lubricants. While hydrochloric acid can determine only detergents so, it is commonly used to measure the TBN of used lubricants. When all basic components have reacted with the acid the amount of acid is converted to KOH/g equivalent of lubricant in analogy with the Total Acid Number (TAN). A potentiometer is commonly used to identify their equilibrium point.

2.5.5 Element and structural analysis [12]

There are two reasons in considering elemental analysis of petroleum product. First, many metals and nonmetals element in crude oils are harmful to the refinery and processing operations, by generally acting as catalyst poisons. The sulfur and nitrogen compounds that are generated during the processes are also potential environmental concerns. Second, the additives and oils contain added organometallic compounds to

enhance their performance. Although much of this chemistry is proprietary, certain aspects are universally known. Generally, the presence of sulfur, phosphorus, alkaline earth metal, zinc, copper, etc. compounds defines the composition of the additives and lubricating oils.

All proper elemental analytical techniques are used for the analysis of petroleum products. Several monographs are available on this subject: a recent monograph has been published by ASTM, containing papers from several authors covering a wide variety of techniques [13]. Most outstanding among these techniques are atomic spectroscopy (atomic absorption spectroscopy, AAS, and inductively coupled plasma atomic emission spectroscopy, ICPAES), X-ray fluorescence (XRF), and micro-elemental techniques.

2.6 Wear analysis

2.6.1 Scanning Electron Microscope [1]

The Scanning Electron Microscope (SEM) is one type of electron microscope. It is the prime technique for imaging and examining wear and damage mechanisms. The most important features of SEM are high spatial resolution and large depth of field, and the possibility to combine imaging with elemental analysis using Energy Dispersive Spectroscopy (EDS). It works by scanning a finely focused electron beam over the surface to be imaged. The incident electrons, with energy typically of 5–20 keV, interact with the sample atoms within a few microns of the surface. This interaction generates various signals emitting from the surface, for example electrons and X-ray photons. The SEM image is formed from the intensity of electron emissions from the surface. When the electron beam is scanned over the surface, the intensity of emitted electrons from each position point of the surface sets the intensity of the corresponding point of the image, as showed in Figure 2.11.

SEM is made in vacuum, which means that the samples must be clean and dry. Non-electrically insulating surfaces, which do not get negatively charged by the electron irradiation, can be analyzed by SEM after, for example, being coated with a thin layer of a gold alloy. However, the development of advanced SEM systems is fast and today most samples can be studied with SEM techniques.

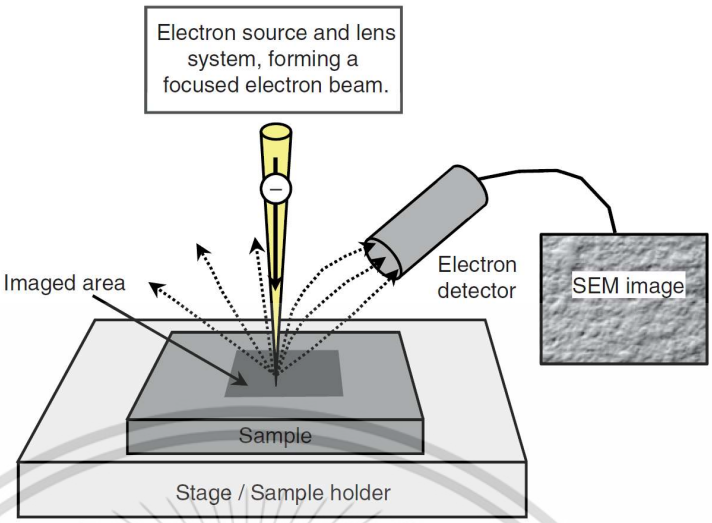

Figure 2.11 Principle of SEM [1].

2.6.2 Confocal Microscope [23]

Confocal microscopy is better than conventional wide field optical microscopy in many aspects. Not only that it can control depth of field, but it can also eliminate or reduce background information away from the focal plane and collect serial optical sections from thick samples. The confocal microscopy works basically by using spatial filtering techniques to delete out-of-focus light or glare in samples, whose thickness is larger than the immediate plane of focus. In recent year, the use of confocal microscopy becomes more popular. It does not require more specification of samples than that of conventional fluorescence microscopy to produce extremely high-quality image.

Figures 2.12 diagrammatically shows the principle of confocal microscopy. It works by scanning epi-fluorescence laser. The laser system emits a consistent beam of light that goes through a pinhole in a confocal plane, with its scanning point on the sample. There is a second pinhole aperture in front of the detector or a photomultiplier tube. As the laser is reflected by a dichromatic mirror and scanned across the specimen in a defined focal plane, secondary fluorescence emitted from points on the specimen in the same focal plane, pass back through the dichromatic mirror and are focused as a confocal point at the detector pinhole aperture.

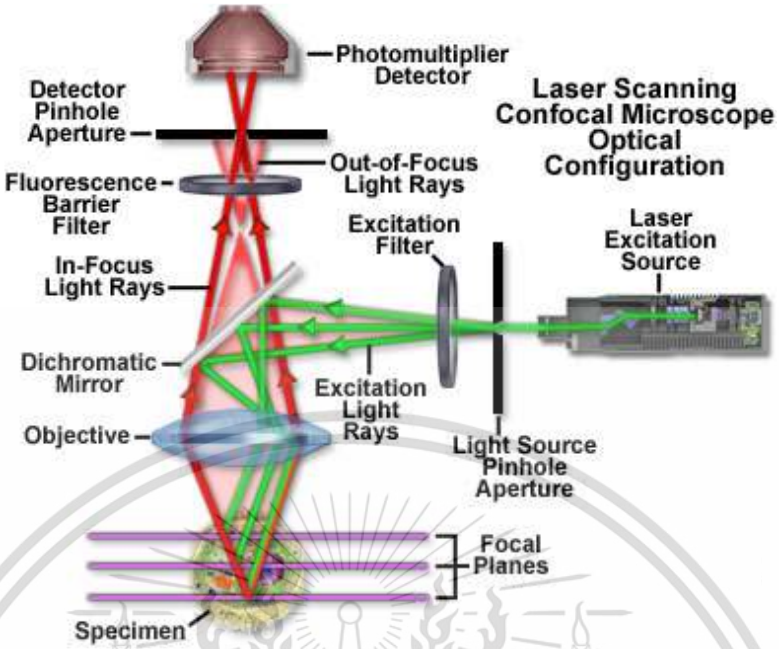

Figure 2.12 Principles of Confocal Microscopy [23].

2.7 Literature reviews

2.7.1 Particle Emission Characteristic

Soot is a microscopic particle that contains carbons. It is produced in the process of incomplete combustion of hydrocarbons. Figure 2.13 [14] shows an artist's conception of diluted and cooled diesel PM, which consists of carbon, ash, and unsaturated hydrocarbons. The unsaturated hydrocarbons are essentially acetylene and polycyclic aromatic hydrocarbons. These mentioned components have exceptionally high levels of acidity and volatility. Measurements have shown that it usually contains 90% carbon, 4% oxygen, 3% hydrogen, and the remainder combination of nitrogen, sulfur, and traces of metal. soot particles from diesel combustion, both Individual or primary, have been measured to be approximately 40 nm. The particles can agglomerate up to a maximum of approximately 500 nm, with an average soot agglomerate size of 200 nm, because of its colloidal properties. Figure 2.14 shows the TEM micrograph of soot from diesel engine.

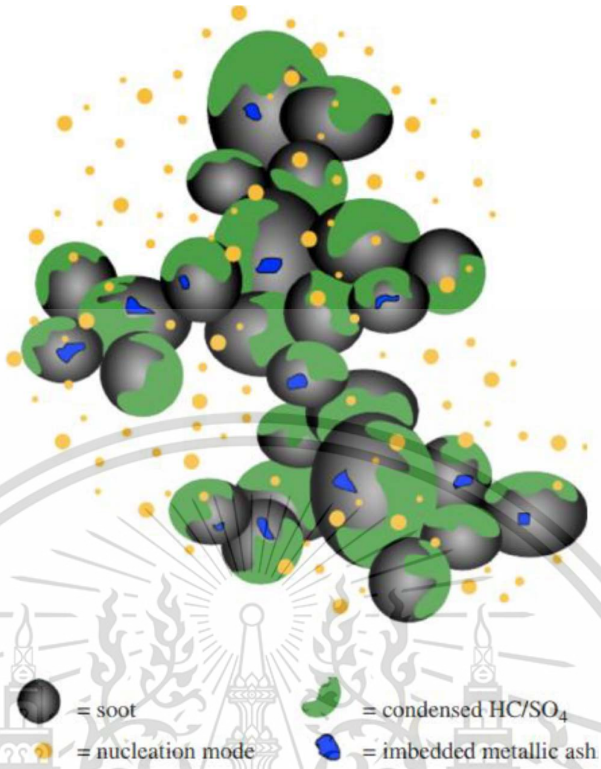

Figure 2.13 Artist's conception of diesel particulate matter [14]

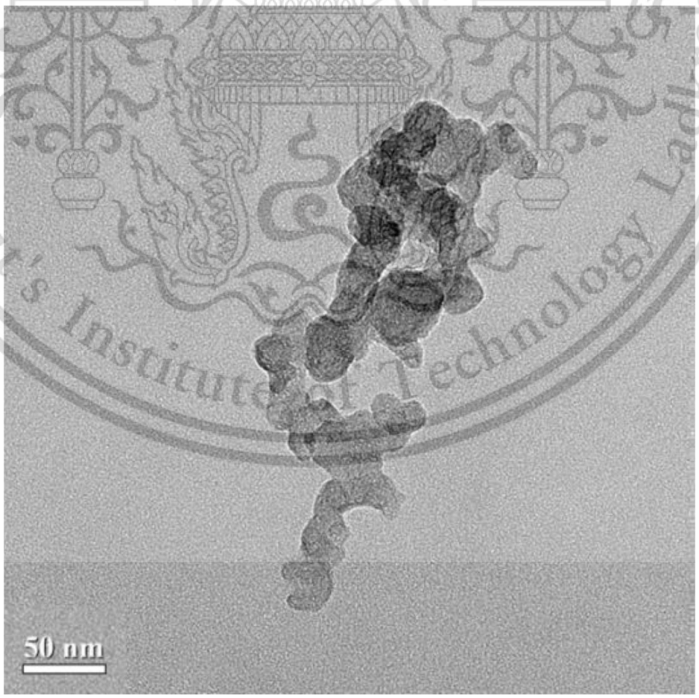

Figure 2.14 TEM micrograph of diesel engine soot [15]

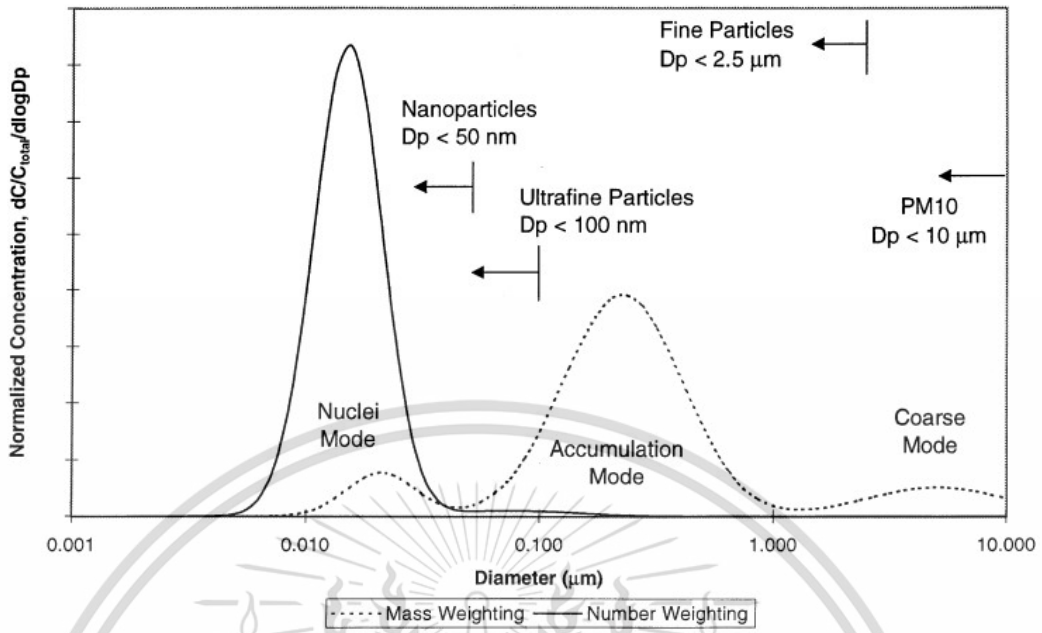

Figure 2.15 Idealized diesel exhaust particle number and mass weighted size distribution [16].

Figure 2.15 shows the ideal number and mass weighted size distributions of diesel exhaust particle, proposed by D. B. Kittelson [14]. The particle size distribution is a trimodal distribution: consisting of nucleation, accumulation and coarse mode. The nucleation mode contains particle from a few nanometers to 50 nm, while in agglomeration mode, there are larger particle in the range of 0.01 – 0.3 microns. The particle in coarse mode which involves both nucleation and accumulation mode are larger than 1 micron.

The impact of small Compression Ignition (CI) engine operation conditions on diesel and biodiesel particulate matters (PMs) was investigated by Siricholathum et al [17] They found that the smoke intensity of biodiesel engine's PMs was around a half of the smoke intensity of diesel engine's PMs. The physical characterization of those PMs was also investigated by using TEM. Figure 2.16 shows TEM micrographs of diesel and biodiesel engine's PMs under 80% engine load and 2,400 rpm of engine speed. The primary particle size was in the range of 10-60 nm and it was observable that a large amount of particle diameters was in the range of 30-40 nm. Figure 2.17 shows that the measured sizes of primary particle size distribution were between 10 and 60 nm. It was clearly seen that a large amount of particle diameters was between 30 and 40 nm.

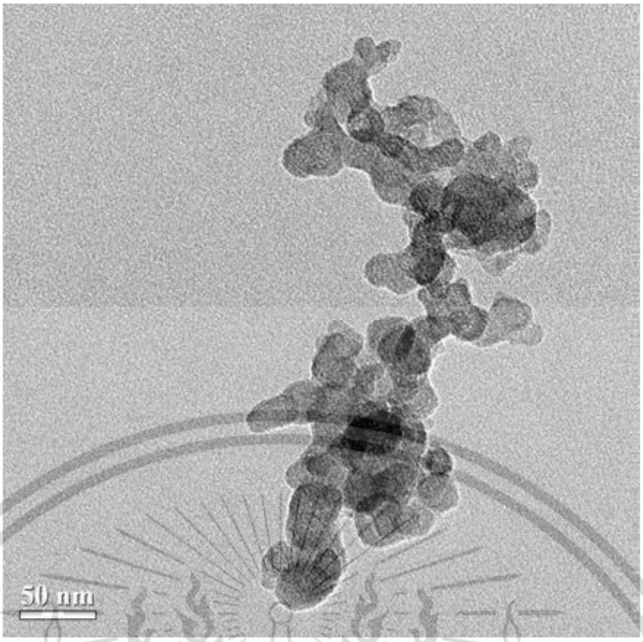

(a) Biodiesel Engine's Ultrafine Particle

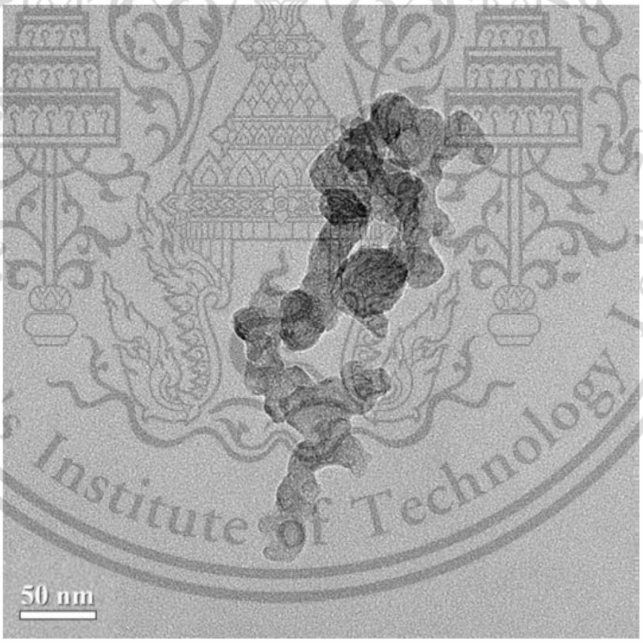

(b) Diesel Engine's Ultrafine Particle

Figure 2.16 TEM images of (a) biodiesel engine's and (b) diesel engine's ultrafine particles in the operation condition 80% of engine load and 2400 rpm of engine speed [15].

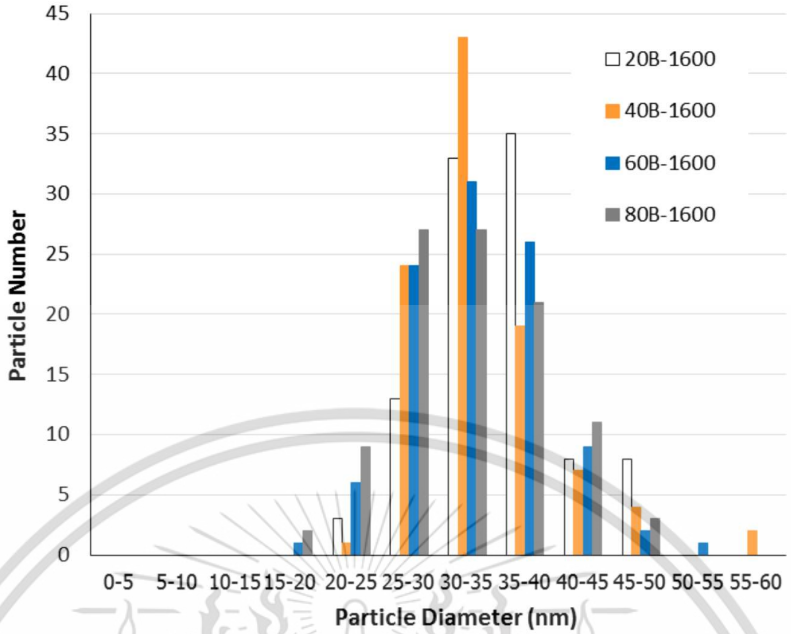

(a) Biodiesel Engine

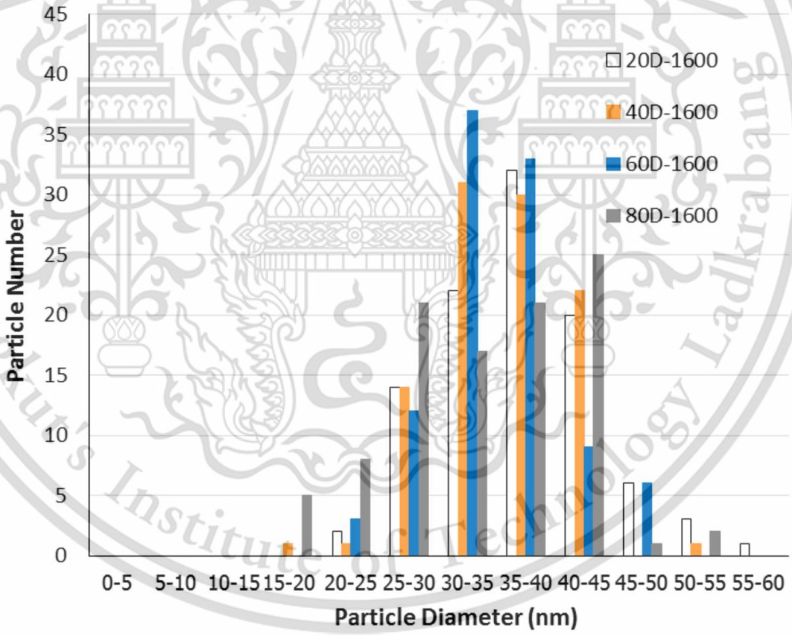

(b) Diesel Engine

Figure 2.17 Size distributions of (a) biodiesel engine's and (b) diesel engine's nanoparticle emission using TEM image processing method. The engine operation condition is 20, 40, 60 and 80% of engine load and 1600 rpm of engine speed [15].

2.7.2 Impact of Soot on metal wear [18]

In case of investigating lubricant from passenger car and truck, it has been showed that soot was contaminating in range of 0 - 1.0% by weight in diesel engine used oil. The results also induced to show that soot may be the cause of increasing metal wear from engine parts. Carbon black can be used to represent soot because of their similar morphology. However, they still have small difference: their particle diameter size. The experiment results showed the soot particle size distribution in different type of liquid: they were highly agglomerated in water, had smaller level of agglomeration in palm oil, and were well dispersed in formulated engine oil.

According to the result of four-ball tribology test, soot in lubricating oil might act as a rolling element and resulted in reducing friction between metal surfaces. Another conclusion was that soot may react with lubricating oil by both physical and chemical reaction and resulted in increasing oil film thickness between contact surfaces. The most significant result was that the dominant cause of making engine wear was the appropriate particle size between 20 nm and 300 nm, which was near oil film thickness between metal surface contacts. High level of proper particle size (20 nm – 100 nm) contaminated in oil will increase probability of rubbing process. Furthermore, soot dispersing oil additives might have a most significant effect on engine wear. Table 2.1 shows wear scar diameter when engine oil is contaminated by carbon black. Figure 2.18 show carbon black and wear particles size distribution before and after Four-ball wear tester.

Table 2.1 Wear scar diameter, roughness and friction torque **[18].**

Wear conditions		Lubricating oil	Lubricating oil with CB
Wear scar diameter	microns	493	537
Roughness	microns	0.07	0.19
Track density	line per mm	237	261
Friction torque	N-mm	2.01	1.62

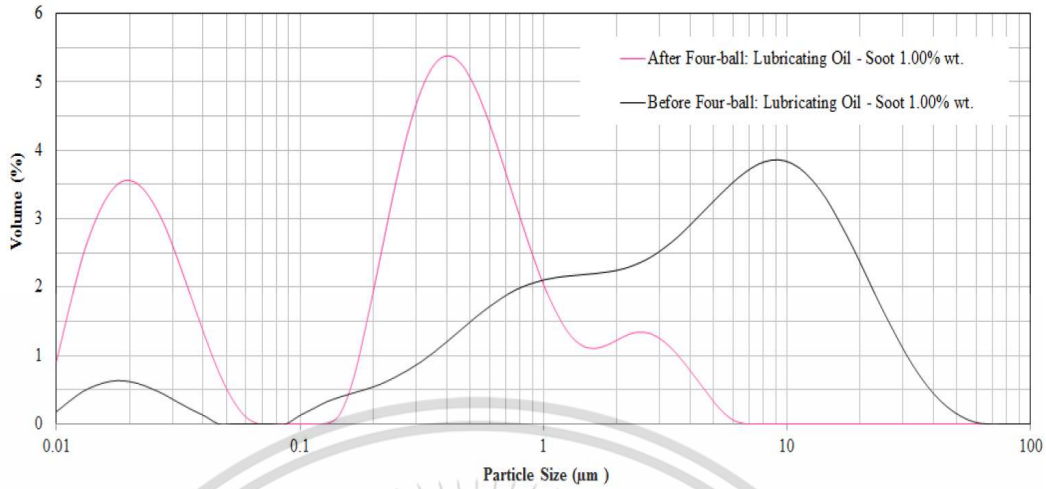

(a) Particle size distribution

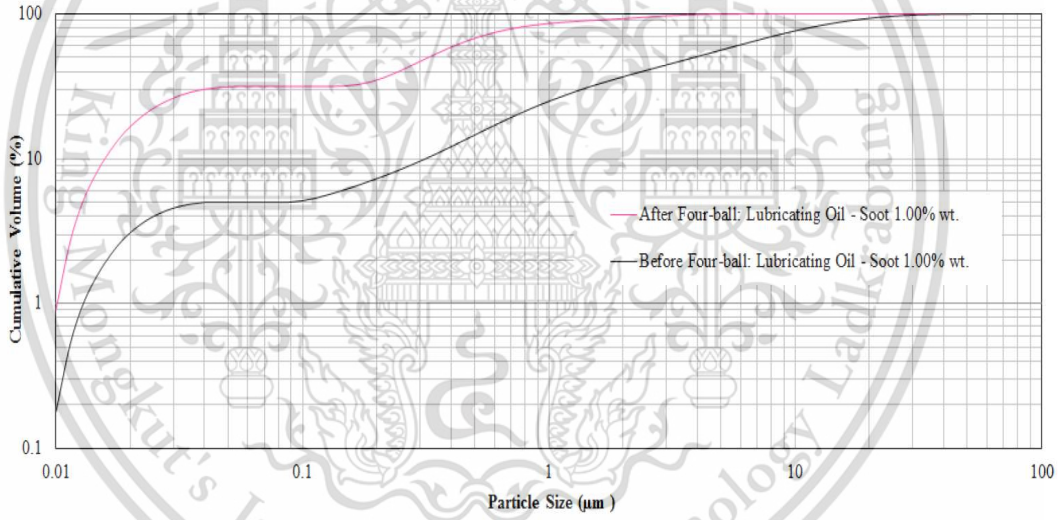

(b) Particle cumulative volume

Figure 2.18 Carbon black and wear particles (a) size distribution and (b) cumulative volume in lubricating oil before and after Four-ball tribology test by Laser Particle Diffraction Spectroscopy [18].

2.7.3 Soot hardness calculation [19]

The TEM micrograph was used to calculate the carbon platelet number to investigate the number of carbon density. Each of platelet is consist of carbon atom from incomplete combustion product as shown in Figure 2.19. The TEM micrographs of 100 nm^2 focused area was changed to be black and white images. Then it was skeletonized by image processing software. The line shows carbon crystallite each of which consist of carbon platelet. Each of platelet is a pair of graphene sheet.

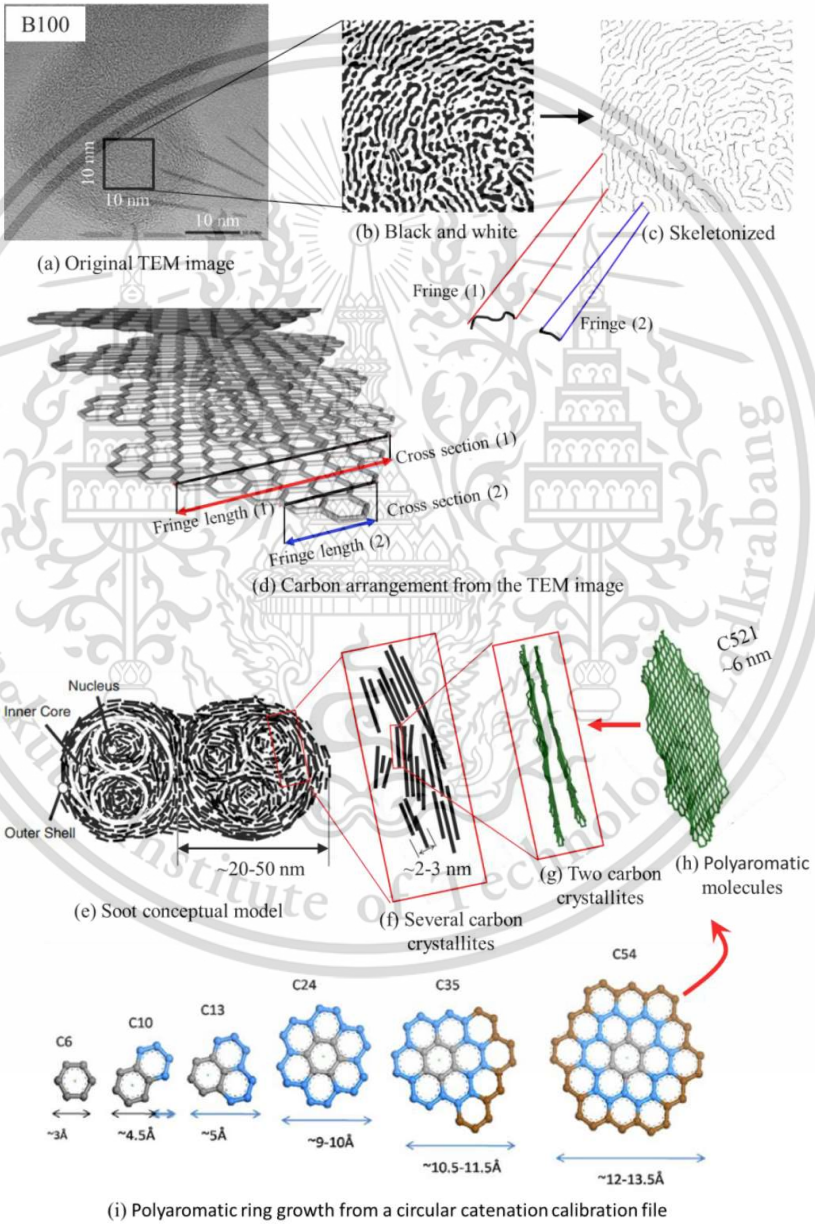

Figure 2.19 Soot primary particle conceptual model for calculation carbon atom density [19].

Table 2.2 shows the properties of various forms of carbon taken from reference [19]. Taking the literature values for the carbon atom density and hardness data of diamond and diamond-like carbon, which are glassy carbon, amorphous carbon and diamond; a plot which in Figure 2.20 is created. The black solid line is the most accurate plot from all four data points, with the R square of 0.95.

Table 2.2 The properties of various forms of carbon [19].

	Density (g/cm^3)	Hardness (kg/mm^2)
Glassy carbon	1.43	250
Evaporated amorphus carbon (a-C:evap)	1.95	0.50
Hydrogenated amorphus carbon (a-C:evap)	1.9	1,500
Daimond	3.52	10,000

Finally, the sot hardness is calculated by the relationship crated by Jao [20]. From the references, shows in Table 2.3, the density of Diesel soot reported by [20, 15] are in the range of 1.79 – 1.86 (g/cm^3) then their hardness are going to be in the range of 968.67 to 1,300 kg/mm^2. Additionally, the density of Biodiesel soot (B20) reported by [7] are in the range of 1.82 – 1.84 (g/cm^3) then their hardness are going to be in the range of 1,100 to 1,200 kg/mm^2. (From Devlin et al [7] they collected the soot of B20 from the difference engines).

Figure 2.20 shows the calculated atom density and mechanical hardness of carbon and the data from the references [20, 15]. The comparison between the hardness of any individual soot particle with the hardness of steel ball by using the correlation [8]. The hardness of steel ball followed by the standard Four-ball wear test is about 799-867 kg/mm^2. It is clearly showed that the hardness of soot is much higher than that of the steel ball.

Table 2.3 Carbon atom density and its hardness of soot primary particle from the references [19].

	Source#	Method to measure carbon density?	Carbon density (g/cm^3)	Hardness (kg/mm^2)
B100	calculated	Qualitatively analysis from the TEM images	1.82	1,334
CB N330			1.89	1,460
Diesel			2.0	2,056
Diesel –A	Li et al [2]	Measuring the plasmon energy of the individual soot by using low-loss electron energy-loss spectroscopy (EELS)	1.86	1,330
Diesel-B	Jao et al [1]		1.84	1,200
Diesel-C	Li et al [2]		1.79	968.67
B20-A	Devlin et al [3]		1.84	1,200
B20-B	Devlin et al [3]		1.82	1,100

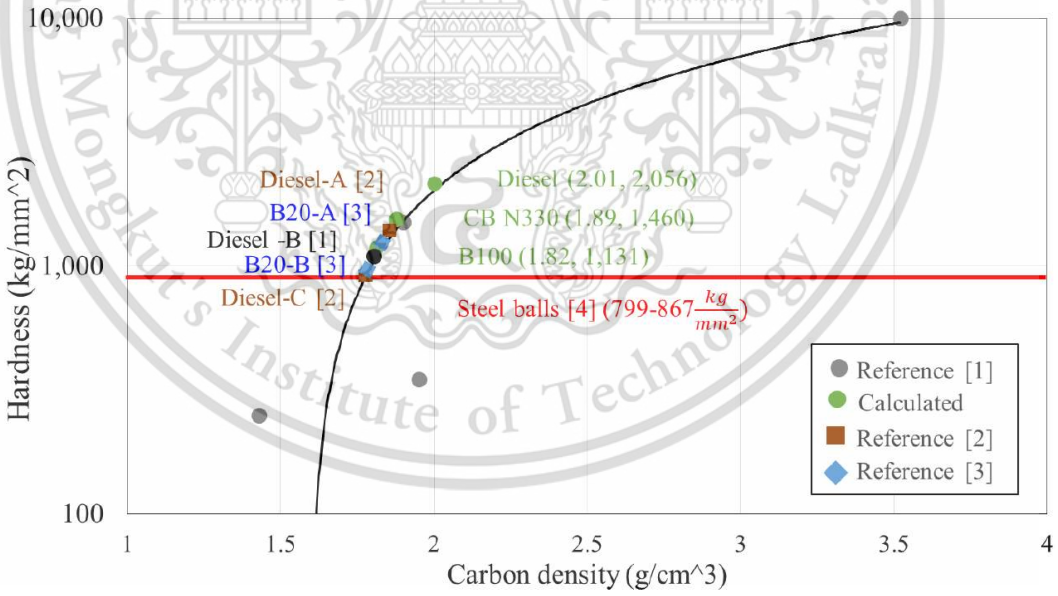

Figure 2.20 Plots of carbon density and its hardness [19].

2.7.4 Tribology Test [11]

Friction and wear experiments are designed to examine tribological characteristics of a tribo system and their variations under working conditions, in order to reveal the influence factors on friction and wear properties, and to reasonably determine design parameters. Because the aspects of friction and wear are complicated, there are many methods and devices needed for experiments, and the results data can be conditional and often difficult to compare. In recent years, researchers have paid more attention on making a standard for these test methods to make them uniform. Friction and wear performances are affected by many factors. Therefore, we can only get a reliable conclusion when the experimental conditions are strictly controlled. Current experimental methods can be divided into the following three categories.

Laboratory Specimen Test

A laboratory specimen test uses the universal testing machine to carry out the experiment with a specimen according to given working conditions. The advantage of the laboratory specimen test is that the environmental and working parameters can be easily controlled. This test can produce high amount of experimental data within a short experimental period. However, the results are often less practical because experimental conditions are not fully met with the actual working conditions. A laboratory specimen test is mainly used to study friction and wear mechanisms and their factors, and to evaluate performances of lubricant.

Simulation Test

After the laboratory specimen test, a simulation test can be further carried out with the real component designed according to selected parameters. The results of this test are more reliable because its test conditions are close to real working conditions. While it can also produce a series of experimental data within a short period and the factors of wear performance can also be studied individually through intensive and strictly controlled experimental conditions. The main purpose of the simulation test is to verify the reliability of the data and the rationality of the wear design of the part.

Actual Test

After the mentioned two tests, an actual test can finally be done, which is much more reliable. However, its experimental period is long and expensive. Its results are influenced by various factors, so it is difficult to analyze the results in-depth. This test is commonly used to test results from the first two experiments.

Figure 2.21 shows the contact and movement types of common friction and wear testing machines.

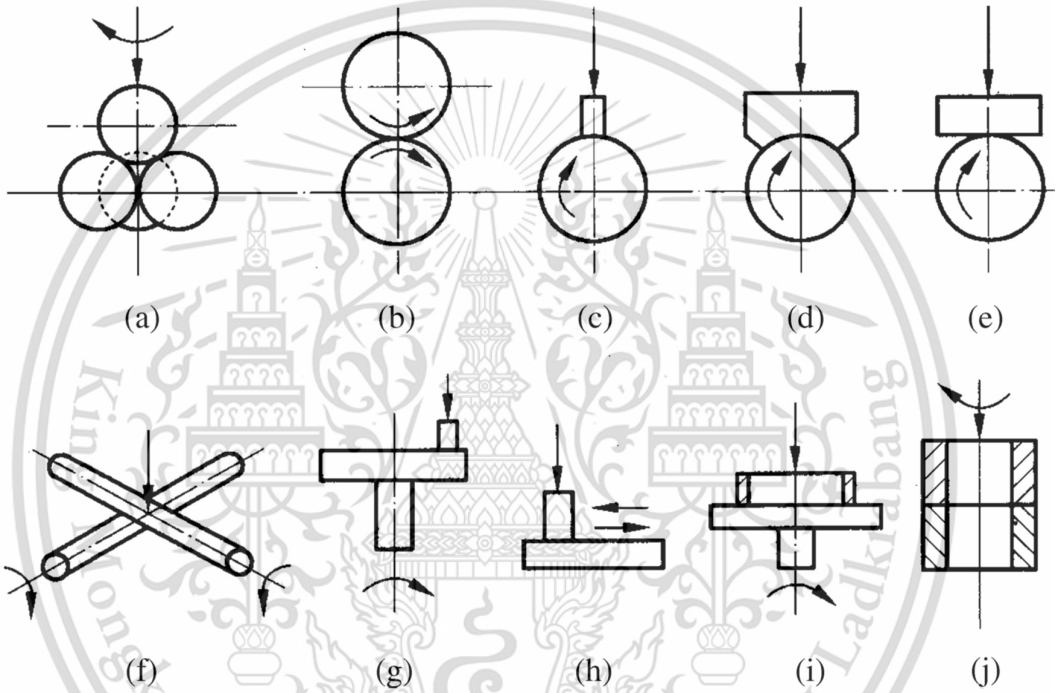

Figure 2.21 Types of contact and movement of friction and wear testers [11].

CHAPTER 3

RESEARCH METHODOLOGY

3.1 Experimental equipment

3.1.1 Engine oil related with API standard

This research used different standard of engine oil. They were normal engine oil that used for diesel engines in the market, based on API standard. Base oil was the same: Group III, but their additive amount in each one was different. In order to study on the effect of soot particles in additives, the amount of additive was measured by x-ray fluorescence (ASTM D6481). The engine oil condition including viscosity and total base number were measured according to ASTM standard test methods.

3.1.2 Carbon black

Figure 3.1 shows Carbon black N330 which was used instead of real engine soot in this research to reduce the impact of unburnt hydrocarbon. Its physical properties were close to soot from diesel engine and average primary particle size was around 31 nanometers, which was also similar with diesel engine soot particles. Carbon black N330 was mixed into engine oil at 1% by weight to simulate the effect of soot contamination in the engine oil. Figure 3.2 shows TEM micrograph of carbon black N330.

Figure 3.1 Carbon Black N330 [21].

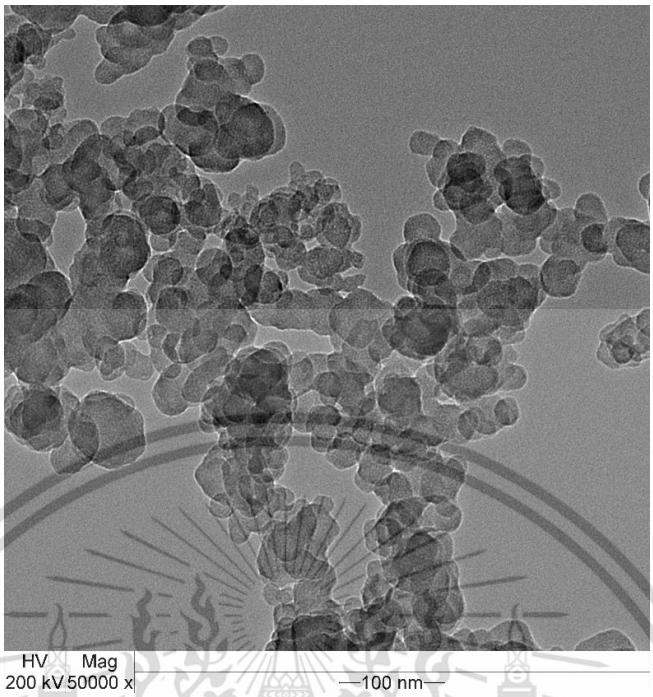

(a) 50,000 magnification

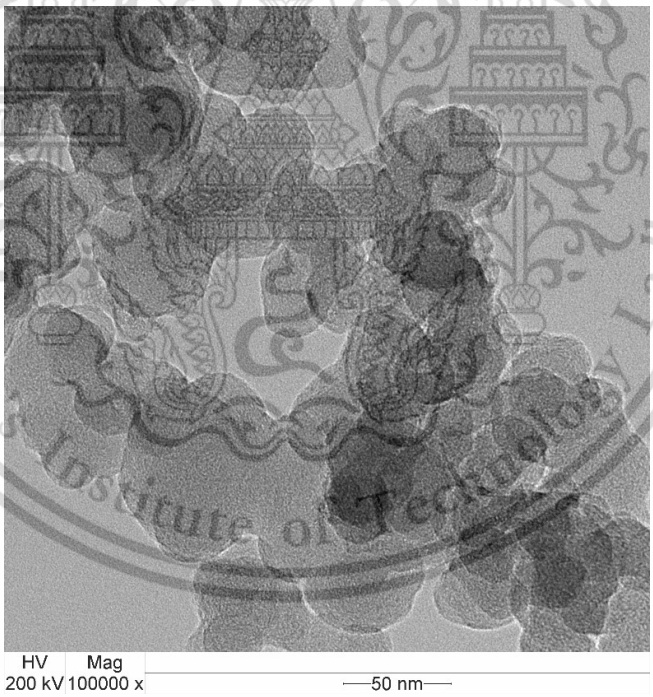

(b) 100,000 magnification

Figure 3.2 TEM Micrograph of carbon black N330 at (a) 50,000 and (b) 100,000 magnification.

3.1.3 Laser Diffraction Particle Size Analyzers

Figure 3.3 shows laser diffraction particle size analyzer which uses the technique of laser diffraction to measure the size of particles. It does this by measuring the intensity of light scattered as a laser beam passes through a dispersed particulate sample. This data is then analyzed to calculate the size of the particles that created the scattering pattern.

Figure 3.3 Laser particle size distribution analyzer (MALVERN, Mastersizer 3000)

3.1.4 Fourier-transform infrared spectrometer

Figure 3.4 shows fourier-transform infrared spectrometer which was used to investigate the engine oil additive structure. Fourier-transform infrared spectroscopy (FTIR) is a technique used to obtain an infrared spectrum of absorption or emission of engine oil additive. When IR radiation is passed through a sample, some radiation is absorbed by the sample and some passes through (is transmitted). The resulting signal at the detector is a spectrum representing a molecular 'fingerprint' of the sample. The usefulness of infrared spectroscopy arises because different chemical structures produce different spectral fingerprints.

Figure 3.4 Fourier Transform Infrared Spectrometer (Perkin Elmer, Spectrum One)

3.1.5 Four ball wear tester

Figure 3.5 shows the Four-ball wear tester which is a tribology bench test. that shows relation between properties to prevent wear of liquids and the sample´s sliding contact. The experiments are done according to ASTM D4172 standard (table 3.1). Equipment used in this experiment are: Four alloy balls with diameter of 12.7 mm (0.5 in.) Grade 25 EP (Extra Polish) 12.7 mm. Three of the balls are fixed at the base while the other one is on them, pressed by 392 newton force, and rotated with speed at 12000 RPM. All four balls are placed inside a container with the engine oil sample. The test is done at 75°C temperature. At the end, this test will cause horizontal circular wear scars to the three balls at the base and will cause vertical straight-line wear scars to the upper ball. The test conditions are shown in Table 3.1.

Figure 3.5 Schematic of Four-ball wear tester followed ASTM - D4172.

Table 3.1 The condition of Four Ball wear tester (ASTM D4172) [24].

Test conditions		**Ball material**	
Parameter	**Specification**	**Parameter**	**Specification**
Rotational speed	1200 rpm	Ball material grade	25 EP
Load	392 N	Surface roughness	0.005 microns
Duration per load	60 min	Ball hardness (Rock well)	64 – 66 (HRC)
Temperature	75°C		

3.1.6 Optical Microscope

Figure 3.6 shows optical microscope (OM) which is used to measure the wear scar diameter of three lower ball after wear testing. Average of wear scar diameters were used to compare the performance engine oil in each standard.

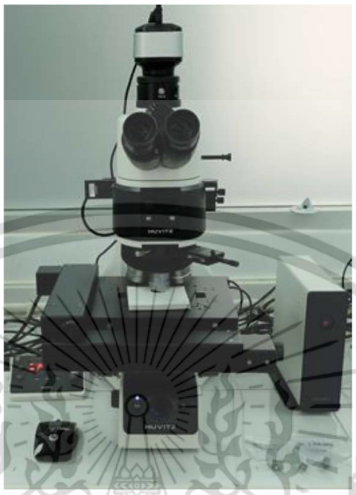

Figure 3.6 Optical Microscope

3.1.7 Confocal Microscope

Figure 3.7 show confocal microscopy which is a kind of microscopy that uses focal point technique to increase resolution and contrast of the image. It uses a spatial pinhole to block out unnecessary lights out of the focus. This imaging technique can create three-dimensional structure by using multiple two-dimensional ones captured at different depths. In this research, confocal microscopy will be used to measure surface roughness of the three balls at the base of four ball test. Each one will be measured five times, the average measurement will be used. The purpose of this process is to see more details of wear scar.

Figure 3.7 LEXT OLS4000 3D Laser Measuring Microscope

3.1.8 Scanning Electron Microscope

Figure 3.8 shows scanning electron microscope and energy dispersive X-ray spectrometer (SEM-EDX) which are used to investigate the worn surface. SEM is used to observe the worn surface in micro scale. EDX is used to investigate elements which remained on ball surface after wear test.

Figure 3.8 SEM-EDX JEOL JSM-IT-500HR

3.2 Experimental procedure

3.2.1 The study of engine oil property

A formulated engine oil which had the same base oil as SAE15W40 was used in this research. The engine oil condition including viscosity and total base number were measured according to ASTM standard test methods. Oil additives were measured by x-ray fluorescence. The standard for testing the new engine oil are following:

- Kinematic viscosity @ 40ºC (ASTM D-445)
- Kinematic viscosity @ 100ºC (ASTM D-445)
- Viscosity Index (ASTM D2270)
- Total base number (ASTM D-4739)
- Element analysis (ASTM D6481)

3.2.2 The impact of oil additive with soot on metal wear

The wear preventative properties of the engine oil and engine oil with soot contamination was investigated using Four ball wear tester. The test methods and conditions followed the standard ASTM D4172 as showed in Table 3.1. The major conditions for this wear test was to investigate the impact of oil additive on metal wear. The engine oil with different types and treat rate of additive were mixed with carbon black (N330) at 1% by weight per volume. The details of oil samples and Carbon black were shown in Table 3.2.

Table 3.2 Engine oils contaminated with carbon black N330

Samples	Carbon Black	Types and volume of additive	%CB (wt./wt.)
CD	-	BCP 3047 4.85%	-
CD	N330	BCP 3047 4.85%	1%
CF	-	BCP 3047 6.80%	-
CF	N330	BCP 3047 6.80%	1%
CF-4	-	BCP 3047 7.50%	-
CF-4	N330	BCP 3047 7.50%	1%
CH-4	-	BCP 1059 12.70%	-
CH-4	N330	BCP 1059 12.70%	1%
CI-4	-	BCP 1059 14.00%	-
CI-4	N330	BCP 1059 14.00%	1%

After the four ball wear tests, the balls and the tested oil were collected for the surface analysis

1) Wear scar diameter measurement by Optical microscopy.

The ball wear scar diameter of the three lower ball and one upper ball were measured using OM. After that, the average wear scar diameter of the three lower balls is used to compare the effect of contaminant on metal wear

2) Surface roughness by Confocal Microscopy

This imaging technique can create three-dimensional structure by using multiple two-dimensional ones captured at different depths. In this research, confocal microscopy will be used to measure surface roughness of the three balls at the base of four ball test. Each one will be measured five times, one after another at about 80 μm and the average measurement will be used. The purpose of this process is to see more details of wear scar.

3) Microscopic surface analysis by using SEM-EDX

The microscopic worn surface of the four balls of each oil samples were investigated using SEM. SEM is a powerful tool for studying worn surface and wear elements analysis. SEM micrograph at 500 magnification used to analyze the wear scar which were covered by 24 x 18 tables, the size of each block was 10.66 microns.

CHAPTER 4

RESULTS AND DISCUSSIONS

4.1 Engine oil properties

Different kinds of engine oil used in this research. They are common oil, based on the API standard, used for diesel engines in the market. The additive amount in each one was different, but their base oil was the same: Group III. They also had the same viscosity at 15W40. In order to studied on the effect of soot particles in additives, they were tested according to ASTM standard and the amount of additive was measured by x-ray fluorescence. Then engine oil is divided into 2 groups according to their amount of additive: Low grade with lower additives from 4.8% to 7.5% and high grade from 12.7% to 14%.

Table 4.1 Engine oil properties

		BCP 3047			BCP 1059	
	Base Oil	Group lll 15-W40				
	API Standard	**CD**	**CF**	**CF-4**	**CH-4**	**CI-4**
	Additive package	4.85%	6.80%	7.50%	12.70%	14%
Magnesium (Mg)	%wt	0.11	0.17	0.16	-	-
Calcium (Ca)	%wt	-	-	-	0.32	0.32
Sulfur (S)	%wt	0.41	0.50	0.43	0.52	0.51
Zinc (Zn)	%wt	0.09	0.13	0.13	0.13	0.14
Phosphorus (P)	%wt	0.08	0.11	0.11	0.12	0.12
TBN	mgKOH/g	6.90	10.1	10.2	9.6	10.4
Viscosity @40°C	cSt	113	120	110	114	113
Viscosity @100°C	cSt	15.0	15.5	15.2	15.3	15.3
Vicosity Index	-	138	136	144	140	140

4.1.1 Fourier-transform infrared spectroscopy

Infrared spectroscopy is a widely used technique for the analysis of lubricating oil. Taking advantage of FTIR spectroscopy in the process of identifying the molecular structure of a compound. Therefore, Fourier-transform infrared spectroscopy is chosen for investigate the chemical structure of engine oil additive. Figure 4.1 shows four different spectrum engine oils. The plot showed the spectrum of C-H stretching(2900 cm^{-1}), C-H scissoring(1470 cm^{-1}) and methyl rock(1380 cm^{-1}). It clearly seen that these four types of FT-IR spectrum were similar. Therefore, the soot dispersant additives structure in these four types were the equivalent, only differed in quantity.

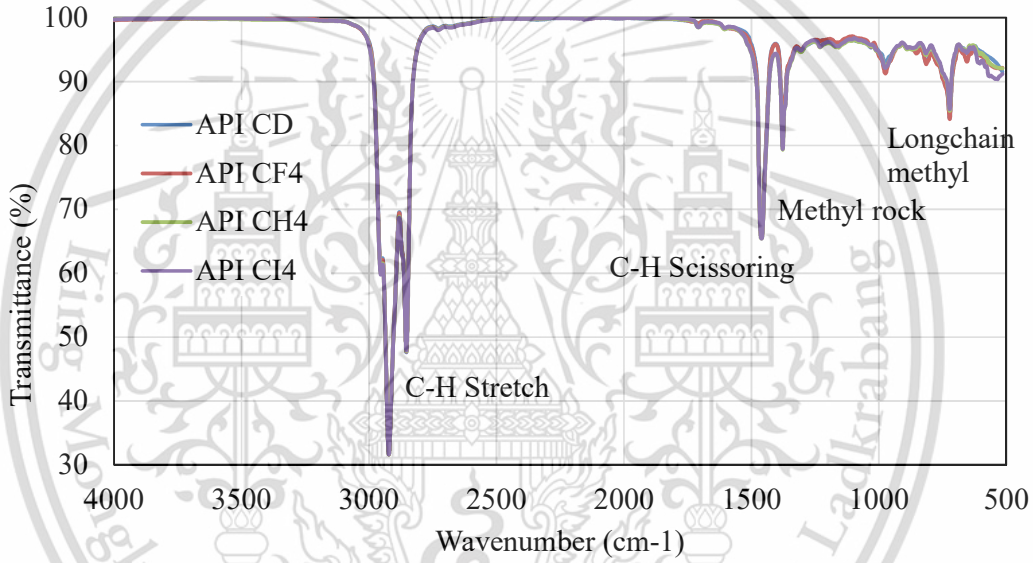

Figure 4.1 Fourier Transform Infrared Spectroscopy

4.1.2 Laser particle size distribution

Figure 4.2 shows size distribution of carbon black N330 which contaminated in formulated engine oil at 1% by weight, using laser particle size distribution analyzer. This graph focuses only soot between 0.01-1 um, because they are the size that can enter into contact area and cause wear on contact surfaces, while soot particles that are larger than 1um are too large to enter into the contact area. The result showed that carbon black N330 can disperse well in API CF4 and CD engine oil, because there was noticeably many of 20-30 nanometer particles that dispersed in the mentioned engine oil. Followed by CI4 and CH4 engine oil respectively.

The dispersing of different sizes of particles in engine oil can specify the performance of soot dispersant additive in each type of engine oil. Also, the difference in sizes of particles impacted directly to metal wear, because its roughness value varied according to the particle size distribution.

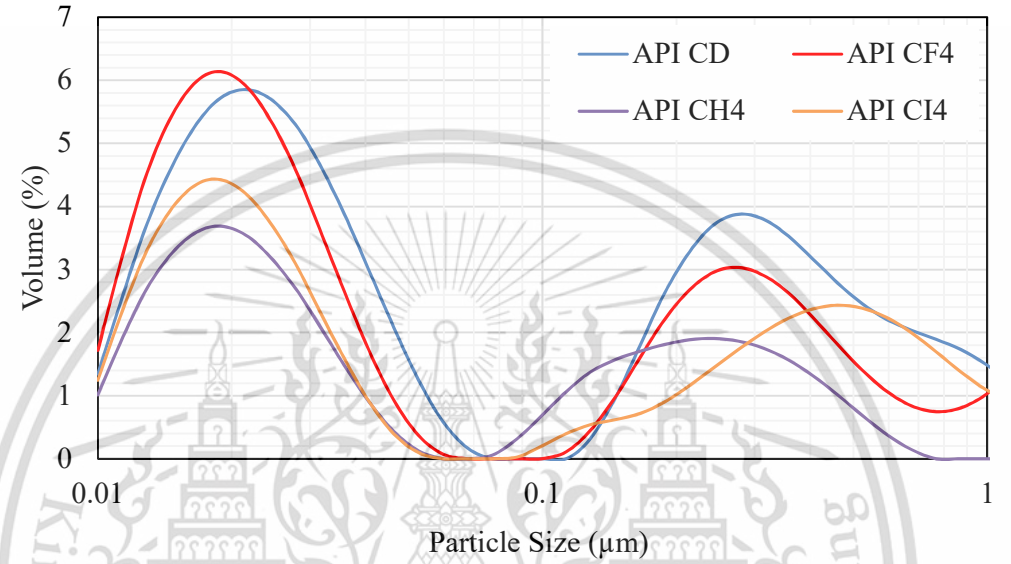

(a) Particle size distribution

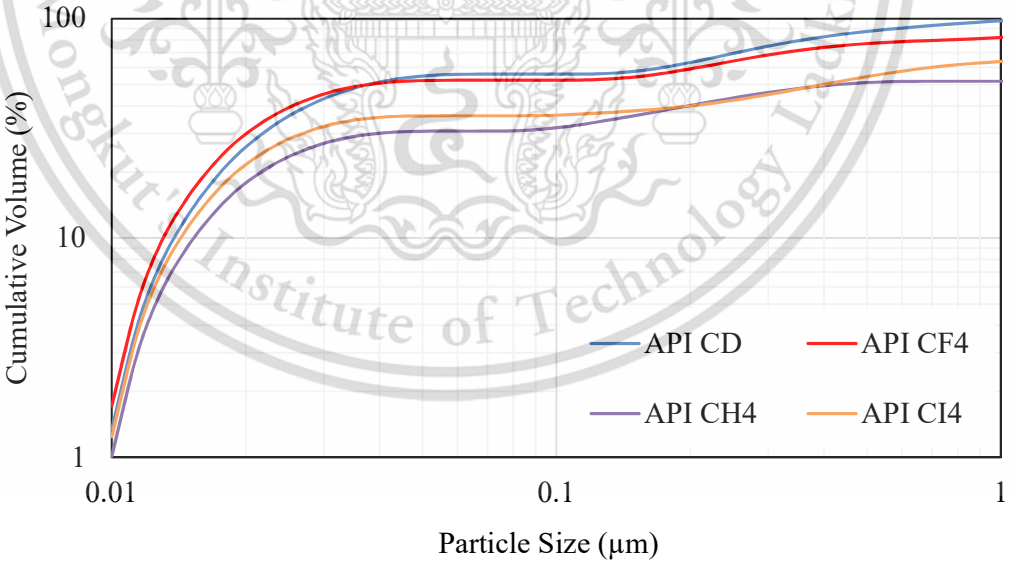

(b) Particle cumulative volume

Figure 4.2 Carbon black N330 (a) size distribution and (b) cumulative volume in engine oil by Laser Particle Diffraction Spectroscopy.

4.2 Impact of anti-ware additive

Figure 4.3 shows average ware scar diameter of new oil from Four-ball wear tester. From the test results, the wear in the group of low-grade engine oil are clearly larger. The main reason of this, is their lower amount of anti-ware additive, that prevent the additive from generating enough oil film layer to protect the surface. Results in more wears than in high grade engine oil.

.

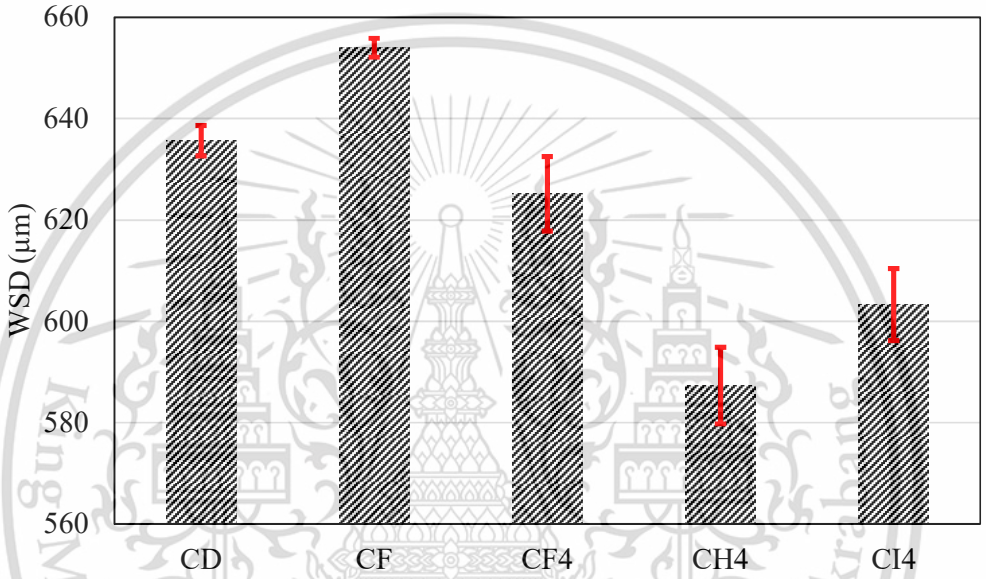

Figure 4.3 The average wear scar diameter measured by OM (µm)

4.3 Impact of soot on metal wear

4.3.1 Wear scar diameter

Four-ball wear tester was used to investigate the effect of soot and oil additive on metallic wear and carbon black N330 was used to simulate engine's soot. Engine oil were contaminated with carbon black N330 1% by weight. After wear test, three lower balls were used to measure the wear scar diameter (WSD) using a high-resolution optical microscope (OM) as showed in Figure 4.4 and 4.5. The results showed that API CD engine oil that was contaminated with carbon black, the largest increase rate of wear scar was found at approximately 7.7%. On API CF the increase rate of wear scar was 3.5% and API CF-4, API CH-4 and API CI-4 the wear scar was not significantly different. Therefore, it was noticeable that wear scar diameters

increase significantly in 2 types of engine oil because of their carbon black contaminating. The average of wear scar diameter of four ball indicate that carbon black particle can enter to the contact area and then cause wear. When soot particles cause too much damage on oil film layer, additives in engine oil will build a new layer to protect the surfaces again. So, when different types of engine oil are contaminated with soot, there are clearly higher wear increase rate in low-grade engine oil as it has less amount of anti-ware additive.

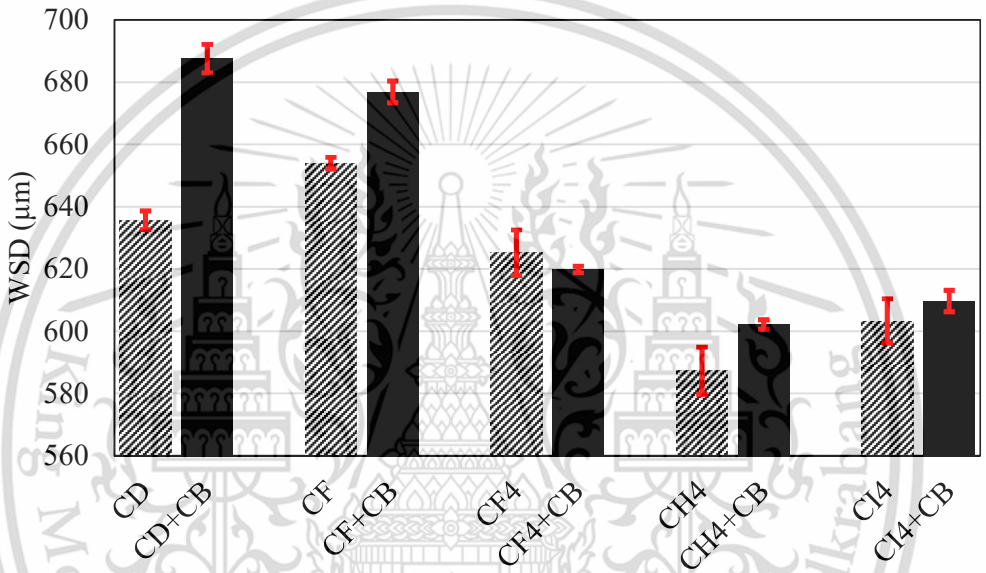

Figure 4.4 The average wear scar diameter of carbon black contaminated engine oil measured by OM (µm)

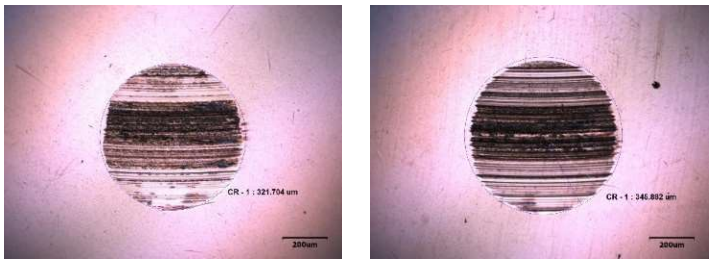

(a) API CD (b) API CD with CB N330

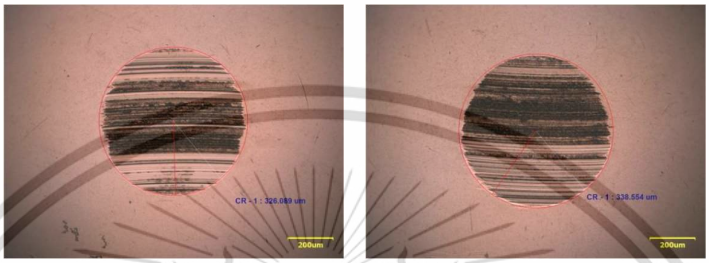

(c) API CF (d) API CF with CB N330

(e) API CF-4 (f) API CF-4 with CB N330

(g) API CH-4 (h) API CH-4 with CB N330

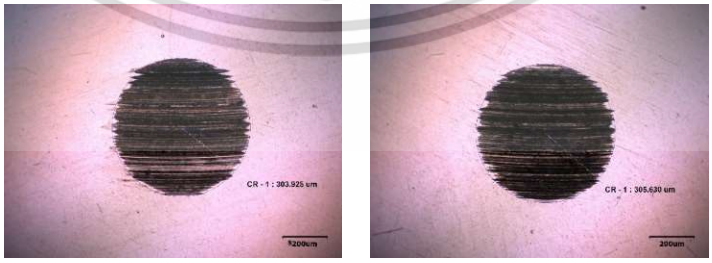

(i) API CI-4 (j) API CI-4 with CB N330

Figure 4.5 Wear scar diameter measured by OM.

4.3.2 Surface roughness

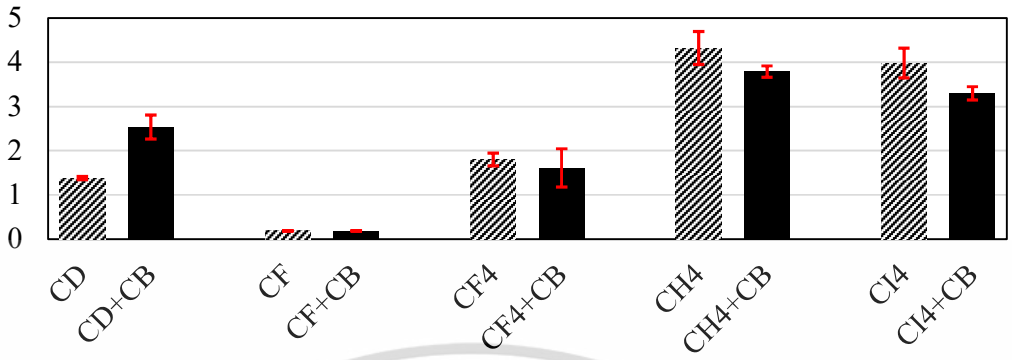

Figure 4.6 Ra value from confocal microscope at low magnification 20x (μm)

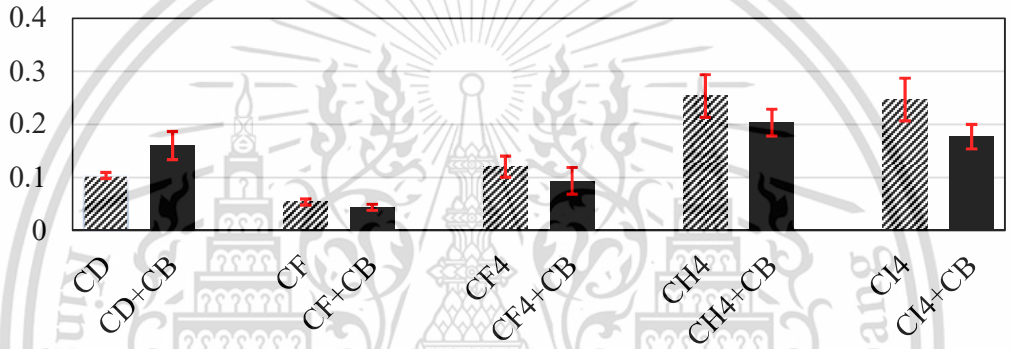

Figure 4.7 Ra value from OM at high magnification 100x (μm)

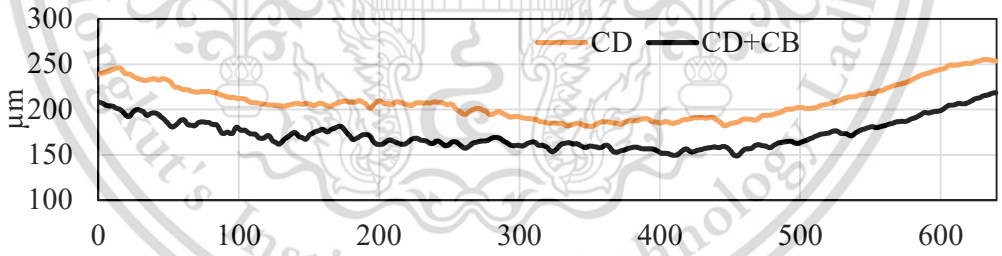

(a) Wear profile of low-grade engine oil

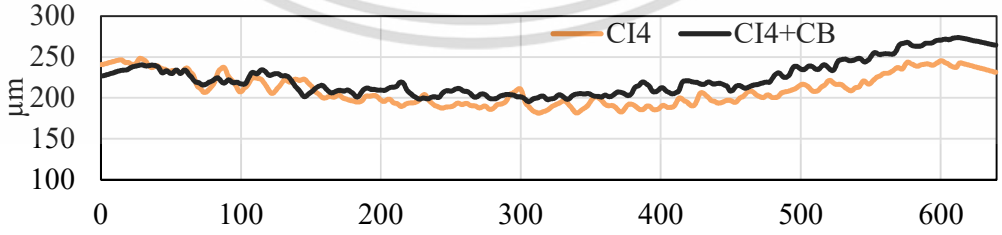

(b) Wear profile of high-grade engine oil

Figure 4.8 Example of wear profile between (a) low-grade and (b) high grade engine oil.

Figure 4.9 show the worn surface after four-ball wear test, Figure 4.6 and 4.7 show surface roughness value of the metal ball. Figure 4.6 shows surface roughness value of the metal ball at low magnification, to study overall-surface metallic wear behavior. Figure 4.7 shows its roughness value at high magnification from optical microscope

The results show that, from both type of Ra value, the results show in the same direction which the roughness value of metal ball will decrease when engine oil is contaminated with carbon black N330. This is because carbon black particles entered and cause 3 body abrasive wear on the surface. Also, small size particles entered into the contact area and polish the ball surfaces, leaving lower roughness value.

However, there is an exception in the case of API CD engine oil that the roughness value increased. That is because its amount of additive is too low, that it could not prevent carbon black particles from further damaging the surfaces like other types of engine oil.

Figure 4.8 show the profiles of wear on metal ball surface. Figure 4.8 (a) shows wear profile low-grade engine oil. When it is contaminated with CB, some part of the surface became rougher, the wear became deeper, and there were more grooves. These damages were not caused only by carbon black particle, but also by small metal particle that had been broken from ball surface as another damage from carbon black particles. This surface braking occurred because there were not enough anti-wear additives to protect all the surfaces. On the other hand, when high-grade engine oil is contaminated with carbon black, the ball surfaces became smoother, because of the strong oil film layers of anti-ware additive as shown in Figure 4.8(b). These layers let carbon black get into the contact area and polish ball surfaces, leaving abrasive wears.

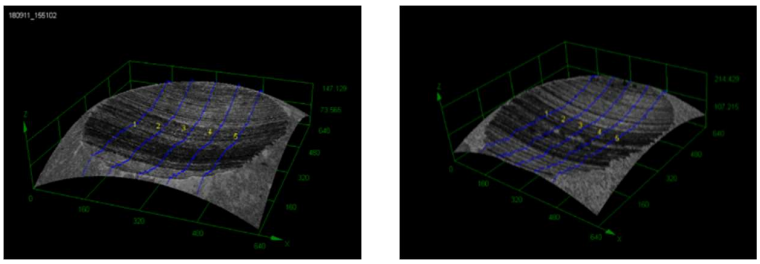

(a) API CD (b) API CD with CB N330

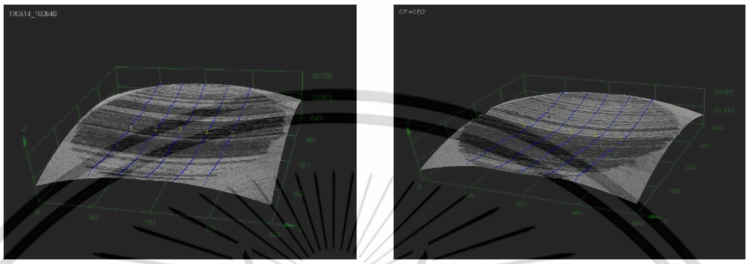

(c) API CF (d) API CF with CB N330

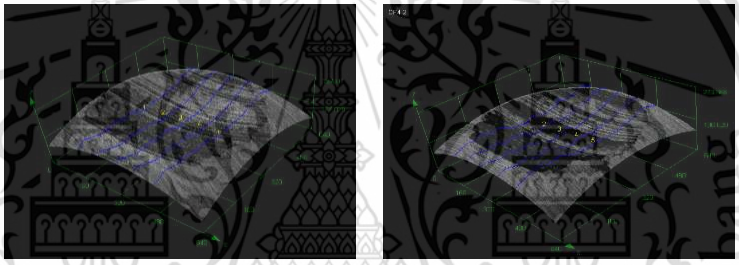

(e) API CF-4 (f) API CF-4 with CB N330

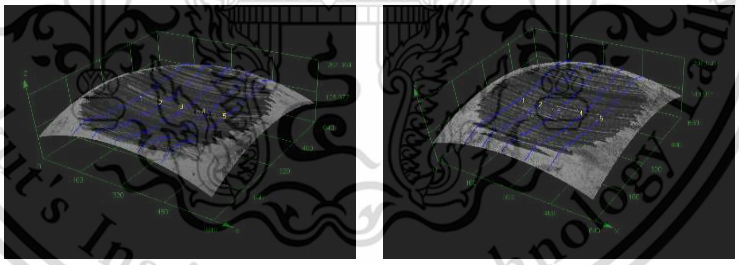

(g) API CH-4 (h) API CH-4 with CB N330

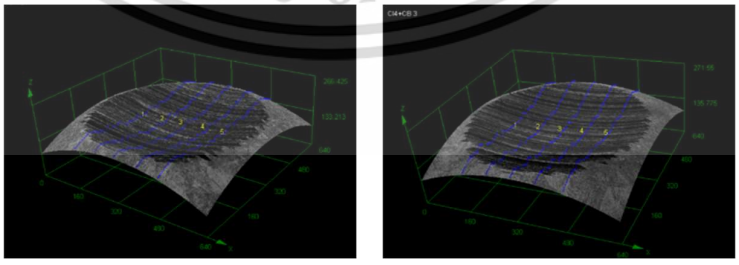

(i) API CI-4 (j) API CI-4 with CB N330

Figure 4.9 Roughness measurement by confocal microscope

4.3.3 Wear mechanism

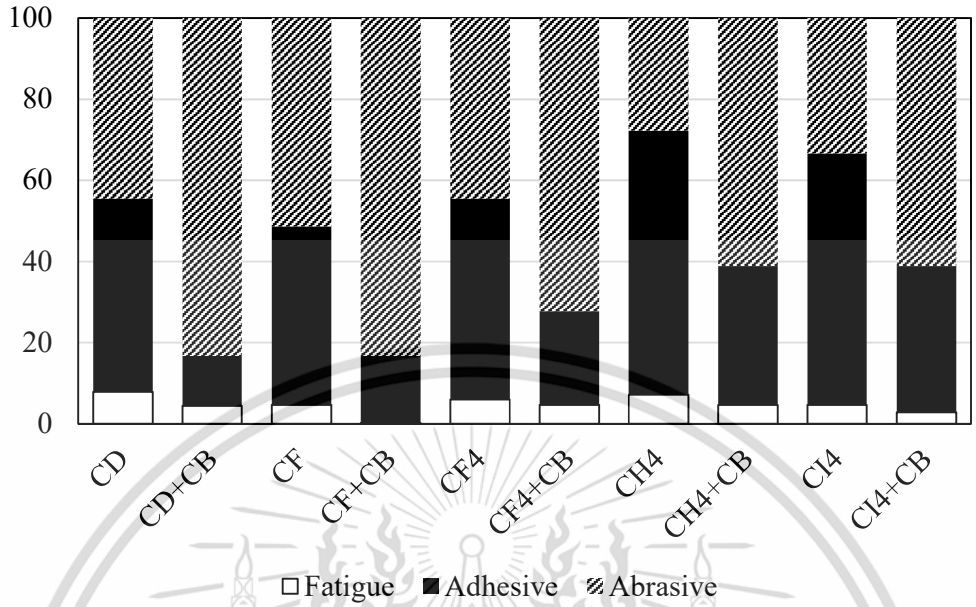

Figure 4.10 Average wear mechanism (%)

Table 4.2 Qualitatively analyze wear mechanisms when engine oil is contaminated with carbon black N330.

	CD	CF	CF4	CH4	CI4
Fatigue	-44.1%	-95.0%	-23.1%	-35.5%	-40.0%
Adhesive	-74.3%	-62.6%	-53.3%	-47.3%	-41.8%
Abrasive	+87.5%	+62.2%	+62.5%	+120.0%	+83.3%

Figure 4.11 shows SEM micrograph at 120 magnification of the wear scar found on the balls of engine oil API CD(a), API CF(c), API CF-4(e), API CH-4(g), API CI-4(i) without soot and contaminated engine oil API CD(b), API CF(d), API CF-4(f), API CH-4(h), API CI-4(j) with CB N330 1% wt. This figure shows the wear scar of stationary ball under the same test conditions according to ASTM D4172. Figure 4.12 and 4.13 show SEM micrograph at 500 magnification of the wear scar. The result shown that, there were some areas of plastic deformation on uncontaminated oil. It was mentioned in the research that the plastic deformation of the worn surface which was larger than 20 microns was reflected to adhesive wear

[3]. Moreover, some of subsurface cracks and pitting were found in the plastic deformation zone that was mentioned as fatigue wear. From the SEM micrograph of wear scar that contaminated with carbon black N330, the increasing of wear track parallel to the sliding direction is clearly seen, which suggests a mechanism of abrasive wear. From the above, when the engine oil was contaminated with carbon black, the mechanism of wear was three body abrasive wear because the hardness of the carbon black is higher than the steel ball [22]. Figure 4.14 show the quantitative analysis, SEM micrograph at 500 magnification of the wear scar were covered by 24 x 18 tables. The size of each block was 10.66 microns. The wear mechanisms characterize as follows: The fine wear track or grove along with the sliding direction which was defined by a gray color was reflected to abrasive wear [3]. The plastic deformation which was larger than 20 microns defined by a blue color was reflected to adhesive wear [3]. Moreover, the pitting and subsurface crack which was defined by a red color was reflected to fatigue wear.

Figure 4.10 and Table 4.2 shows qualitatively analyze wear mechanisms, the result show that the engine oil without carbon black has more adhesive wear than the engine oil with carbon black also when the carbon black was added the abrasive wear increase significantly. This indicates that the predominant wear mode of soot contaminated engine oil was three body abrasive wear because the hardness of the carbon black is higher than the steel ball. In case of new oil, adhesive wear occurred because of three factors: the boundary lubrication of the anti-ware additive, the shearing force of the steel balls´ sliding motion, and the direct contact between two metal surfaces.

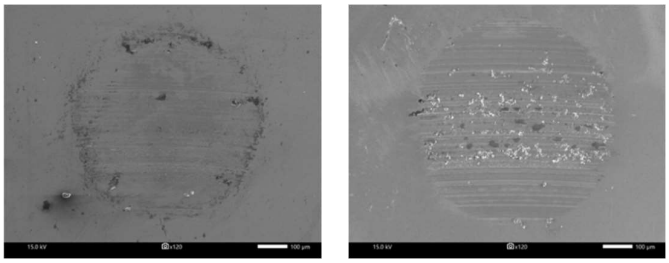

(a) API CD (b) API CD with CB N330

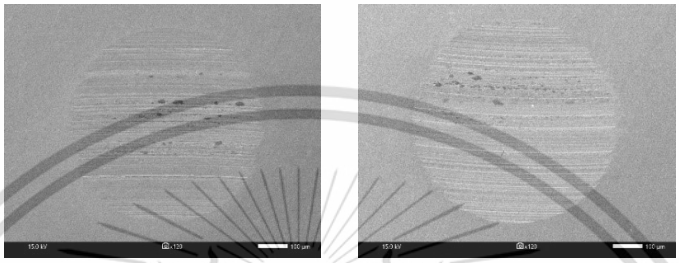

(c) API CF (d) API CF with CB N330

(e) API CF-4 (f) API CF-4 with CB N330

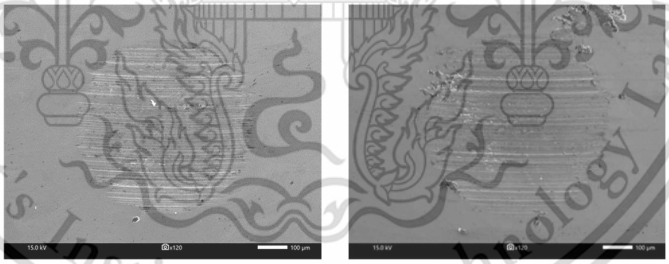

(g) API CH-4 (h) API CH-4 with CB N330

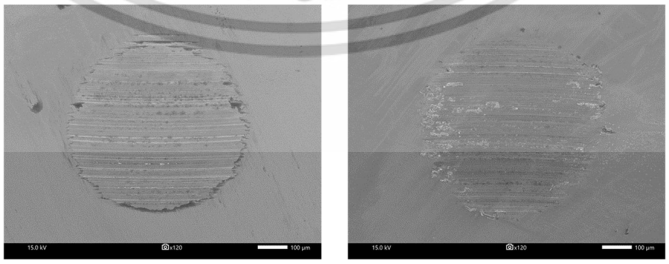

(i) API CI-4 (j) API CI-4 with CB N330

Figure 4.11 SEM Micrographs of wear scar at 120 magnification

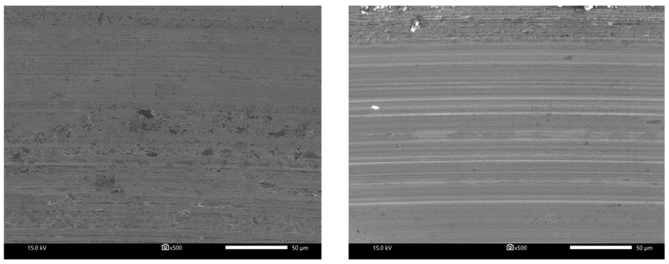

(a) API CD (b) API CD with CB N330

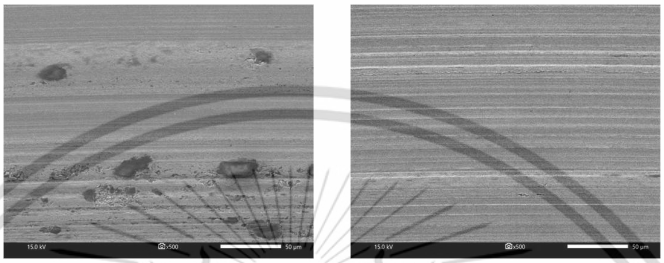

(c) API CF (d) API CF with CB N330

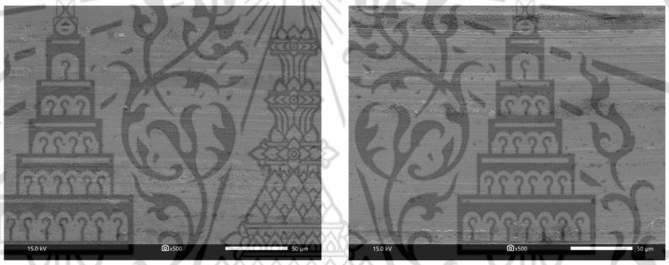

(e) API CF-4 (f) API CF-4 with CB N330

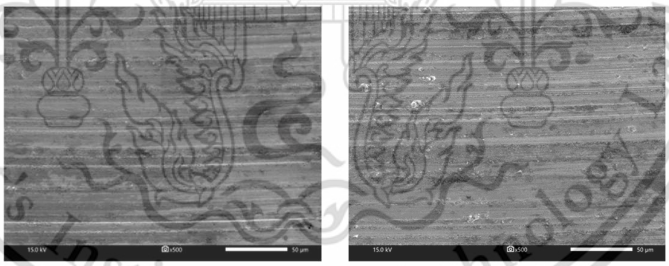

(g) API CH-4 (h) API CH-4 with CB N330

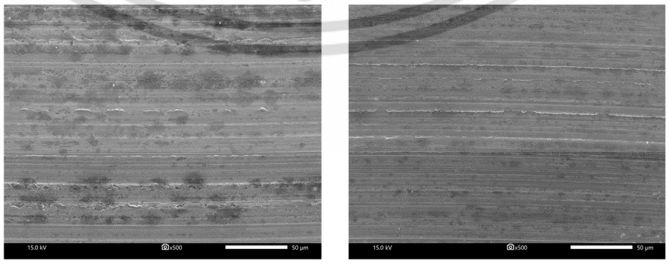

(i) API CI-4 (j) API CI-4 with CB N330

Figure 4.12 SEM micrograph of wear scar at 500 magnification

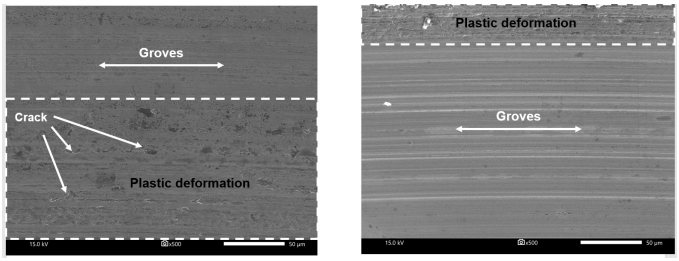

(a) API CD (b) API CD with CB N330

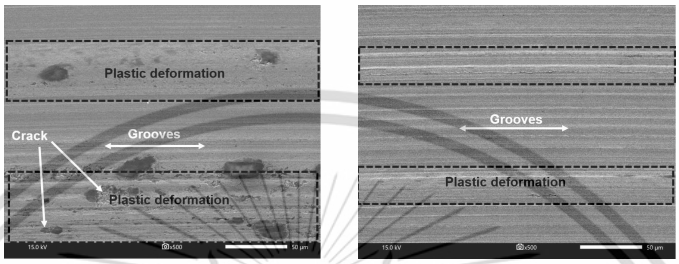

(c) API CF (d) API CF with CB N330

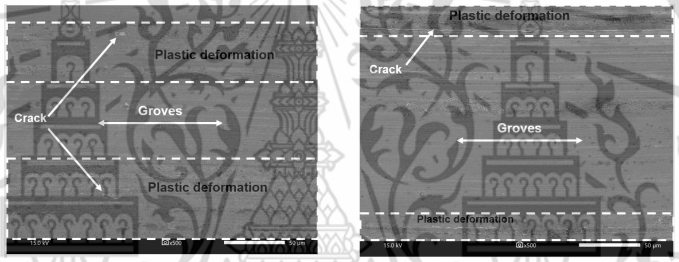

(e) API CF-4 (f) API CF-4 with CB N330

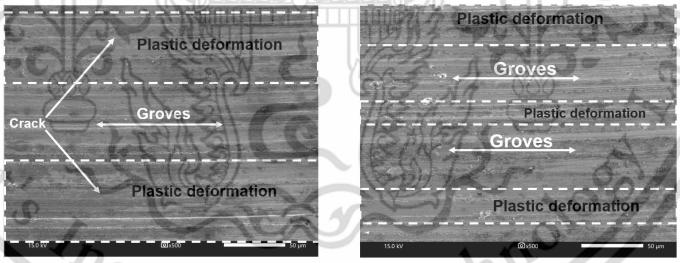

(g) API CH-4 (h) API CH-4 with CB N330

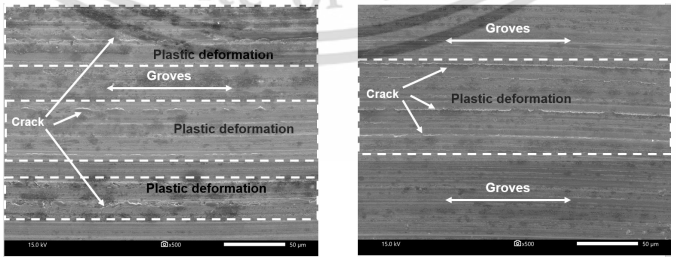

(i) API CI-4 (j) API CI-4 with CB N330

Figure 4.13 SEM micrograph of wear scar at 500 magnification with wear description

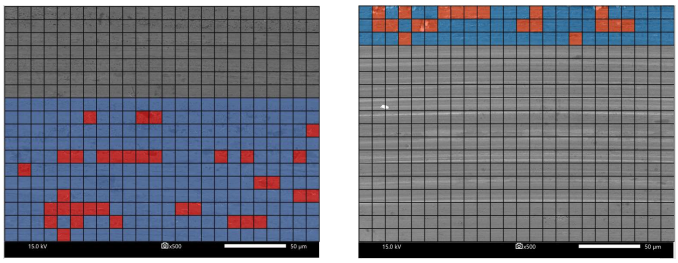

(a) API CD (b) API CD with CB N330

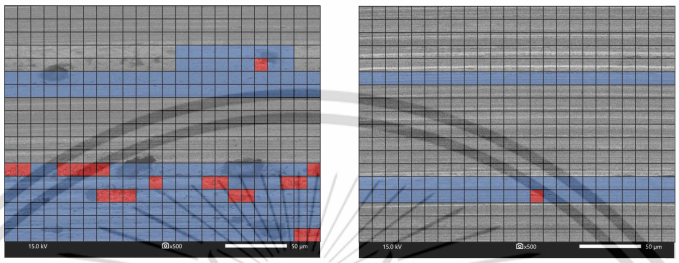

(c) API CF (d) API CF with CB N330

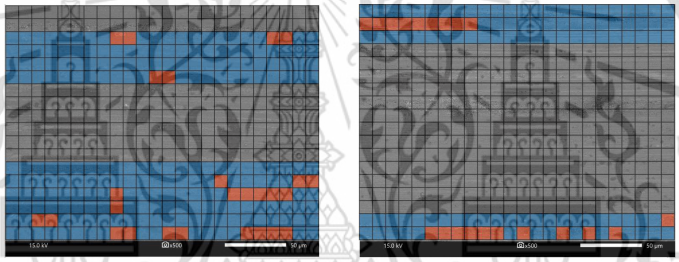

(e) API CF-4 (f) API CF-4 with CB N330

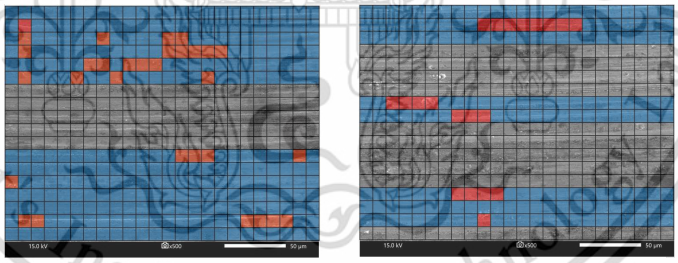

(g) API CH-4 (h) API CH-4 with CB N330

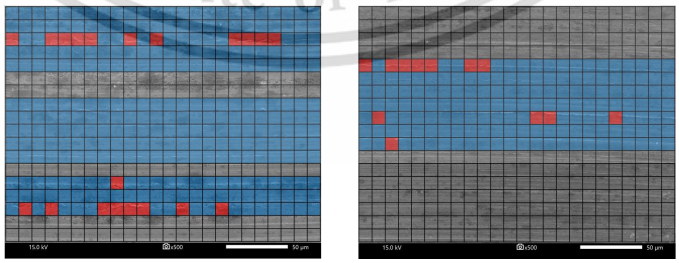

(i) API CI-4 (j) API CI-4 with CB N330

Figure 4.14 SEM micrographs of wear scar with colored wear analysis

4.3.4 Ball surface element analysis

The oil additive that remain on the ball surface were observed by EDX analysis. As mention before, the base of additive element in API CD, API CF and API CF-4 was magnesium and calcium in API CH-4 and API CI-4. Table 4.3 and 4.4 showed elemental analysis of ball surface of low-grade and high-grade engine oil respectively. Figure 4.15 and 4.16 showed percentage of element of ball surface and EDX spectrum respectively. The results showed that the additive element still remained on the ball surface. Therefore, it was proved that engine oil additive had spread all over the area, including between the contact surfaces, which means that it performed its role on soot particles on ball surfaces. The additive that contained in the engine oil improves the dispersing of contaminated carbon black. When the carbon black is dispersed, it will serve to polish the ball's surface. This behavior of additive would be a main impact on metal wear mechanism. From Table 4.4, the result showed that there wear Zn remaining on the surfaces in high-grade engine oil, while in low-grade engine oil, there were no remain of Zn on the surface. So, it can be concluded that, anti-wear additive that build oil film layers on metal surfaces has an important role on preventing metallic wear, both in the case of with and without carbon black contamination.

Table 4.3 Element analysis of ball surface (Low grade engine oil)

	Ball	CD	CD+CB	CF	CF+CB	CF4	CF4+CB
Fe	91.8	86.8	93.7	87.7	94.7	88.3	90.9
C	6.8	3.4	2.3	3.3	2.6	4.3	3.8
O	0.0	4.6	1.7	3.7	0.0	3.1	2.2
Mg	0.0	0.7	0.0	1.5	0.0	0.4	0.3
Si	0.0	0.0	0.3	0.3	0.3	0.3	0.3
S	0.0	2.0	0.5	1.0	0.4	1.2	0.7
Cr	1.4	1.3	1.5	1.4	1.6	1.6	1.5
Zn	0.0	1.2	0.0	0.0	0.0	0.0	0.0

Table 4.4 Element analysis of ball surface (High grade engine oil)

	Ball	CH4	CH4+CB	CI4	CI4+CB
Fe	91.8	80.9	76.7	87.3	85.4
C	6.8	6.7	7.6	4.8	4.2
O	0.0	5.6	6.9	3.2	4.1
Ca	0.0	0.8	0.7	0.4	0.6
Si	0.0	0.0	0.0	0.0	0.0
S	0.0	1.9	1.9	1.1	1.5
Cr	1.4	1.5	1.4	1.4	1.4
Zn	0.0	2.3	2.1	1.3	2.3

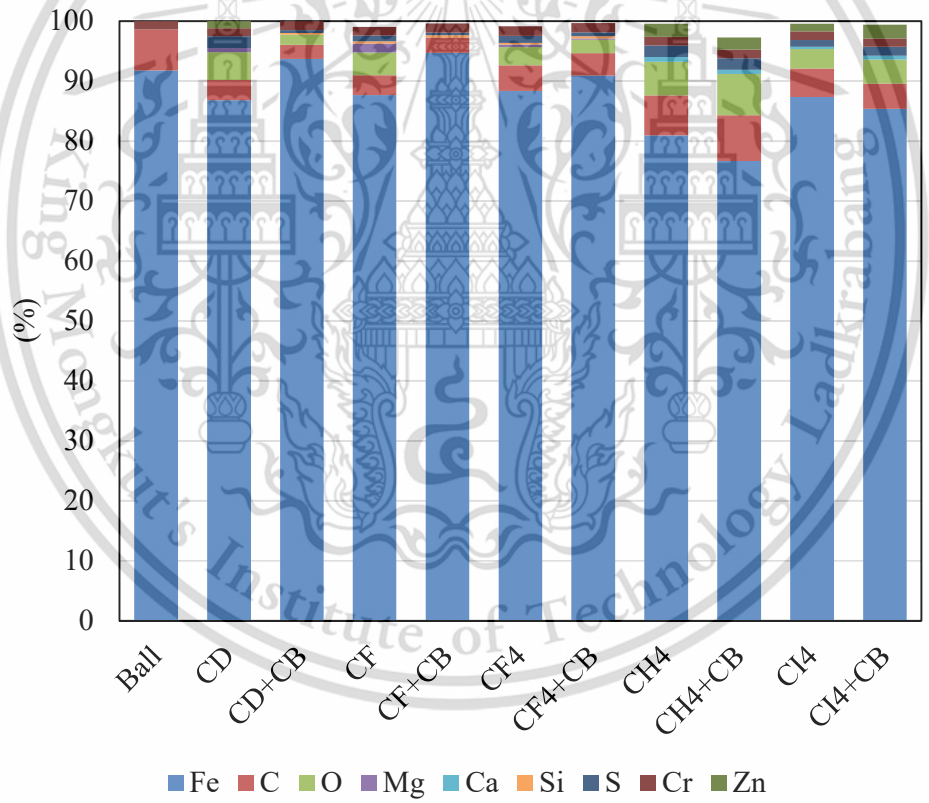

Figure 4.15 Elemental analysis of ball surface.

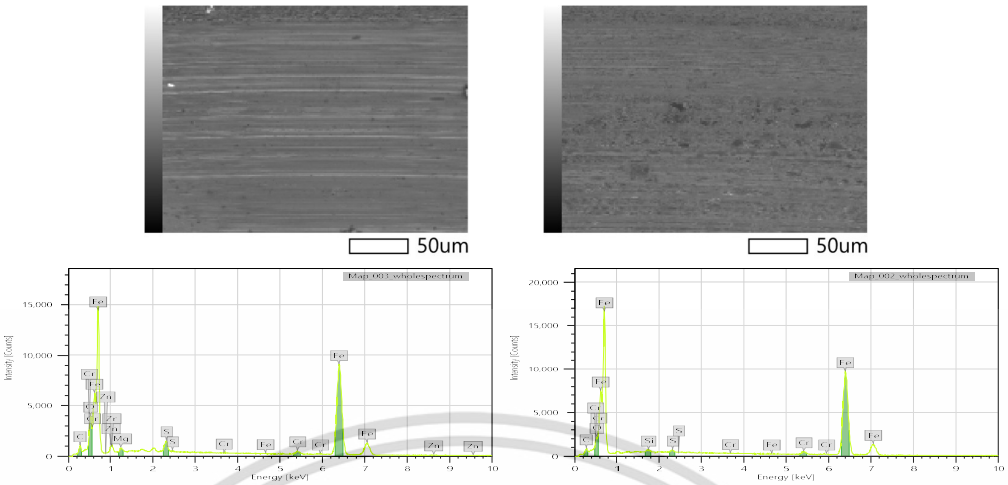

(a) API CD (b) API CD+CB

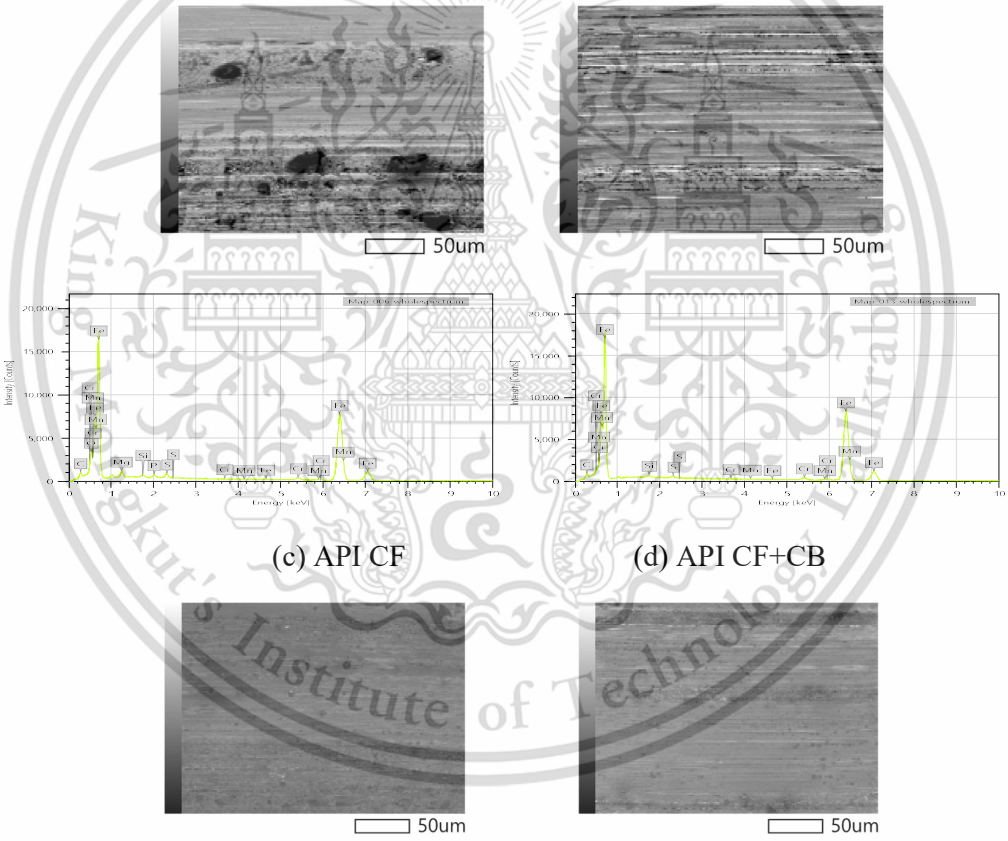

(c) API CF (d) API CF+CB

(e) API CF4 (f) API CF4+CB

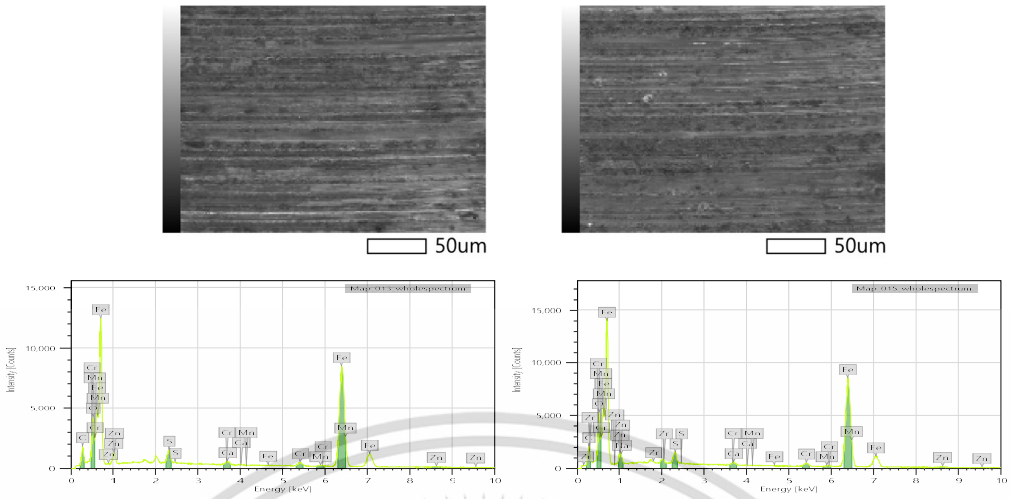

(g) API CH4 (h) API CH4+CB

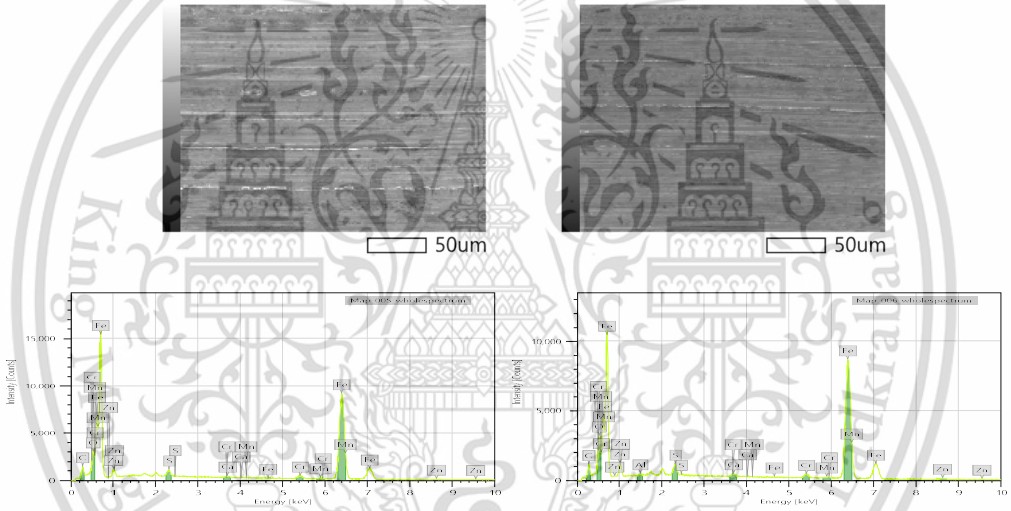

(i) API CI4 (j) API CI4+CB

Figure 4.16 SEM micrograph with EDX analysis.

CHAPTER 5

CONCLUSIONS

This research used different standards of engine oil which depended on the amount of additive. Engine oils were divided into 2 groups according to their amount of additive: low-grade with lower additives from 4.8 to 7.5 percent and high-grade from 12.7 to 14 percent. Carbon black N330 was mixed with formulated engine oil at 1% by weight. The primary particle size was about 31 nanometers.

After four-ball wear tests, the results showed that wear scar diameter in the group of low-grade engine oil were clearly larger. The main reason of this was their lower amount of anti-ware additive, that prevent the additive from generating enough oil film layer to protect the surface, results in more wears than in high-grade engine oil.

When the engine oil was contaminated with carbon black N330, the results showed that wear scar diameter in API CD and API CF engine oil accelerated the most clearly. On the other hand, there was almost no change in the high-grade engine oils. Soot was the reason of the increase of metallic wear, and the amount of anti-wear additives had an important role in preventing them.

The roughness value of metal ball will decrease when engine oil was contaminated with carbon black because carbon black particles entered into the contact area and polish the ball surfaces. In the case of API CD engine oil that the roughness value increased because its amount of additive was too low, that it could not prevent carbon black particles from further damaging the surfaces.

Abrasive wear clearly increased in any case when engine oil was contaminated with carbon black, because the carbon black was the cause of three body abrasive wear. When they enter into contact area, they would scratch and damage the ball's surfaces into metal particles that mixed within engine oil. So, it could be concluded that carbon black was the reason of evidently increasing of abrasive wear.

The additive element still remained on the worn surface. So, it was proved that engine oil additive had spread all over the area, including between the contact surfaces. Anti-wear additive that build oil film layers on metal surfaces has an important role on preventing metallic wear, both in the case of with and without CB contamination.

REFERENCES

[1] M. Torbacke, Å. K. Rudolphi and E. Kassfeldt, Lubricants: Introduction to Properties and Performance, United Kingdom: John Wiley & Sons Ltd, 2014.

[2] T. Mang, K. Bobzin and T. Bartels, Industrial Tribology: Friction, Germany: WILEY-VCH Verlag & Co. KGaA, 2011.

[3] G. W. Stachowiak and A. W. Batchelor, ENGINEERING TRIBOLOGY, ELSEVIER, 1993.

[4] K. G. Budinski, Friction, wear, and erosion atlas, CRC Press, 2014.

[5] M. Torbacke, Å. K. Rudolphi and E. Kassfeldt, Lubricants: Formulating Lubricants, United Kingdom: John Wiley & Sons Ltd, 2014.

[6] S. N. Nayak and P. A. Lakshminarayanan, Critical Component Wear in Heavy Duty Engine, John Wiley & Sons (Asia) Pte Ltd, 2011.

[7] S. Q. A. Rizvi, A Comprehensive Review of Lubricant Chemistry, Technology, Selection, and Design, Baltimore: ASTM stock number: MNL59, 2009.

[8] Farng, L.O., Ashless antiwear and extreme pressure additives, in Lubricant Additives: Chemistry and Applications (ed. L.R. Rudnick), Marcel Dekker Inc., New York, 2003.

[9] Phillips,W.D., Ashless phosphorus containing lubricating oil additives, in Lubricant Additives: Chemistry and Applications (ed. L.R. Rudnick), Marcel Dekker, Inc., New York, 2003.

[10] T. Mang and W. Dresel, Lubricants and Lubrication: Rheology of Lubricants, Germany: WILEY-VCH GmbH, 2007.

[11] W. Shizhu and H. Ping, Principles of Tribology: Properties of Lubricants, China: John Wiley & Sons (Asia) Pte Ltd, 2012.

[12] G. E. Totten, S. R. Westbrook and R. J. Shah, Fuels and Lubricants Handbook: Performance/Property Testing Procedures, USA: ASTM International, 2003.

[13] Modern Instrumental Methods of Elemental Analysis of Petroleum Products and Lubricants, ASTM STP 1109, R. A. Nadkami, Ed., ASTM International, West Conshohocken, PA, p. 19, 1991.

[14] M. Maricq, "Review Chemical Characterization of particulate emissions from," *Journal of Aerosal Science*, 2007.

[15] P. Karin, J. Boonsakda, K. Siricholathum, E. Saenkhumvong, C. Charoenphonphanich and K. Hanamura "Morphology and oxidation kinetics of CI engine's biodiesel particulate matters on cordierite diesel particulate filters using TGA," *International Journal of Automotive Technology*, vol. 18, No. 1, p. 31−40, 2017.

[16] D. B. Kittelson, "Engines and nanoparticles: A review," *Aerosol Science*, vol. 29, 1998.

[17] K. Siricholathum, P. Karin, C. Charoenphonphanich, K. Hanamura and N. Chollacoop, The impact of biodiesel particulate matter morphology and oxidation kinetic on filter trapping and regeneration mechanism, master's degree thesis KMITL, 2015.

[18] P. Karin, C. Supanamok and K. Hanamura," Impact of soot on metal wear characteristics using laser diffraction spectroscopy", *Journal of Research and Applications in Mechanical Engineering,* vol.4, No.2, 126-134, 2016.

[19] W. Amornprapa, P. Karin, N. Chollacoop and K. Hanamura, Impact of carbon black particle size on metallic wear using four-ball wear, Master degree thesis KMITL, 2017.

[20] "Schematics of transmission electron microscopy operation," [Online]. Available: http://www.hkphy.org/atomic_world/tem/tem02_e.html. [Accessed 2017].

[21] N. DATABASE, "Carbon Black," 2016. [Online]. Available: http://web.eng.nu.ac.th/eng2012/ceri/nanodatabase/info_index.php?cat_id=13.

[22] P. Karin, W. Amornprapa, P. Khamsrisuk, P. Budsayahem, P. Chammana, K. Sriprapha and K. Hanamura, Effect of Biofuel and Soot on Metal Wear Characteristic using Electron Microscopy and 3D Image Processing, SAE Technical Papers, JSAE 20179095 / SAE 2017-32-0095.

[23] Thomas J. Fellers and Michael W. Davidson "Confocal Microscopy Introduction," [Online]. Available: https://www.olympus-lifescience.com/en/microscope-resource/primer/techniques/confocal/confocalintro/. [Accessed 2019].

[24] A. D. −. 94, "Standard Test Method for Wear Preventive Characteristics of Lubricating Fluid," 2016.

APPENDIX A

FOUR BALL REPORTS

InS Thai Ltd.
Thai-French Innovation Institute (8th Floor),
King Mongkut's University of Technology North Bangkok,
1518 Pracharat 1 Rd., Wongsawang, Bangsue, Bangkok 10800, Thailand.
Tel: +66 (0)2 585 9946, +66 (0)2 585 9964, +66 (0)2 585 9982, Fax: +66 (0)2 585 9951
www.ins-thai.com

ANALYSIS REPORT:
King Mongkut's Institute of Technology Ladkrabang
Four ball – Wear resistance according to ASTM D4172

Sample description	Lubricants
Customer Sample Reference	See table 1
Internal Sample Reference	See table 1
Date of Receipt	08/08/2018
Date of Analysis	09/08/2018 – 05/09/2018
Analysis Report Reference	R1808105KML-01

TESTS & SAMPLES

TEST	STANDARD	CONDITIONS	CUSTOMER SAMPLE REF.	INTERNAL SAMPLE REF.
4-Ball Method	ASTM D4172	– *Rotational speed: 1200±10 rpm* – *Load: 392±2 N (40±2 kgf)* – *Duration per load: 60±1 min* – *Temperature: 75±2 °C*	See Table 1	See Table 1

Table 1: List of samples reference

Customer Reference	InS Thai Reference
1. API CD + BCP 3047 4.85% (418487)	S1808105KML-01
2. API CD + BCP 3047 4.85%	S1808105KML-02
3. API CF-4 + BCP 3047 7.5% (418489)	S1808105KML-03
4. API CF-4 + BCP 3047 7.5%	S1808105KML-04
5. API CH-4 + BCP 1059 12.7% (418490)	S1808105KML-05
6. API CH-4 + BCP 1059 12.7%	S1808105KML-06
7. API CI-4 + BCP 1059 14% (418491)	S1808105KML-07
8. API CI-4 + BCP 1059 14%	S1808105KML-08

InS Thai Ltd.
Thai-French Innovation Institute (8th Floor),
King Mongkut's University of Technology North Bangkok,
1518 Pracharat 1 Rd., Wongsawang, Bangsue, Bangkok 10800, Thailand.
Tel: +66 (0)2 585 9946, +66 (0)2 585 9964, +66 (0)2 585 9982, Fax: +66 (0)2 585 9951
www.ins-thai.com

SAMPLE PREPARATION & TESTING

According to the four balls testing standard (ASTM D4172), the samples are tested at 75°C. The normal load applied is 392 N. Running time is 60 minutes.

Figure 1: Four balls testing machine and direction of applied load

After the test, the diameter of wear scar is measured by optical microscope at ×100 magnifications. The wear scar diameters of the three lower balls are measured and the average values are calculated.

InS Thai Ltd.
Thai-French Innovation Institute (8th Floor),
King Mongkut's University of Technology North Bangkok,
1518 Pracharat 1 Rd., Wongsawang, Bangsue, Bangkok 10800, Thailand.
Tel: +66 (0)2 585 9946, +66 (0)2 585 9964, +66 (0)2 585 9982, Fax: +66 (0)2 585 9951
www.ins-thai.com

RESULTS

Table 2 presents the wear scars diameter measured on the three lower balls. The variation of wear scar diameter is small indicating a good sample installation. Figure 2 shows the comparison of wear scar size between different samples.

Table 2: Wear scars diameter measured by microscope

Sample no.	Ball 1 (µm)	Ball 2 (µm)	Ball 3 (µm)	Average (µm)	Ball 4 (µm)
1	643.41	639.07	633.45	638.64	652.15
2	691.76	688.26	682.69	687.57	697.61
3	631.96	617.35	626.20	625.17	694.35
4	620.58	620.58	620.35	620.50	725.15
5	592.00	591.39	578.60	587.33	633.24
6	600.54	603.60	602.34	602.16	643.29
7	595.13	607.85	606.96	603.31	690.46
8	611.26	612.13	605.73	609.71	674.18

* Red-filled cell represent the highest value.

Figure 2: Average wear scar size of three lower balls after testing

Table 3 presents the result of roughness measured on the 4 balls after Four ball test on engine oil sample. Figure 3 shows the comparison of roughness result between different samples.

Table 3: Roughness Measurement by optical microscope.

Sample no.	Ball 1 (µm)	Ball 2 (µm)	Ball 3 (µm)	Average (µm)	Ball 4 (µm)
1	0.110	0.097	0.103	0.103	0.113
2	0.137	0.157	0.190	0.161	0.177
3	0.103	0.143	0.117	0.121	0.103
4	0.120	0.067	0.090	0.092	0.077
5	0.203	0.293	0.260	0.252	0.383
6	0.183	0.227	0.203	0.204	0.227
7	0.237	0.287	0.213	0.246	0.213
8	0.153	0.187	0.193	0.178	0.207

* Red-filled cell represent the highest value.

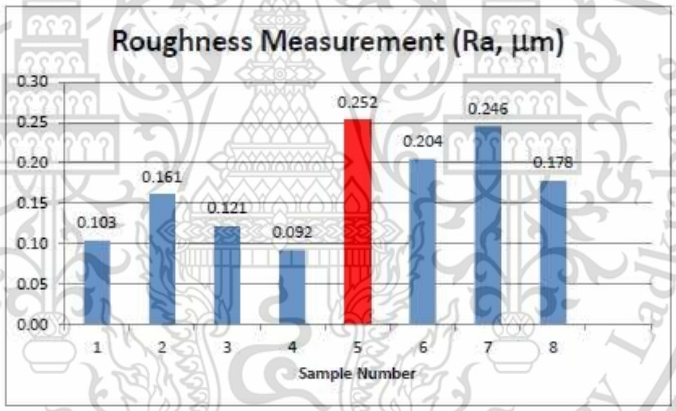

Figure 3: Average roughness of three lower balls after testing

InS Thai Ltd.
Thai-French Innovation Institute (8th Floor),
King Mongkut's University of Technology North Bangkok,
1518 Pracharat 1 Rd., Wongsawang, Bangsue, Bangkok 10800, Thailand.
Tel: +66 (0)2 585 9946, +66 (0)2 585 9964, +66 (0)2 585 9982, Fax: +66 (0)2 585 9951
www.ins-thai.com

Table 4 showed the mass loss of each ball after testing of all lubricant samples.

Table 4: Mass loss measured by high precision balance (4 digit)

Sample no.		Weight (g)		
		Before	After	Weight loss (g)
1	Ball 1	8.3515	8.3515	≤0.0001
	Ball 2	8.3523	8.3521	0.0002
	Ball 3	8.3506	8.3506	≤0.0001
	Ball 4	8.3550	8.3548	0.0002
2	Ball 1	8.3539	8.3536	0.0003
	Ball 2	8.3538	8.3537	0.0001
	Ball 3	8.3539	8.3534	0.0005
	Ball 4	8.3550	8.3546	0.0004
3	Ball 1	8.3534	8.3534	≤0.0001
	Ball 2	8.3529	8.3529	≤0.0001
	Ball 3	8.3531	8.3529	0.0002
	Ball 4	8.3512	8.3512	≤0.0001
4	Ball 1	8.3537	8.3537	≤0.0001
	Ball 2	8.3541	8.3540	0.0001
	Ball 3	8.3538	8.3538	≤0.0001
	Ball 4	8.3514	8.3512	0.0002
5	Ball 1	8.3524	8.3522	0.0002
	Ball 2	8.3518	8.3518	≤0.0001
	Ball 3	8.3542	8.3542	≤0.0001
	Ball 4	8.3550	8.3550	≤0.0001
6	Ball 1	8.3537	8.3537	≤0.0001
	Ball 2	8.3541	8.3540	0.0001
	Ball 3	8.3538	8.3538	≤0.0001
	Ball 4	8.3514	8.3512	0.0002
7	Ball 1	8.3527	8.3524	0.0003
	Ball 2	8.3521	8.3520	0.0001
	Ball 3	8.3536	8.3530	0.0006
	Ball 4	8.3513	8.3512	0.0001
8	Ball 1	8.3508	8.3507	0.0001
	Ball 2	8.3528	8.3527	0.0001
	Ball 3	8.3538	8.3537	0.0001
	Ball 4	8.3508	8.3506	0.0002

InS Thai Ltd.
Thai-French Innovation Institute (8th Floor),
King Mongkut's University of Technology North Bangkok,
1518 Pracharat 1 Rd., Wongsawang, Bangsue, Bangkok 10800, Thailand.
Tel: +66 (0)2 585 9946, +66 (0)2 585 9964, +66 (0)2 585 9982, Fax: +66 (0)2 585 9951
www.ins-thai.com

General conclusion:

- The lowest and highest wear scar diameters of three lower balls were found on Sample 5; API CH-4 + BCP 1059 12.7% (418490) and Sample 2; API CD + BCP3047 4.85%, respectively.
- The lowest and highest roughness of three lower balls were found on Sample 4; API CF-4 + BCP 3047 7.5% and Sample 5; API CH-4 + BCP 1059 12.7% (418490), respectively.

Suggestion:

The mixture sample should be performed 4-Ball test repetition for obtaining high precision and reliability because the dispersion between carbon and lube liquid part is not entirely homogeneous.

Prepared by:	Approved by:
Mr.Panumas Songvut	Dr. Pornsit Lorkit
R&D Scientist	Laboratory Manager
Panumas Songvut	Pornsit L.
2018-09-05	2018-09-05

InS Thai Ltd.
Thai-French Innovation Institute (8th Floor),
King Mongkut's University of Technology North Bangkok,
1518 Pracharat 1 Rd., Wongsawang, Bangsue, Bangkok 10800, Thailand.
Tel: +66 (0)2 585 9946, +66 (0)2 585 9964, +66 (0)2 585 9982, Fax: +66 (0)2 585 9951
www.ins-thai.com

ANALYSIS REPORT:
King Mongkut's Institute of Technology Ladkrabang
Four ball – Wear resistance according to ASTM D4172

Sample description	Lubricants
Customer Sample Reference	See table 1
Internal Sample Reference	See table 1
Date of Receipt	31/05/2019
Date of Analysis	31/05/2019 – 7/06/2019
Analysis Report Reference	R1905114KMIL

TESTS & SAMPLES

TEST	STANDARD	CONDITIONS	CUSTOMER SAMPLE REF.	INTERNAL SAMPLE REF.
4-Ball Method	ASTM D4172	– *Rotational speed: 1200±10 rpm* – *Load: 392±2 N (40±2 kgf)* – *Duration per load: 60±1 min* – *Temperature: 75±2 °C*	See Table 1	See Table 1

Table 1: List of samples reference

Customer Reference	InS Thai Reference
API CF BCP 3047 6.8% (New Oil)	S1905114KML-01
API CF BCP 3047 6.8%	S1905114KML-02

InS Thai Ltd.
Thai-French Innovation Institute (8th Floor),
King Mongkut's University of Technology North Bangkok,
1518 Pracharat 1 Rd., Wongsawang, Bangsue, Bangkok 10800, Thailand.
Tel: +66 (0)2 585 9946, +66 (0)2 585 9964, +66 (0)2 585 9982, Fax: +66 (0)2 585 9951
www.ins-thai.com

SAMPLE PREPARATION & TESTING

According to the four balls testing standard (ASTM D4172), the samples are tested at 75°C. The normal load applied is 392 N. Running time is 60 minutes.

Figure 1: Four balls testing machine and direction of applied load

After the test, the diameter of wear scar is measured by optical microscope at ×100 magnifications. The wear scar diameters of the three lower balls are measured and the average values are calculated.

InS Thai Ltd.
Thai-French Innovation Institute (8th Floor),
King Mongkut's University of Technology North Bangkok,
1518 Pracharat 1 Rd., Wongsawang, Bangsue, Bangkok 10800, Thailand.
Tel: +66 (0)2 585 9946, +66 (0)2 585 9964, +66 (0)2 585 9982, Fax: +66 (0)2 585 9951
www.ins-thai.com

RESULTS

Table 2 and 3 presents the wear scars diameter measured on the three lower balls. The variation of wear scar diameter is small indicating a good sample installation. Figure 3 shows the comparison of wear scar size between different samples.

Table 2: Wear scars by microscope

Ball	S1905114KML-01	S1905114KML-02
1		
2		
3		
4		

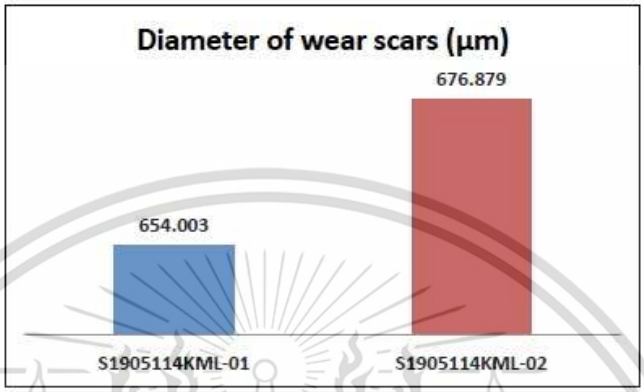

Figure 3: Average wear scar size of three lower balls after testing

Table 3 showed the mass loss of each ball after testing of all lubricant samples.

Table 3: Diameter of wear scars measured

Samples	Ball 1 (µm)	Ball 2 (µm)	Ball 3 (µm)	Average (µm)	Ball 4 (µm)
S1905114KML-01	653.931	652.178	655.900	654.003	653.180
S1905114KML-02	[illegible]	[illegible]	[illegible]	[illegible]	[illegible]

Table 4: Mass loss measured by high precision balance (4 digit)

Customer Reference		Weight (g)		
		Before	After	Weight loss (g)
S1905114KML-01	Ball 1	8.3550	8.3549	≤0.0001
	Ball 2	8.3510	8.3509	≤0.0001
	Ball 3	8.3524	8.3523	≤0.0001
	Ball 4	8.3545	8.3544	≤0.0001
S1905114KML-02	Ball 1	8.3540	8.3539	≤0.0001
	Ball 2	8.3530	8.3529	≤0.0001
	Ball 3	8.3523	8.3522	≤0.0001
	Ball 4	8.3539	8.3538	≤0.0001

InS Thai Ltd.
Thai-French Innovation Institute (8th Floor),
King Mongkut's University of Technology North Bangkok,
1518 Pracharat 1 Rd., Wongsawang, Bangsue, Bangkok 10800, Thailand.
Tel: +66 (0)2 585 9946, +66 (0)2 585 9964, +66 (0)2 585 9982, Fax: +66 (0)2 585 9951
www.ins-thai.com

General conclusion:

- The diameter of sample API CF BCP 3047 6.8 has higher than API CF BCP 3047 6.8% (New oil)
- The mass loss of each ball for all samples were less than or equal to 0.0001 g.

Suggestion:

The mixture sample should be performed 4-Ball test repeatedly for obtaining high precision and reliability because the dispersion between carbon and lube liquid part is not entirely homogeneous.

Prepared by: Mr.Panumas Songvut R&D Scientist Panumas Songvut 2019-06-07	**Approved by:** Dr. Natapat Ampan Laboratory Manager Natapat Am 2019-06-07

APPENDIX B

X-RAY FLUORESCENCE SPECTRA

Eval2 V2.5.500 Admin 6/24/2018 2:48:30 PM
Sample: 612206-8700-CD
Measured on 6/22/2018 1:34:08 PM
Sample measured by Admin
Measurement method: Best Detection-He34mm

Sum	S	Mg	Zn	P
0.70 %	0.411 %	0.119 %	893 PPM	795 PPM

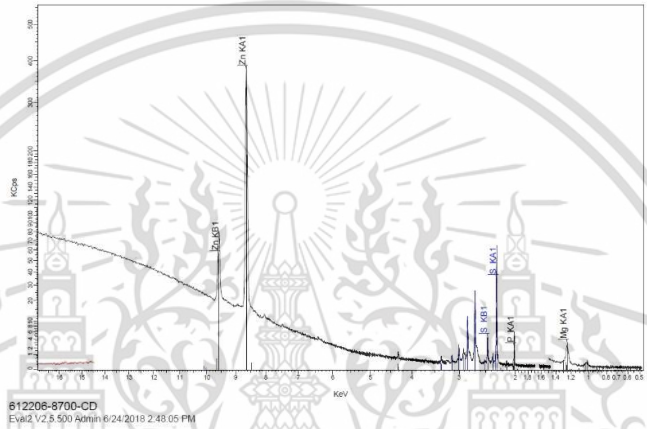

612206-8700-CD
Eval2 V2.5.500 Admin 6/24/2018 2:48:05 PM

Eval2 V2.5.500 Admin 6/24/2018 2:50:54 PM
Sample: 612206-8700-CF
Measured on 6/22/2018 1:52:54 PM
Sample measured by Admin
Measurement method: Best Detection-He34mm

Sum	S	Mg	Zn	P	Si	Ca
0.91 %	0.496 %	0.171 %	0.128 %	0.111 %	27.2 PPM	18.0 PPM

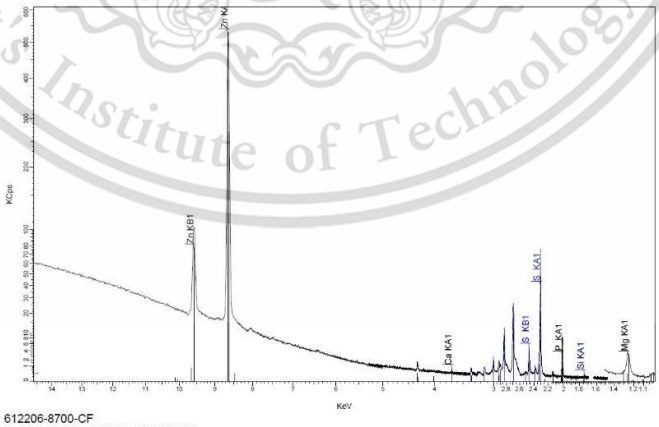

612206-8700-CF
Eval2 V2.5.500 Admin 6/24/2018 2:52:20 PM

Eval2 V2.5.500 Admin 6/24/2018 2:54:28 PM
Sample: 612206-8700-CF4
Measured on 6/22/2018 2:12:58 PM
Sample measured by Admin
Measurement method: Best Detection-He34mm

Sum	S	Mg	Zn	P	Si
0.83 %	0.426 %	0.160 %	0.128 %	0.111 %	29.7 PPM

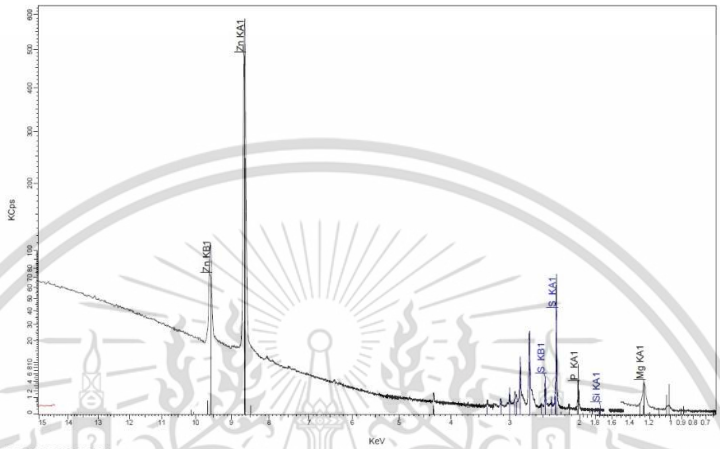

612206-8700-CF4
Eval2 V2.5.500 Admin 6/24/2018 2:55:26 PM

Eval2 V2.5.500 Admin 6/24/2018 2:57:40 PM
Sample: 612206-8700-CH4
Measured on 6/22/2018 2:31:19 PM
Sample measured by Admin
Measurement method: Best Detection-He34mm

Sum	S	Ca	Zn	P	Cl	Si
1.1 %	0.519 %	0.318 %	0.126 %	0.117 %	100 PPM	39.9 PPM

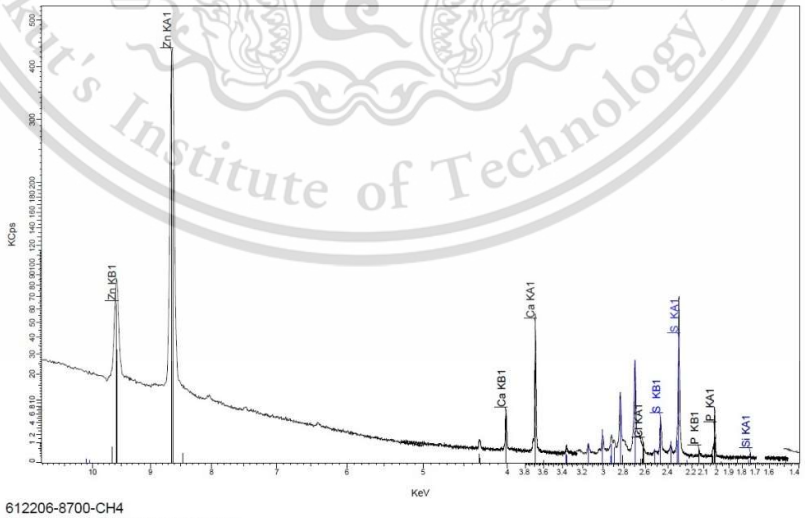

612206-8700-CH4
Eval2 V2.5.500 Admin 6/24/2018 3:00:02 PM

Eval2 V2.5.500 Admin 6/24/2018 3:01:23 PM
Sample: 612206-8700-Cl4
Measured on 6/22/2018 2:49:50 PM
Sample measured by Admin
Measurement method: Best Detection-He34mm

Sum	S	Ca	Zn	P	Cl	Si
1.1 %	0.511 %	0.327 %	0.135 %	0.120 %	110 PPM	49.1 PPM

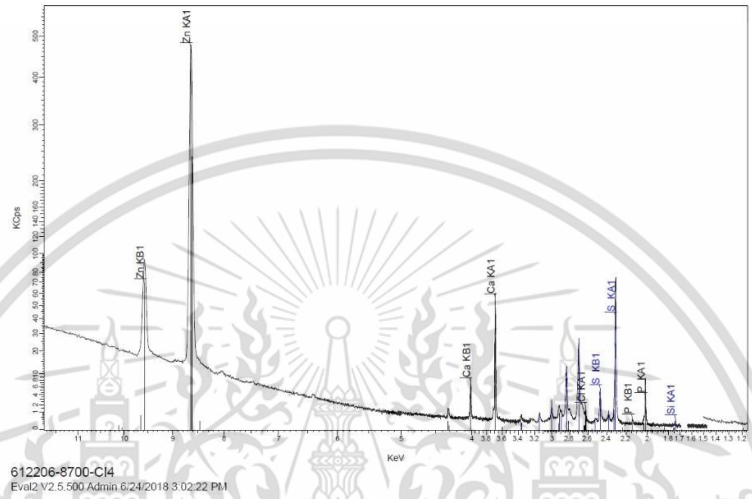

APPENDIX C

Laser particle size distribution spectrum

Scientific and Technological Research Equipment Centre (STREC), Chulalongkorn University

Sample	
Sample Name	API CD BCP 3047 4.85%
Batch/Lot No./Sample detail	
File Name	620103-9372

Instrument	
Instrument Type	Mastersizer3000
Instrument Serial No.	MAL1099267
Accessory Name	Hydro EV

Conditions	
Particle Name	Carbon
Particle Refractive Index	1.870
Particle Absorption Index	3.000
Dispersant Name	Engine oil
Dispersant Refractive Index	1.470
Analysis Model	General Purpose
Scattering Model	Mie
Laser Obscuration	7.73 %
Ultrasound Achieved	0 %
Stirrer Speed Achieved	3000 rpm
Particle Notes	

Result	
Result Units	Volume
Concentration	0.0002 %
Uniformity	4.694
Span	14.687
Specific Surface Area	158200 m²/kg
Weighted Residual	1.94 %
Dv (10)	0.0157 µm
Dv (50)	0.0435 µm
Dv (90)	0.654 µm
D [4,3]	0.228 µm
D [3,2]	0.0379 µm

Frequency (compatible)

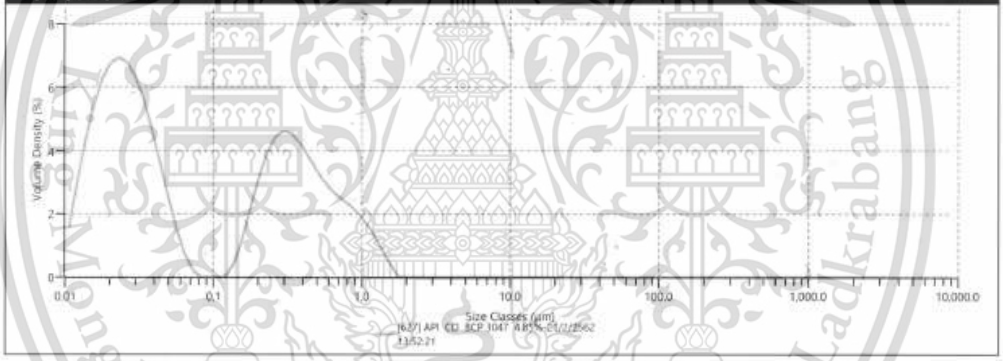

Result table

Size (µm)	% Volume In	Size (µm)	% Volume In	Size (µm)	% Volume In	Size (µm)	% Volume In	Size (µm)	% Volume In	Size (µm)	% Volume In	Size (µm)	% Volume In
0.0100	1.31	0.0679	0.19	0.460	2.85	3.12	0.00	21.2	0.00	144	0.00	976	0.00
0.0114	2.55	0.0771	0.00	0.523	2.52	3.55	0.00	24.1	0.00	163	0.00	1110	0.00
0.0129	3.65	0.0876	0.00	0.594	2.27	4.03	0.00	27.4	0.00	186	0.00	1260	0.00
0.0147	4.55	0.0995	0.00	0.675	2.08	4.58	0.00	31.1	0.00	211	0.00	1430	0.00
0.0167	5.23	0.113	0.00	0.767	1.92	5.21	0.00	35.3	0.00	240	0.00	1630	0.00
0.0189	5.65	0.128	0.31	0.872	1.73	5.92	0.00	40.1	0.00	272	0.00	1850	0.00
0.0215	5.80	0.146	0.96	0.991	1.47	6.72	0.00	45.6	0.00	310	0.00	2100	0.00
0.0244	5.69	0.166	1.79	1.13	1.13	7.64	0.00	51.8	0.00	352	0.00	2390	0.00
0.0278	5.31	0.188	2.60	1.28	0.75	8.68	0.00	58.9	0.00	400	0.00	2710	0.00
0.0315	4.72	0.214	3.26	1.45	0.36	9.86	0.00	66.9	0.00	454	0.00	3080	0.00
0.0358	3.95	0.243	3.70	1.65	0.00	11.2	0.00	76.0	0.00	516	0.00	3500	
0.0407	3.08	0.276	3.88	1.88	0.00	12.7	0.00	86.4	0.00	586	0.00		
0.0463	2.17	0.314	3.81	2.13	0.00	14.5	0.00	98.1	0.00	666	0.00		
0.0526	1.33	0.357	3.56	2.42	0.00	16.4	0.00	111	0.00	756	0.00		
0.0597	0.64	0.405	3.22	2.75	0.00	18.7	0.00	127	0.00	859	0.00		

Malvern

Malvern Instruments Ltd.
www.malvern.com

Mastersizer - v3.40
Page 1 of 1

620103-9372
Created: 10/5/2559
Printed: 2/4/2562 11:33

Scientific and Technological Research Equipment Centre (STREC), Chulalongkorn University

Sample	
Sample Name	API CF4 BCP 3047 7.5%
Batch/Lot No./Sample detail	
File Name	620103-9372

Instrument	
Instrument Type	Mastersizer3000
Instrument Serial No.	MAL1099267
Accessory Name	Hydro EV

Conditions	
Particle Name	Carbon
Particle Refractive Index	1.870
Particle Absorption Index	3.000
Dispersant Name	Engine oil
Dispersant Refractive Index	1.470
Analysis Model	General Purpose
Scattering Model	Mie
Laser Obscuration	9.74 %
Ultrasound Achieved	0 %
Stirrer Speed Achieved	3500 rpm
Particle Notes	

Result	
Result Units	Volume
Concentration	0.0002 %
Uniformity	11.536
Span	44.930
Specific Surface Area	165600 m^2/kg
Weighted Residual	1.23 %
Dv (10)	0.0146 µm
Dv (50)	0.0428 µm
Dv (90)	1.94 µm
D [4,3]	0.516 µm
D [3,2]	0.0362 µm

Frequency (compatible)

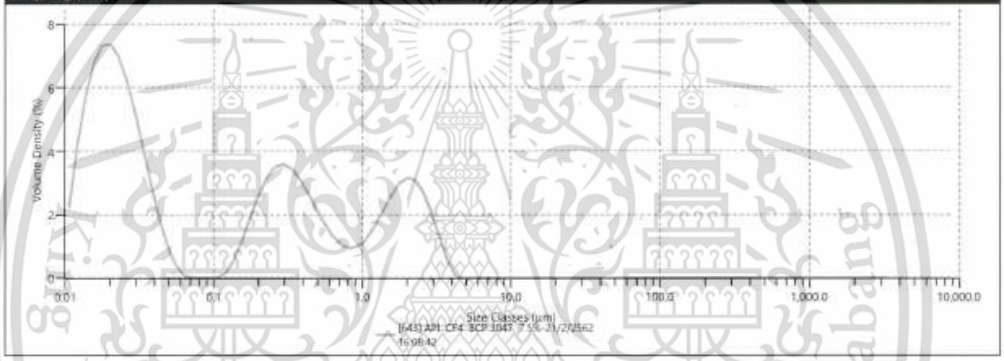

Result table

Size (µm)	% Volume In	Size (µm)	% Volume In	Size (µm)	% Volume In	Size (µm)	% Volume In	Size (µm)	% Volume In	Size (µm)	% Volume In	Size (µm)	% Volume In
0.0100	1.88	0.0679	0.00	0.460	1.83	3.12	7.06	21.2	0.00	144	0.00	976	0.00
0.0114	3.51	0.0771	0.00	0.523	1.43	3.55	0.48	24.1	0.00	163	0.00	1110	0.00
0.0129	4.80	0.0876	0.00	0.594	1.10	4.03	0.00	27.4	0.00	186	0.00	1260	0.00
0.0147	5.68	0.0995	0.00	0.675	0.87	4.58	0.00	31.1	0.00	211	0.00	1430	0.00
0.0167	6.13	0.113	0.11	0.767	0.78	5.21	0.00	35.3	0.00	240	0.00	1630	0.00
0.0189	6.17	0.128	0.45	0.872	0.82	5.92	0.00	40.1	0.00	272	0.00	1850	0.00
0.0215	5.94	0.146	0.96	0.991	1.01	6.72	0.00	45.6	0.00	310	0.00	2100	0.00
0.0244	5.21	0.166	1.60	1.13	1.33	7.64	0.00	51.8	0.00	352	0.00	2390	0.00
0.0278	4.36	0.188	2.19	1.28	1.73	8.68	0.00	58.8	0.00	400	0.00	2710	0.00
0.0315	3.39	0.214	2.66	1.45	2.15	9.86	0.00	66.9	0.00	454	0.00	3080	0.00
0.0358	2.42	0.243	2.94	1.65	2.48	11.2	0.00	76.0	0.00	516	0.00	3500	
0.0407	1.52	0.276	3.01	1.88	2.66	12.7	0.00	86.4	0.00	586	0.00		
0.0463	0.80	0.314	2.89	2.13	2.60	14.5	0.00	98.1	0.00	666	0.00		
0.0526	0.31	0.357	2.62	2.42	2.27	16.4	0.00	111	0.00	756	0.00		
0.0597	0.06	0.405	2.24	2.75	1.71	18.7	0.00	127	0.00	859	0.00		

Scientific and Technological Research Equipment Centre (STREC), Chulalongkorn University

Sample	
Sample Name	API CH-4 BCP 1059 12.5%
Batch/Lot No./Sample detail	
File Name	620103-9372

Instrument	
Instrument Type	Mastersizer3000
Instrument Serial No.	MAL1099267
Accessory Name	Hydro EV

Conditions	
Particle Name	Carbon
Particle Refractive Index	1.870
Particle Absorption Index	3.000
Dispersant Name	Engine oil
Dispersant Refractive Index	1.470
Analysis Model	General Purpose
Scattering Model	Mie
Laser Obscuration	12.19 %
Ultrasound Achieved	0 %
Stirrer Speed Achieved	3000 rpm
Particle Notes	

Result	
Result Units	Volume
Concentration	0.0004 %
Uniformity	29.538
Span	101.178
Specific Surface Area	99110 m^2/kg
Weighted Residual	5.88 %
Dv (10)	0.0173 µm
Dv (50)	0.492 µm
Dv (90)	49.8 µm
D [4,3]	14.6 µm
D [3,2]	0.0605 µm

Frequency (compatible)

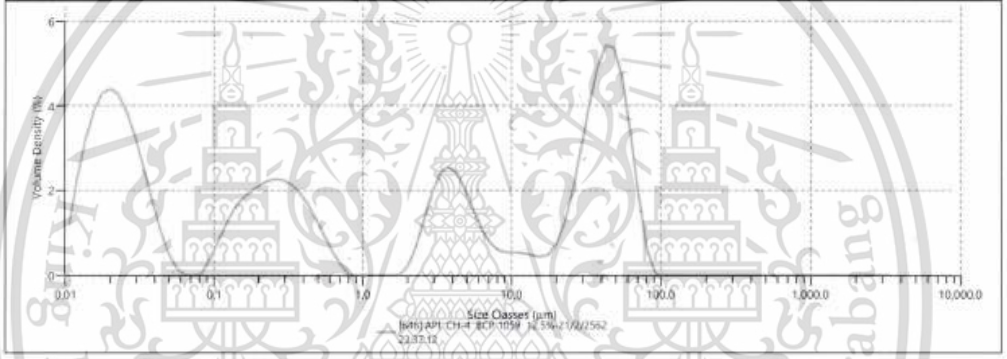

Result table

Size (µm)	% Volume In	Size (µm)	% Volume In	Size (µm)	% Volume In	Size (µm)	% Volume In	Size (µm)	% Volume In	Size (µm)	% Volume In	Size (µm)	% Volume In
0.0100	1.01	0.0679	0.00	0.460	1.08	3.12	2.04	21.2	1.01	144	0.00	976	0.00
0.0114	1.94	0.0771	0.00	0.523	0.75	3.55	2.16	24.1	1.66	163	0.00	1110	0.00
0.0129	2.71	0.0876	0.29	0.594	0.44	4.03	2.02	27.4	2.49	186	0.00	1260	0.00
0.0147	3.27	0.0995	0.64	0.675	0.18	4.58	1.68	31.1	3.57	211	0.00	1430	0.00
0.0167	3.60	0.113	1.01	0.767	0.00	5.21	1.27	35.3	4.13	240	0.00	1630	0.00
0.0189	3.70	0.128	1.21	0.872	0.00	5.92	0.90	40.1	4.57	272	0.00	1850	0.00
0.0215	3.58	0.146	1.51	0.991	0.00	6.72	0.63	45.6	4.52	310	0.00	2100	0.00
0.0244	3.37	0.166	1.85	1.13	0.00	7.64	0.49	51.8	3.89	352	0.00	2390	0.00
0.0278	2.72	0.188	1.77	1.28	0.00	8.68	0.45	58.9	2.78	400	0.00	2710	0.00
0.0315	2.13	0.214	1.86	1.45	0.00	9.85	0.46	66.9	1.48	454	0.00	3080	0.00
0.0358	1.80	0.243	1.90	1.65	0.00	11.2	0.44	76.0	0.45	516	0.00	3500	
0.0407	0.92	0.276	1.87	1.88	0.15	12.7	0.40	86.4	0.00	586	0.00		
0.0463	0.44	0.314	1.78	2.13	0.55	14.5	0.36	98.1	0.00	666	0.00		
0.0526	0.13	0.357	1.61	2.42	1.11	16.4	0.39	111	0.00	755	0.00		
0.0597	0.00	0.405	1.38	2.75	1.66	18.7	0.59	127	0.00	859	0.00		

Malvern

620103-9372

Malvern Instruments Ltd.
www.malvern.com

Mastersizer - v3.40
Page 1 of 1

Created: 10/5/2559
Printed: 2/4/2562 11:34

Scientific and Technological Research Equipment Centre (STREC), Chulalongkorn University

Sample	
Sample Name	API CI-4 BCP 1059 14%
Batch/Lot No./Sample detail	
File Name	620103-9372

Instrument	
Instrument Type	Mastersizer3000
Instrument Serial No.	MAL1099267
Accessory Name	Hydro EV

Conditions	
Particle Name	Carbon
Particle Refractive Index	1.870
Particle Absorption Index	3.000
Dispersant Name	Engine oil
Dispersant Refractive Index	1.470
Analysis Model	General Purpose
Scattering Model	Mie
Laser Obscuration	12.72 %
Ultrasound Achieved	0 %
Stirrer Speed Achieved	3000 rpm
Particle Notes	

Result	
Result Units	Volume
Concentration	0.0004 %
Uniformity	4.217
Span	13.590
Specific Surface Area	117800 m²/kg
Weighted Residual	1.80 %
Dv (10)	0.0161 µm
Dv (50)	0.437 µm
Dv (90)	5.95 µm
D [4,3]	1.94 µm
D [3,2]	0.0509 µm

Frequency (compatible)

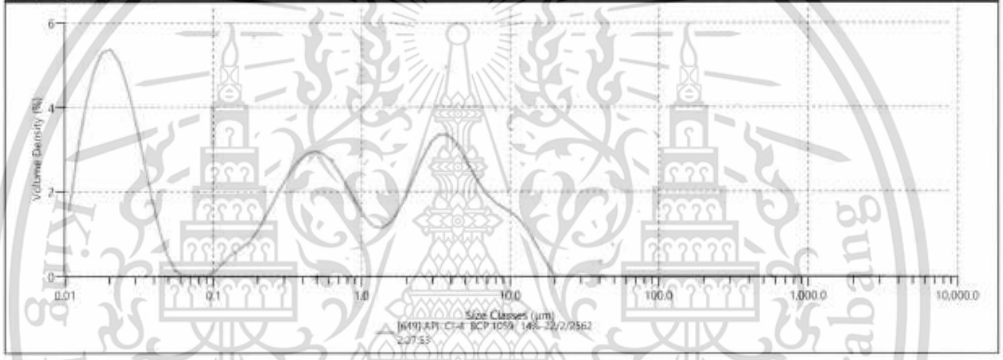

Result Table

Size (µm)	% Volume In	Size (µm)	% Volume In	Size (µm)	% Volume In	Size (µm)	% Volume In	Size (µm)	% Volume In	Size (µm)	% Volume In	Size (µm)	% Volume In
0.0100	1.27	0.0679	0.00	0.460	2.47	3.12	0.81	21.2	0.00	144	0.00	976	0.00
0.0114	2.43	0.0771	0.00	0.523	2.41	3.55	2.80	24.1	0.00	163	0.00	1110	0.00
0.0129	3.38	0.0826	0.00	0.594	2.25	4.03	2.64	27.4	0.00	186	0.00	1260	0.00
0.0147	4.06	0.0995	0.13	0.675	2.01	4.58	2.17	31.1	0.00	211	0.00	1430	0.00
0.0167	4.44	0.115	0.31	0.767	1.71	5.21	2.07	35.3	0.00	240	0.00	1630	0.00
0.0189	4.50	0.128	0.46	0.872	1.41	5.92	1.79	40.1	0.00	272	0.00	1850	0.00
0.0215	4.27	0.146	0.56	0.991	1.15	6.72	1.17	45.6	0.00	310	0.00	2100	0.00
0.0244	3.79	0.166	0.69	1.13	0.97	7.64	1.43	51.8	0.00	352	0.00	2390	0.00
0.0278	3.12	0.188	0.91	1.28	0.93	8.68	1.31	58.9	0.00	400	0.00	2710	0.00
0.0315	2.36	0.214	1.20	1.45	1.04	9.86	1.21	66.9	0.00	454	0.00	3080	0.00
0.0358	1.59	0.243	1.52	1.65	1.27	11.2	1.08	76.0	0.00	516	0.00	3500	
0.0407	0.93	0.276	1.82	1.88	1.61	12.7	0.85	86.4	0.00	586	0.00		
0.0463	0.38	0.314	2.09	2.13	1.98	14.5	0.56	98.1	0.00	666	0.00		
0.0526	0.09	0.357	2.30	2.42	2.35	16.4	0.27	111	0.00	756	0.00		
0.0597	0.00	0.405	2.43	2.75	2.65	18.7	0.06	127	0.00	859	0.00		

APPENDIX D

Fourier Transform Infrared Spectroscopy

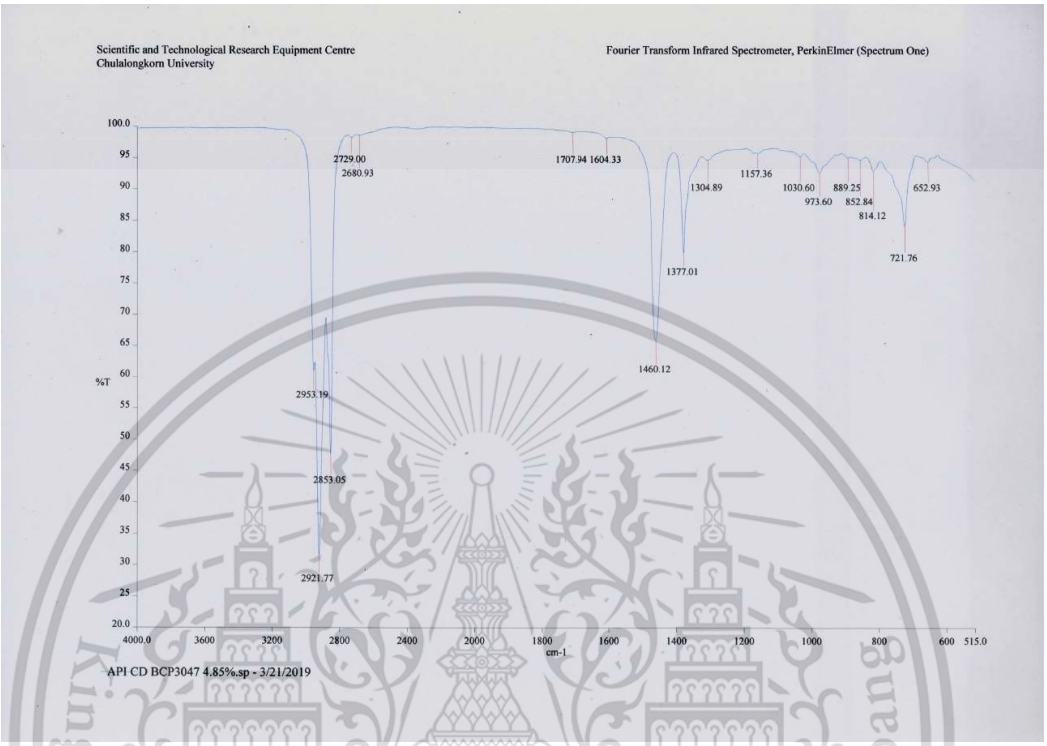

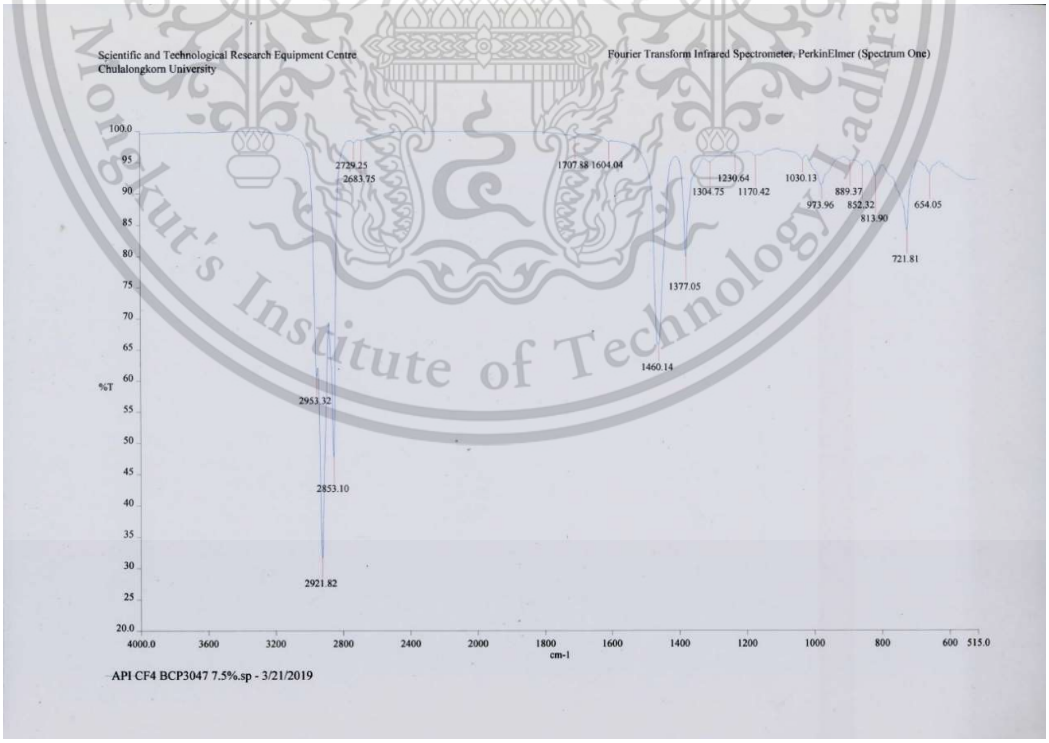

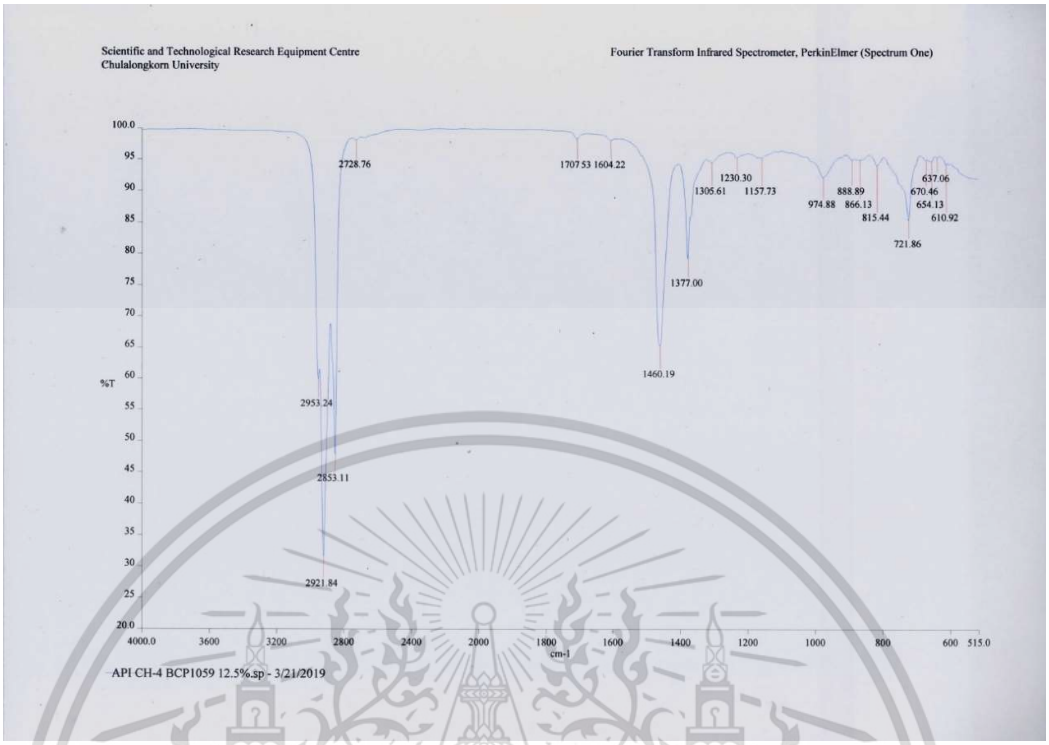

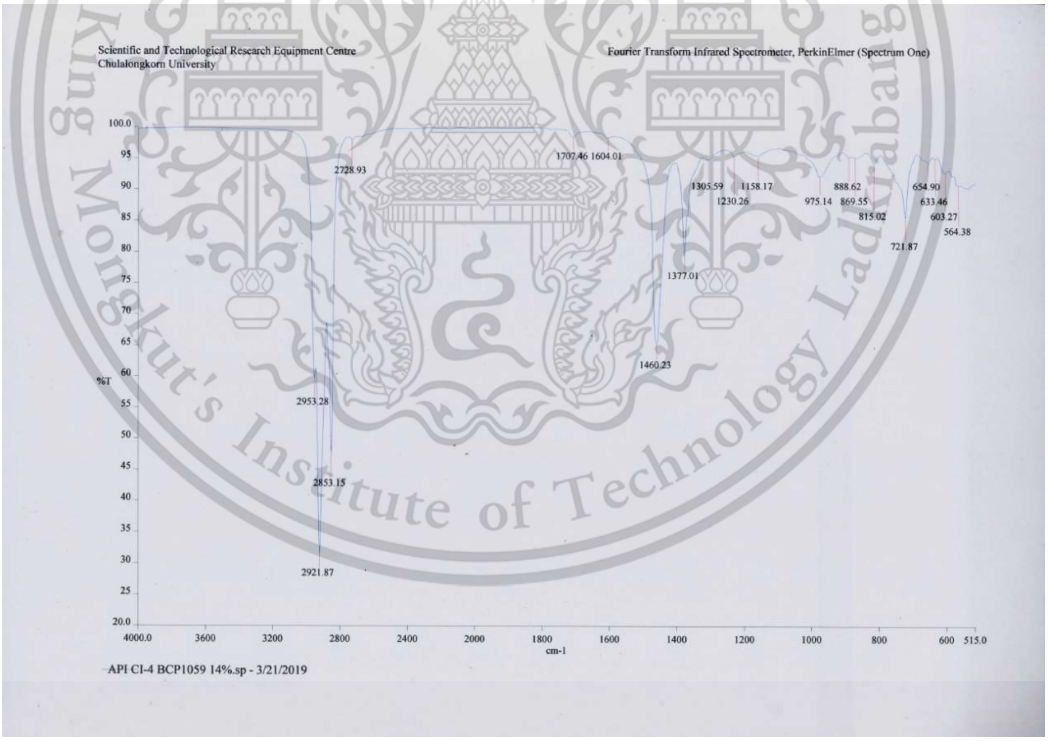

APPENDIX E

PUBLICATION

Key Engineering Materials
ISSN: 1662-9795, Vol. 798, pp 113-121
doi:10.4028/www.scientific.net/KEM.798.113
© 2019 Trans Tech Publications Ltd, Switzerland

Submitted: 2018-09-30
Revised: 2019-01-08
Accepted: 2019-01-08
Online: 2019-04-10

Impact of Oil Additive Characteristics on Biofuel Engine Wear Using Electron Microscopy and Confocal Microscopy

Panyakorn Rungsritanapaisan[1,a], Preechar Karin[1,b*], Dhritti Tanprayoon[2,c], Ruangdaj Tongsri[2,d] and Katsunori Hanamura[3,e]

[1]Automotive Engineering Program, International College, King Mongkut's Institute of Technology Ladkrabang, Bangkok 10520, Thailand

[2]National Metal and Materials Technology Center, National Science and Technology Development Agency, Pathumthani 12120, Thailand

[3]School of Engineering, Tokyo Institute of Technology, Tokyo 152-8552, Japan

[b*]preechar.ka@kmitl.ac.th

Keywords: Internal Combustion Engine, Biofuels, Lubricating oil, Wear, Particulate matter

Abstract. Soot particles are produced during combustion process in the diesel engine. These particles will later exhaust into the thermosphere and part of them will contaminate the engine oil. When the lubricant is contaminated with soot, diesel engine abrasion or in a worst-case scenario lubricant starvation occurs. This situation will eventually lead into engine wear. High volume of soot also raises acid level of the area. If this state co-occurs with high temperature of the engine and volatile gases during operation, engine corrosion may also be produced. This research study the effect of additive volume on the dispersion of soot in engine oil and effect of additive on size and volume of soot which affect to mechanism of wear in metal by tribology four-ball tester, image analysis by scanning electron microscope and particle size analysis by laser diffraction technique.

1. Introduction

Diesel engine is widely used nowadays because it is more efficient and fuel-saver than gasoline engine. EGR system is used to control emission by efficiently reducing Nitrogen oxide (NOx). Unfortunately, the EGR system causes more wear in diesel engine, as it let lubricant oil be contaminated by soot, especially in valve train. Therefore, many researchers studied the soot's effects in lubricant: Hiromitsu Sato used TEM to test the size of soot from many engine samples. He found out that the average diameters of those primary soot particles were between 20 to 40 nanometers, and that their sizes were not influenced by their combustion methods. Also, those wear sizes increased directly to the amount of soot in lubricants tested [1].

P. Karin tested lubricant in 2,000 cc., 2,500 cc. and 7,684 cc. used diesel engines. He found out that their contaminated soot was from 0 to 1% by weight respectively. And with four-ball tribology test, he found out that soot in lubricant might help reduce friction between metal surfaces with its larger lubricant film. However, 20 – 300 nanometers soot would cause wear because of its better chance of friction [2].

David B. Kittelson grouped their sizes into large particle (0.1 – 0.3 micrometers), emitted directly from combustions in diesel engine and mainly consisted of carbon, and nuclei-mode small particle (5 – 50 nanometers), occurred on the cooling process of exhaust system, mainly consisted of hydrocarbon and sulfate. 90% of the particles emitted by diesel engines were the nuclei-mode type [3].

Enzhu Hu found out that wear sizes grew bigger when there was more carbon black, because the carbon black united. EDS test showed that they also adsorbed additives, as there were additive components in the carbon black extracted from lubricant. The average of friction coefficient tended to respectively increase when carbon black increased. Engine wear sizes and friction coefficient in lubricant are larger than those in engine oil, because there was higher kinematic viscosity in engine oil [4].

2. Experimental

2.1 Materials and samples preparation

Different kinds of engine oil used in this research are sponsored by Bangchak Corporation Public Company Limited. They are common oil, based on the API standard, used for diesel engines in the market. The additive amount in each one is different, but their base oil is the same: Group III. They also have the same viscosity at 15W40. In order to study on the effect of soot particles in additives, they are tested according to ASTM standard (Table 1) and the amount of additive is measured by x-ray fluorescence.

Carbon black is a synthetic soot, which has the same size and physical characteristics as soot from the actual engine. Because there are other compounds in the soot caused by actual engine, such as unburn hydrocarbon or metal ash, therefore, carbon black is used instead of real engine soot in this research to reduce the impact of those components. There are many kinds of carbon black. Carbon black N330 is chosen for this research because its physical properties are close to soot from biodiesel engine (Table 2). Its Average Primary Particle size is around 31 nanometers, which is also similar with biodiesel engine soot particles.

Table 1. Engine oil properties

		Base oil	Group III 15W-40	
		API Standard	CD	CI-4
		Additive package	4.84%	14%
Magnesium (Mg)	%wt	ASTM D6481	0.1256	-
Calcium (Ca)	%wt	ASTM D6481	-	0.3205
Zinc (Zn)	%wt	ASTM D6481	0.0984	0.1349
Phosphorus (P)	%wt	ASTM D6481	0.0868	0.1254
Total Base Number	mgKOH/g	ASTM D2896(B)-11	6.5	10.5
Viscosity @40°C	cSt	ASTM D445-15a	112.5	112.6
Viscosity @100°C	cSt	ASTM D445-15a	14.96	15.18
Viscosity Index	-	ASTM D2270	138	141
CCS@-20°C	cPs	ASTM D5293-15	5336	4900

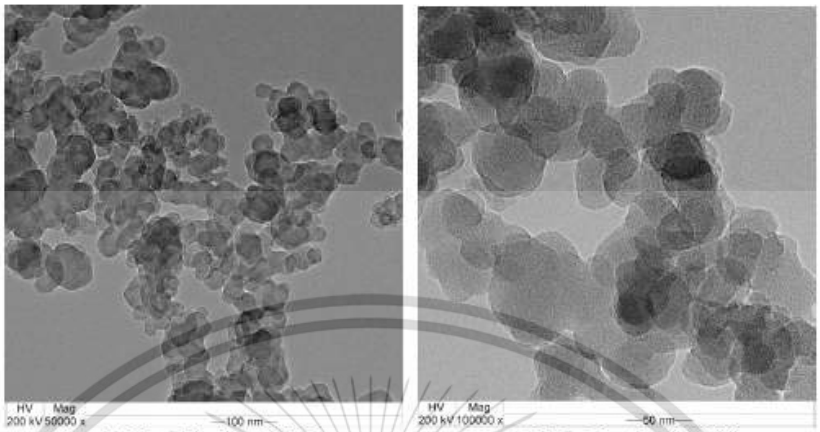

(a) Magnification 50,000x (b) Magnification 100,000x

Figure 1. TEM image of the carbon black N330

Table 2. Comparison of atom and soot density of CB N330, Diesel and B100 [5]

Items		CB N330	Diesel	Biodiesel
Total Fringe length	nm	203.91	227.45	208.38
Total C atoms		19879.89	176595.83	14700.46
Control volume	nm^3	209.92	171.61	162.27
Density	g/cm^3	1.89	2.01	1.82

Table 3. Engine oils mixed with carbon black.

Samples	Carbon Black	Average Primary Particle size according to standard (nm)	% CB (wt. / vol.)
API CD	-	-	-
API CD	N330	31	1 %
API CI-4	-	-	-
API CI-4	N330	31	1 %

In order to simulate the contamination of soot in the engine oil used, Carbon black N330 is added into the engine oil at 1% by weight. The purpose of this test is to determine the additive influence to the contaminating soot in both types of engine oil. The experiments are done according to ASTM4172 standard (Table 3) and to study the effects from soot contaminating, engine oils are divided into two groups: contaminated with soot and not contaminated.

2.2 Experimental method

Four ball test

Four ball wear test is a tribological testing method that shows relation between properties to prevent wear of liquids and the sample´s sliding contact. The experiments are done according to ASTM4172 standard (table 4). Equipment used in this experiment are: Four alloy balls with

diameter of 12.7 mm (0.5 in.) Grade 25 EP (Extra Polish) 12.7 mm. Three of the balls are fixed at the base while the other one is on them, pressed by 392 newton force, and rotated with speed at 12000 RPM/round. All four balls are placed inside a container with the engine oil sample. The test is done at 75°C temperature. At the end, this test will cause horizontal circular wear scars to the three balls at the base and will cause vertical straight-line wear scars to the upper ball.

Table 4. Four ball testing condition

Test conditions		Ball material	
Parameter	Specification	Parameter	Specification
Rotational speed	1200 rpm	Ball material grade	ANSI B3.12
Load	392 N	Surface roughness	0.005 microns
Duration per load	60 min	Ball hardness (Rock well)	64 – 66 (HRC)
Temperature	75°C		

Confocal

Confocal Microscopy is a kind of microscopy that uses focal point technique to increase resolution and contrast of the image. It uses a spatial pinhole to block out unnecessary lights out of the focus. This imaging technique can create three-dimensional structure by using multiple two-dimensional ones captured at different depths. In this research, confocal microscopy will be used to measure surface roughness of the three balls at the base of four ball test. Each one will be measured five times, one after another at about 80 μm (Fig. 2) and the average measurement will be used. The purpose of this process is to see more details of wear scar.

Figure 2. Roughness measurement by confocal microscope

3. Results and Discussion

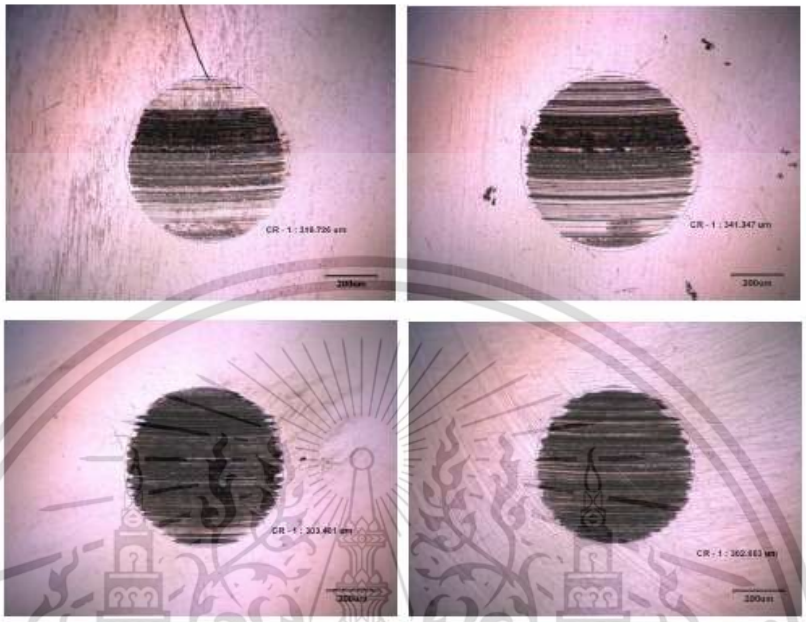

Figure 3. Wear scar diameter are measured by optical microscope

Table 5. Wear scar diameter (μm)

	Wear scar diameter		Arithmetical mean roughness (Ra)	
	New oil	With CB N330	New oil	With CB N330
API CD	638.64 ±1%	687.57 ±1%	1.38 ±5%	2.54 ±5%
API CI-4	603.31 ±1%	609.71 ±1%	3.98 ±5%	3.30 ±5%

After the measurement, it is found that wear scar diameters increase when the engine oil is contaminated with soot at 1% by weight. Test of API CD engine oil that is contaminated with CB is where the largest increase rate of scar is found, which is approximately at 7.7%. In the meantime, wear scar diameters found in the test of API CI-4 engine oil, that is contaminated with CB, also increase approximately at 1.1%. Therefore, it is noticeable that wear scar diameters increase in both types of engine oil because of their CB (soot) contaminating.

For roughness value, the result from API CD testing shows that the Ra value increased significantly about 84% when the oil was contaminated with CD. But when the oil was contaminated with CB like the case of API CI-4 engine oil, the result shows that the Ra value reduced by approximately 17.1%. This indicates that when the oil is contaminated with soot, differentiation of additive will play an important role in reducing surface roughness.

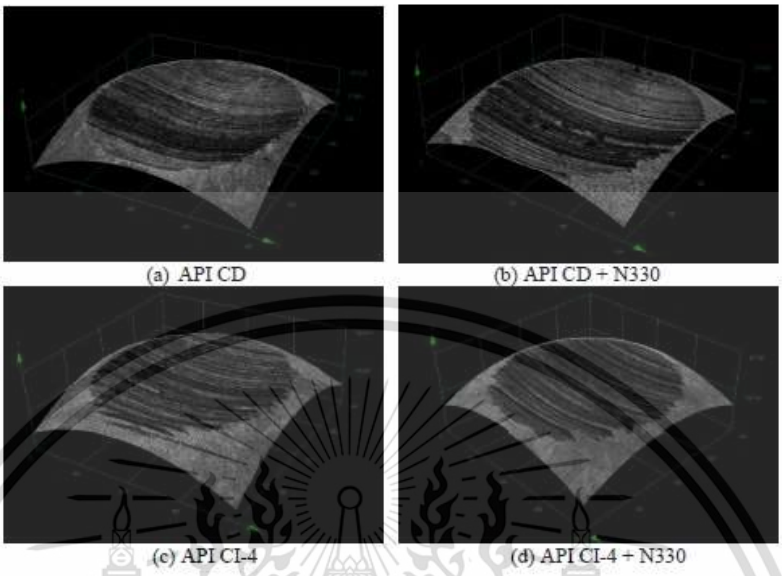

(a) API CD (b) API CD + N330

(c) API CI-4 (d) API CI-4 + N330

Figure 4. Overview of black and white 3D image

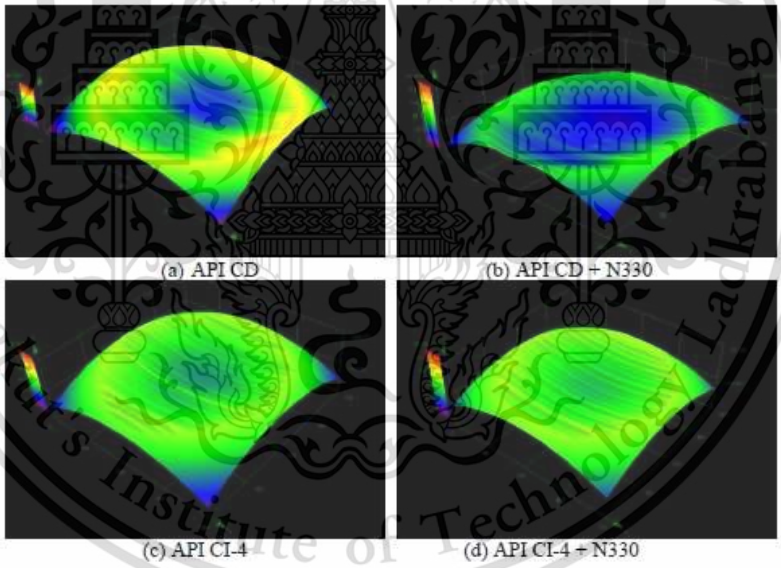

(a) API CD (b) API CD + N330

(c) API CI-4 (d) API CI-4 + N330

Figure 5. Overview of depth profile color 3D image

From figure 4,5 the result shows that the ball surfaces in API CD oil that is contaminated with soot is more rough. Especially in depth profile color picture (Fig. 5b). When the oil is contaminated with soot, the wear surface is very deep. As the blue space in the image can be seen increased. This shows the role of soot when contaminated in engine oil. While the API CI-4 oil, Fig. 5c and 5d, was contaminated with soot in the same amount as the API CD, but there is not much difference in the depth of the wear surface. This demonstrates the ability of the additive to reduce wear when the oil is contaminated with soot.

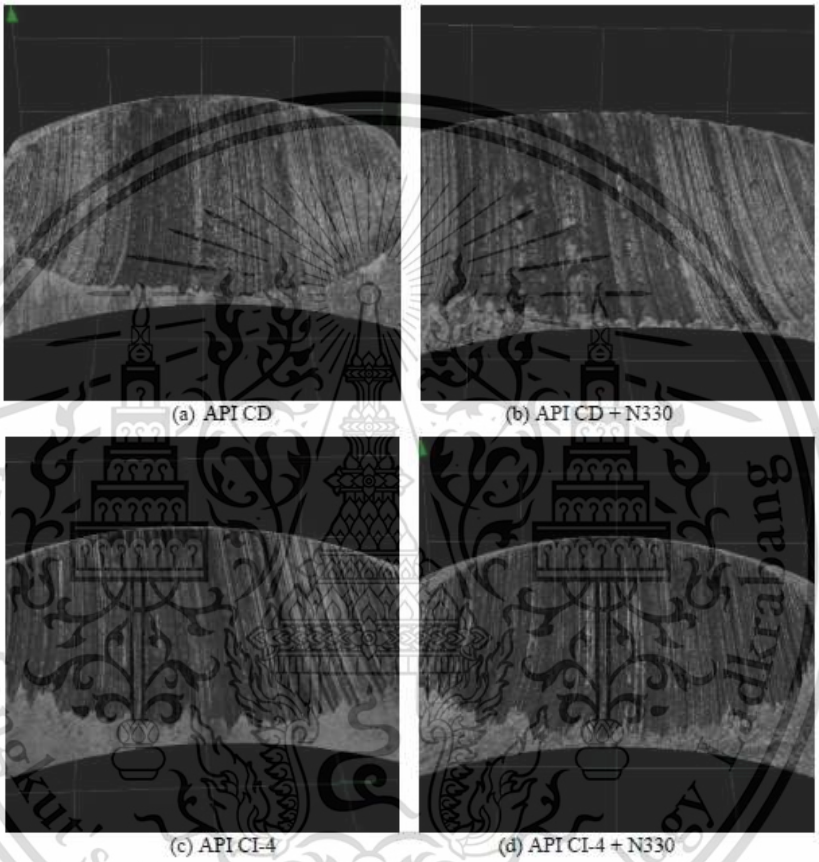

(a) API CD (b) API CD + N330

(c) API CI-4 (d) API CI-4 + N330

Figure 6. High magnification of depth profile black and white 3D image

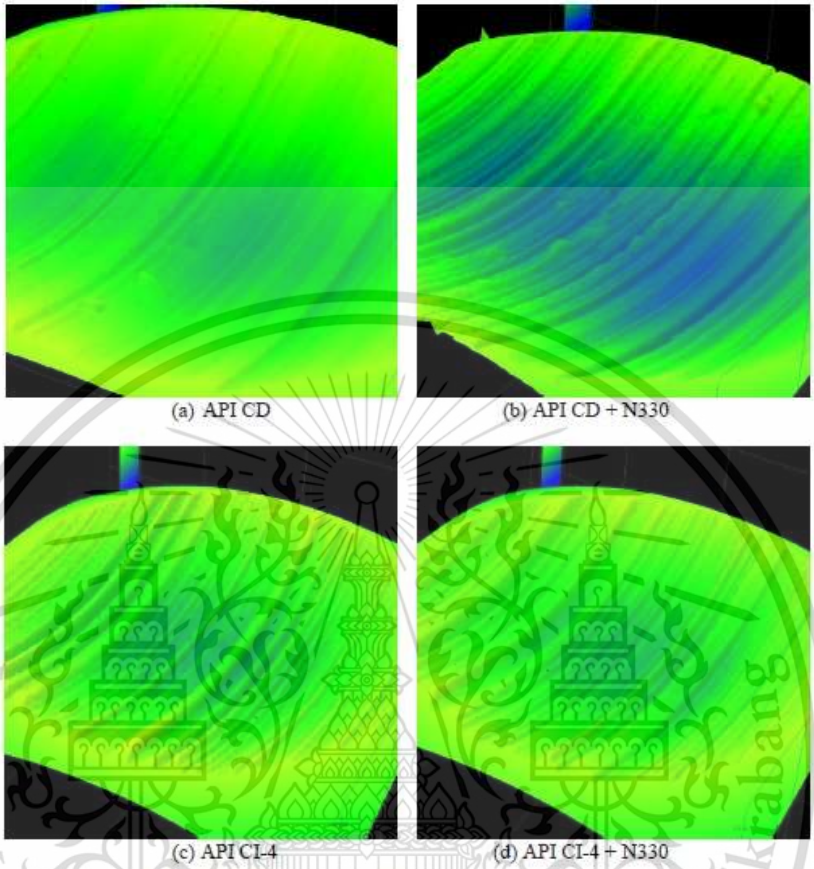

(a) API CD (b) API CD + N330

(c) API CI-4 (d) API CI-4 + N330

Figure 7. High magnification of depth profile color 3D image

In Figure 6a, 6b, 7a and 7b, it is noticeable that the roughness of ball surface increases when the oil is contaminated with soot, a large groove with adhesive wear is found. On the other hand, figure 6c, 6d, 7c and 7d show that the API CI-4 oil made smaller and smoother tear marks, which most of them are abrasive wear.

4. Conclusion

This paper describes the impact of oil additive to soot by simulating engine oil that is contaminated with carbon black. The results showed that, when the engine oil is contaminated with carbon black, as shown in the results of the four ball test, the wear scar diameters significantly increased. This was caused when carbon black entered into the contact surface between the balls. There is carbon black in the oil film when the balls contact each other, and consequently increased wear. In the roughness, the oil containing additives API CI-4 has a lower roughness value than the API CD, because the additive that contained in the engine oil improve the dispersing of contaminated carbon black. When the carbon black is dispersed, it will serve to polish the ball's

surface, resulting in a lower roughness value in the CB contaminated API CI-4 engine oil, than the API CD engine oil that has soot contaminating.

5. Acknowledgements

The authors wish to express their thanks to The Thailand Research Fund (TRF) for supporting research funding and National Metal and Materials Technology Center for supporting laboratory equipment and also Bangchak Corporation Public Company Limited (BCP) for supporting lubricant to accomplish this research.

References

[1] H. Sato, N. Tokuoka, H. Yamamoto and M. Sasaki. (1999). Study on Wear Mechanism by Soot Contaminated in Engine Oil (First Report: Relation Between Characteristics of Used Oil and Wear), SAE TECHNICAL PAPER SERIES 1999-01-3573.

[2] P. Karin, C. Supannamok and K. Hanamura. (2016). Impact of Soot on Metal Wear Characteristics Using Laser Diffraction Spectroscopy, Journal of Research and Applications in Mechanical Engineering, Vol. 4, No.2, pp. 126-134.

[3] D. B. Kittelson. (1998). Engines and nanoparticles: A review. Aerosol Science, vol. 29.

[4] E. Hu, X.Hu, T. Liu, L. Fang, K. D. Dearn and H. Xu. (2013). The role of soot particles in the tribological behavior of engine. Wear 304, pp. 152-161.

[5] P. Watanawongskorn, P. Karin, K. Hanamura and N. Chollacoop. (2017). Impact of morphology and nanostructure on particulate matter's oxidation kinetics from biofuel combustion, Master degree thesis KMITL.

AUTHOR BIOGRAPHY

Author:	Mr. Panyakorn Rungsritanapaisan
Degree:	Master of Engineering
Date of Graduation:	27th July 2019
Date of Birth:	20th April 1995
Place of Birth:	Bangkok,Thailand

Undergraduate and Graduate Education:

Master of Engineering in Automotive Engineering,
King Mongkut's Institute of Technology Ladkrabang, Bangkok, 2019

Bachelor's degree in Materials Engineering,
Kasetsart University, Bangkok, 2016

Major: Automotive Engineering

Presentations and Publications:

[1] Panyakorn Rungsritanapaisan, Preechar Karin, Dhritti Tanprayoon, Ruangdaj Tongsri, and Katsunori Hanamura "Impact of Oil Additive Characteristics on Biofuel Engine Wear Using Electron Microscopy and Confocal Microscopy", *Key Engineering Materials,* ISSN: 1662-9795, Vol. 798, pp 113-121, 2019.